Ornithological assessment in relation to plans for offshore wind farm development in the Hesselø area, Kattegat

Ib Krag Petersen

Lindesay Scott-Hayward

Monique Mackenzie

Rasmus Due Nielsen

Jacob Sterup

Aarhus University/DCE

University of St. Andrews, Scotland

Contents

Summary

In August 2021 Energinet commissioned the Danish Center for Environment and Energy (DCE), Aarhus University, in collaboration with Univ. of St. Andrews, Scotland, to carry out an assessment of the potential effects on bird distributions in and around the Hesselø OWF area in southeastern Kattegat.

Results from seven aerial line transect surveys of birds, conducted in relation to the above wind farm plans, was used to present data on bird abundance and distribution. This was supplemented by bird survey data from the Danish national monitoring program, NOVANA, from which data were selected from a larger area from the winters of 2008, 2013, 2016 and 2020. Based on these data, persistency maps could be modelled for each of the species/species groups, across all surveys. Persistency maps indicate where the bird utilize an area more intensively than other parts. Thus, persistency maps also indicate areas of higher sensitivity for the species.

From a list of bird species recorded within the study area, four species or species groups were selected for further analysis. The selection of the species was based on their abundance in and near the potential Hesselø OWF, combined with the conservation status of each species. Red-throated Diver/Black-throated Diver, Northern Gannet, Black-legged Kittiwake and Razorbill/Common Guillemot were the four species/species groups selected.

Through a literature study, the effect from offshore wind farms on the distribution of the above four species/species groups was assessed, on basis of which displacement scenarios could be determined. Using these scenarios, the number of displaced birds pr. species/species group could be estimated. Also, the potential change in distribution between the winter 2020 distribution and other mid-winter survey could be assessed, including the re-distribution of displaced birds. These assessments indicate how a wind farm project in the area could add to a cumulative effect on the selected species.

Red-throated Diver/Black-throated Diver was found in low numbers in the vicinity of the proposed wind farm site. Being listed on Appendix 1 of the EU Birds Directive, this species group was included in the analysis. Less than 0.1 % of the flyway population was displaced.

Gannet and Kittiwake was present in the proposed wind farm area in very fluctuating numbers. The number of displaced birds for the two species was less than 0.01 and 0.002 % of the flyway populations, respectively.

Razorbill/Common Guillemot was found to be the most abundant species group in and near the proposed wind farm area, appearing in highly fluctuating numbers. They could not be identified to species, and each of the two species consist of more subpopulations. The subpopulation composition in the study area is poorly known, but under described assumptions the estimated percentage of displaced birds was approximately 0.5 % of the Razorbill ssp. *torda* population, 0.2 % of the Razorbill ssp. *islandica*, 0.03 % for Common Guillemot ssp. aalge (East Atlantic), and 0.04 % for Common Guillemot ssp. *albionis*.

Introduction

In August 2021 Energinet requested input for an assessment of the potential ornithological impacts in relation to the plan for Hesselø Offshore Wind Farm (OWF) in the Middelgrund area, in the Danish part of Kattegat. The purpose of the report is to provide ornithological input for a Strategic Impact Assessment for plans to develop this OWF. The assessment focuses on evaluation of potential effects of possible changes in the distribution of birds within and around the area of the proposed Hesselø OWF.

The analyses are based on aerial line transect survey data from a total of 11 aerial surveys of birds. Seven surveys were conducted in relation to the plans for offshore wind farms in the Middelgrund area. These surveys were commissioned by the Danish Energy Agency, and conducted by DCE, Aarhus University between December 2018 and November 2019 (Petersen & Sterup 2019a, 2019b). The Middelgrund Study Area covers an area of ca. 3,900 km^2. Data from an additional four surveys on bird distributions was included from the Danish national waterbird monitoring program, NOVANA. These surveys covered the entire Middelgrund study area plus areas of the Danish part of Kattegat to the north and west of the site, hereafter referred to as the Kattegat Study Area. The surveys conducted in relation to the Hesselø OWF from the Middelgrund Study Area are abbreviated “MG”-surveys below, while the NOVANA data are referred to as “W” surveys.

Based on the collected data, bird species of special relevance in relation to the development of a wind farm in the proposed Hesselø OWF area were identified. This was based on the numerical abundance of bird species in the vicinity of the proposed wind farm site and the conservation status of the species. In this way four bird species or species groups were identified, namely Red-throated Diver *Gavia stellata*/Black-throated Diver *Gavia arctica*, Northern Gannet *Morus bassanus* (hereafter Gannet), Black-legged Kittiwake *Rissa tridactyla* (hereafter Kittiwake) and Razorbill *Alca torda*/Guillemot *Uria aalge*.

For each of these species/species groups estimations of abundances and fine scale geographical distribution was analyzed, using Distance Sampling principles and a spatial modelling frameworks. This resulted in predicted distributions for each of the species/species groups and surveys.

Based on the predicted density surfaces persistency values could be modeled for each of the species, aiming to quantify the spatial importance within the study area as estimated across all surveys.

A literature study delivered input for displacement/attraction scenarios to each of the four species/species groups in relation to offshore wind farms. On the background of these the expected number of displaced/attracted birds could be predicted. The data were also used to model the potential distributional effect of displacements/attractions in relation to numbers throughout the general study area. This was achieved by redistributing those individuals that were displaced/attracted to other parts of the study area based on the previous modelling of densities in all areas. Output from these models was used to describe the potential cumulative impact of a wind farm project in this area.

The population status of the selected species was assessed, and the percentage of the flyway populations affected by the proposed wind farm could be estimated.

In the present report analyses of the potential sensitivity to marine birds from a proposed offshore wind farm area, exclusively related to the distribution of resting marine birds, is presented. No data on bird migration or bird flying altitudes was available for this analysis, and the potential effect of collisions between birds and turbines was not included in the analysis.

The report was a collaboration between DCE, Aarhus University and the CREEM group at University of St. Andrews. The data collection, curation and general analysis was performed by DCE, while CREEM performed and provided the Distance Sampling and spatial modelling analyses.

Data and Methods

Survey area

This assessment concerns plans for the development of the proposed Hesselø OWF in an area of almost 247 km^2 of Kattegat between Anholt and the island of Hesselø (Figures 1 & 2) situated ca. 20 km from Hesselø, 20 km from Anholt and at its shortest distance is ca. 8 km from the Danish/Swedish EEZ-border. The area within the proposed wind farm area ranges in water depths from 24 to 39 meters.

The study area (here described as the Middelgrund Study Area) around the proposed Hesselø OWF area was established within which ornithological data was collected between December 2018 and November 2019, covering an area of 3,894 km^2. We have also included existing data from an even greater study area, including Ålborg Bugt and the waters between Læsø and Anholt, using data from the Danish national monitoring scheme (NOVANA) survey from that area collected in the winters of 2008, 2013, 2016 and 2020. Data on the abundance and distribution of waterbirds from this area were included in this analysis. Throughout this report, we refer to this area as the Kattegat Study Area, which covers not only the entire Middelgrund Study Area, but also marine areas west and northwest (see Figure 1) and covers an area of 12,308 km^2.

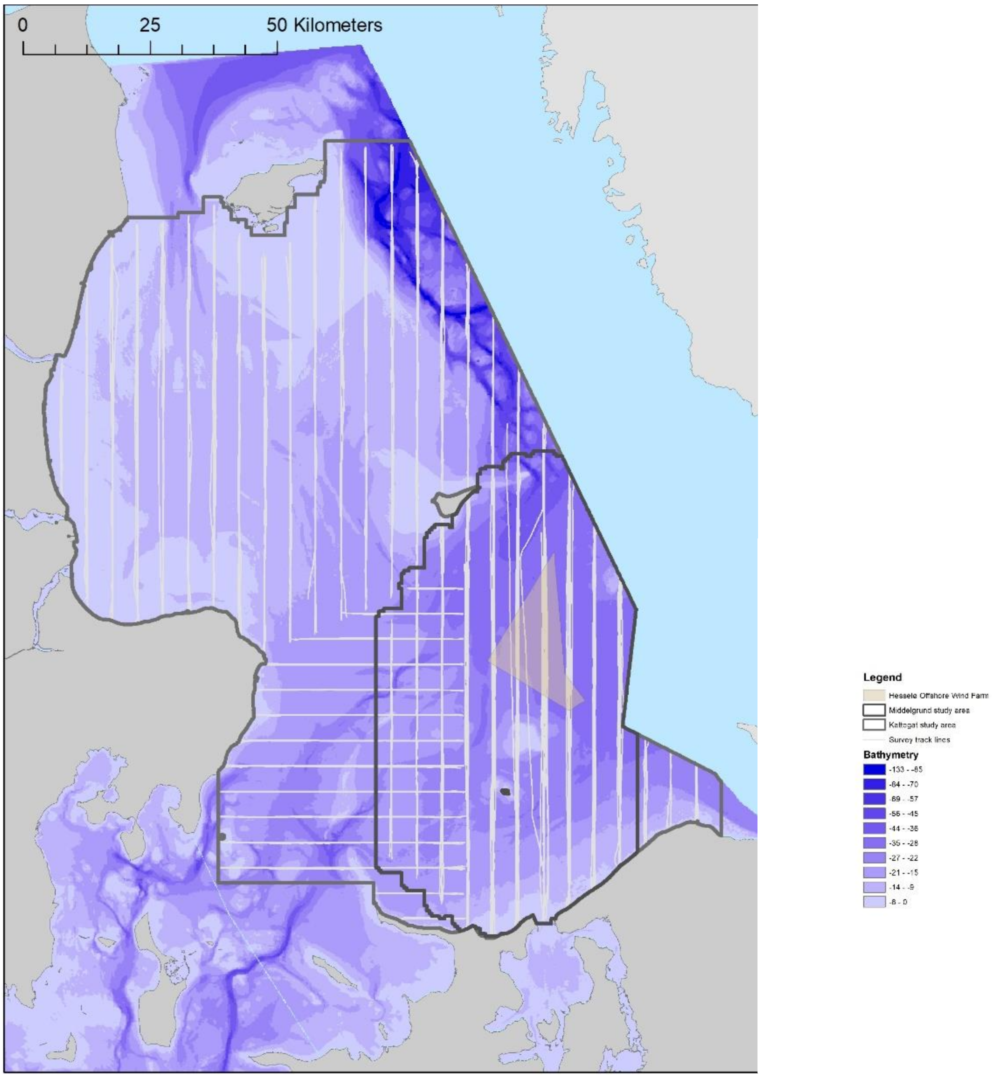

Figure 1. Map of the study areas surveyed for resting birds around the proposed offshore wind fan site in Kattegat. The wind farm site (Hesselø OWF Site), along with the extension of the Middelgrund and the Kattegat study areas are indicated. The combined transect lines surveyed are shown, as is the bathymetry of the area.

Birds Directive areas

Six EU Special Protection Areas (SPAs) are already designated under the Birds Directive within the Kattegat Study Area, which covers all of the Middelgrund Study Area, two of which overlap peripherally with the Middelgrund Study Area (Figure 2). On the Swedish side a number of marine Birds Directive SPA's are designated, two of which border to the Danish/Swedish EEZ-border.

The marine Birds Directive areas (SPA's) in the Danish part of Kattegat was very recently revised (1st December 2021). Neither the geographical extend nor the bird species designated for those areas will alter the conclusions drawn in this report.

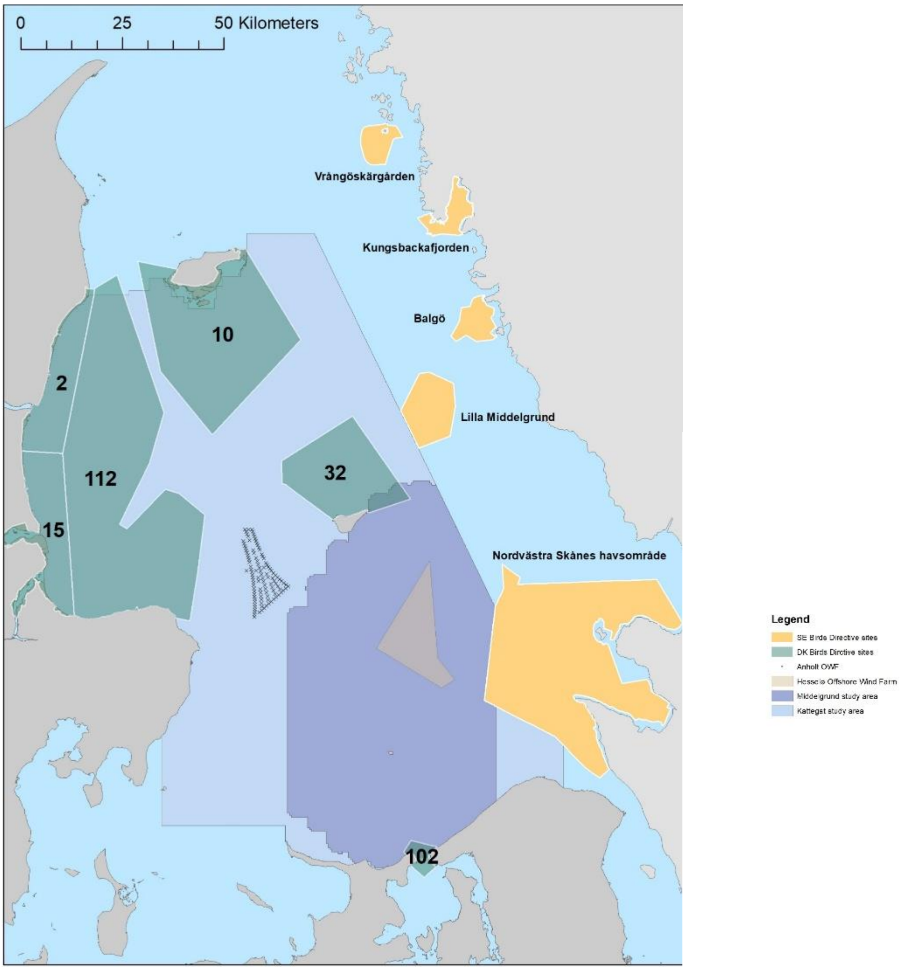

Figure 2. Map of the Middelgrund and Kattegat Study Areas, with indication of the potential offshore wind farm area and the Danish Special Protection Areas within the Study Areas (green). Five marine Swedish Birds Directive (yellow) areas in adjacent marine waters are also shown. The proposed Hesselø OWF impact area and the extant Anholt OWF are indicated.

The six Danish SPAs support 12 different migratory bird species for which the sites have been designated (listed in Table 1). The species were selected on the background of three criteria, namely F4, F5 and F7 (Table 1). The criteria cover the following:

- F4 Regular occurrence of numbers of international importance
- F5 Regular occurrence of >20,000 waterbirds
- F7 An occurrence of limited but important number of a species during challenging life stages (e.g. ice winters or moulting)

Table 1. List of the migratory bird species named in the designation of each of the six EU Special Protection Areas within the Middelgrund and Kattegat Study Areas (identified by codes in Figure 2), showing qualifying designation criteria. Breeding birds have not been included. This table is based on data from the designation lists from before 1st December 2021 revision of the SPA's

Species	SPA_02	SPA_10	SPA_102	SPA_112	SPA_15	SPA_32
Mute Swan					F4	
Light-bellied Brent Goose	F4			F4	F4	
Dark-bellied Brent Goose		F4				

Shelduck	F4, F5				F4	
Greater Scaup	F4				F4	
Golden-eye			F4, F7		F4	
Common Eider	F5, F7	F4	F4, F7	F4	F4	F4
Common Scoter	F4	F4, F7		F4, F7	F4, F7	F4, F7
Velvet Scoter	F4, F7	F4, F7			F4, F7	F4, F7
Goosander			F4, F7		F4	
Red-breasted Merganser			F4, F7			
Dunlin	F5	F5				

Data collection

Data on bird abundance and distributions were collected using standard methods; human observers during aerial surveys, flying transects between designated GPS waypoints at regular speed and altitude. Observations are recorded within distance bands of the aircraft to allow for modelling of differential detectability at increasing distance from the observers, following standard Distance Sampling line transect survey methods (Buckland et al. 2001, 2015). The survey methods used in these surveys are fully described in detail in Petersen & Sterup (2019a).

The data used for this assessment comes from a total of 11 aerial surveys. Of these, seven surveys were commissioned by Energistyrelsen, covering the Middelgrund Study Area of ca. 3,900 km^2. These data were collected between December 2018 and November 2019. The remaining four surveys, covering the Kattegat Study Area were collected under the national Danish monitoring programme, NOVANA in the winters of 2008, 2013, 2016 and 2020 (Table 2).

Table 2. Timing of the 11 surveys covered in this analysis. The length of the transects covered for each survey is given.

Survey time	Total length of transects (Km)
17. December 2018	736
10. January 2019	731
1. March 2019	676
1. April 2019	739
17. April 2019	735
9. September 2019	576
6. November 2019	652
Winter 2008	2,444
Winter 2013	2,385
Winter 2016	2,445
Winter 2020	2,384

The precise survey track lines flown during each survey is presented in each of the species distribution maps provided below.

Each of the Middelgrund surveys were conducted in a single day. During the NOVANA surveys, which covered a larger area, data were collected over several days, or, in some cases, using two survey aircraft operating on the same day (Table 3). In 2008 the surveys comprised of five campaigns, covering four dates between 7 February and 16 March, in 2013 of four campaigns, covering two dates between 13 and 26 February, in 2016 of five campaigns, covering three dates between 15 January and 13 February and in 2020 of five campaigns, covering three dates between 30 January and 14 February (Table 3).

Table 3. Survey dates and aircraft used for each of the NOVANA survey campaigns during the winters of 2008, 2013, 2016 and 2020.

Survey timing	Date	Aircraft
Winter 2008	07/02/2008	OY-CAG
Winter 2008	09/02/2008	OY-CDC
Winter 2008	10/02/2008	OY-CDC
Winter 2008	10/02/2008	OY-CAG
Winter 2008	16/03/2008	OY-CAG
Winter 2013	13/02/2013	OY-BSE
Winter 2013	13/02/2013	OY-CAG
Winter 2013	26/02/2013	OY-CAG
Winter 2013	26/02/2013	OY-ILS
Winter 2016	15/01/2016	OY-ILS
Winter 2016	15/01/2016	OY-GPS
Winter 2016	12/02/2016	OY-GNS
Winter 2016	13/02/2016	OY-BSE
Winter 2016	13/02/2016	OY-CDC
Winter 2020	30/01/2020	OY-BSE
Winter 2020	30/01/2020	OY-MLS
Winter 2020	03/02/2020	OY-BSE
Winter 2020	03/02/2020	OY-SPS
Winter 2020	14/02/2020	OY-SPS

Data from the mid-winter surveys is part of national monitoring schemes, and cover most of the inner Danish waters. Data from outside the Kattegat study area was not included in this analysis.

Some species are difficult to differentiate during the aerial surveys, and are therefore treated as combined species groups in this report. This is the case for Red-throated Diver /Black-throated Diver, for Razorbill *Alca torda*/Guillemot *Uria aalge* and for Arctic Tern *Sterna paradisaea*/Common Tern *Sterna hirundo*.

Data analysis

Distance Sampling Analysis

Distance sampling analyses were conducted for each of four selected bird species/species groups by pooling the information from 11 surveys within the Kattegat Study Area. The four species/species groups are diver species (Red-throated Diver/Black-throated Diver), Gannet *Morus bassanus*, Kittiwake and alcids (Razorbill/Guillemot). The selection criterion is defined below.

When fitting detection functions, the effects of covariates, other than perpendicular distance, are incorporated into the detection function model (Multiple Covariate Distance Sampling, MCDS, Marques et al. 2004, 2007, Buckland et al. 2001). In these cases, the probability of detection becomes a multivariate function, g(y;v), which represents the probability of detection at perpendicular distance y and covariates, v (v=v_1…v_Q) where Q is the number of covariates). In this study, using a half-normal detection function ($e^{(-y^2/\sigma^2)}$) the covariates were incorporated via the scale term, σ, where for sighting j, σ has the form:

$$\sigma_j = \exp\left(\beta_0 + \sum_{q=1}^{Q}(\beta_q v_{jq})\right)$$

where β_0 and β_q (q = 1 … Q) are parameters to be estimated. Both half-normal and hazard rate detection functions were fitted with AIC used to choose between the two models. The candidate variables trialed were bird group size, sea state, sun intensity, behaviour and observer (Table 4). The detections were recorded in four bins (A-D) with cut offs at 119, 388, 956 and 1426m out from the flown transect lineand were predominantly observed from both sides of the plane.

Table 4: Table detailing the covariates used in the detection function fitting.

Covariates	Values
Sea State	0, 0.5, 1, 1.5, 2, 2.5, 3 (calm to rough)
Glare	1 (full sun), 2, 3 (cloudy), 9 (sun and cloud)
Behaviour	S (sitting or diving) and F (flying or flushing)
Observers	Up to 12 different observers

Spatial Analysis Framework

Executive summary of the spatial modelling methods

The data collected by these surveys are bird counts and since the variation in the number of birds tends to increase as the average number of birds increases (i.e., there is a mean-variance relationship) an overdispersed Poisson-based count model was used.

Additionally, since bird numbers are often thought to be related to environmental characteristics, such as water depth and the distance from land, these variables were considered as part of each analysis. To ensure these relationships were suitably informed by the data (and not fixed in nature based on prior thinking), a flexible approach to these relationships was taken, and the shape of these relationships was evidence-based. For example, a species could show a preference for a particular depth range (i.e., the shape of the relationship between bird numbers and depth could rise and fall) or it could be more simplistic (e.g., numbers could systematically increase/decrease with depth) or alternatively be more complex. In the case of distance from land, the relationship could indicate a general increase or decrease in bird numbers as the distance from land increases or it could show more curvature and/or indicate some “preferred” distance range.

The model selection approach used in the following analyses selects the details of these relationships informed by the data, while ensuring that the resulting relationships are not “overfitted” to the data available – so the underlying relationships in each case were sought, rather than a “fine-tuned” version of these relationships which would fit perfectly to the data set collected for each species, in each survey, but not represent any other set of observations from this survey or area (even if they were collected at a similar time from the same area).

While including environmental relationships in models can be relatively simple to understand, it is important to note that if these terms are included in a model (in this way) they are assumed to be true everywhere across the survey region– that is, if bird numbers are assumed to be highest at some number of kilometres from land, this is assumed to be true for *all* areas of land, including along the entire coastlines and around the small island located in the centre.

This is often unrealistic in practice since there are many (other) influences in addition to the variable(s) under consideration which act together to determine which locations are attractive/unattractive to birds (some of which might be changing daily). Additionally, all of the variables giving rise to bird numbers in particular locations are unlikely to be available for consideration/selection in model and thus localised spatial patterns often remain. For this reason, and to account for localised surface patterns, a spatial surface was also considered for inclusion in each model. These terms were also permitted to be flexible (and informed by the data) but were chosen in order not to be “overfitted” to any particular survey – instead to represent the underlying spatial patterns likely to be observed at a similar time in the same survey area.

If a spatial term was chosen for a model (with some appropriate level of flexibility), this term was assumed to ‘absorb’ (and thus replace) the ‘one-dimensional’ distance from land relationship since any systematic relationships from land (coastline and/or island) are estimated by this term instead. If a ‘distance from land’ relationship is of inherent biological interest however, it is still possible (using this modelling approach) to estimate what this relationship looks like (and potentially how this changes along the coastline and/or from the island) by post processing the model predictions within and across surveys. This enables accurate estimates at the survey level, and some insights about this relationship and how this might change across the survey area and across surveys.

To achieve this balance between fit to the survey data and to avoid “fine-tuning” each model to represent the exact observations sampled for each survey, a “10 fold cross validation” procedure was used. This simply divides the data up into buckets (folds) with (relatively) equal numbers of observations (in this case sections of transects) and uses nine of these folds to choose a model and the remaining fold (which is left out of model fitting and selection) to “test” the model. This prevents overfitting since a finely tuned model would fit almost perfectly to the nine folds but would look very different from the ‘left-out’ fold since it was not included in the model fitting and choice, even though it was collected as part of each survey.

The additional feature of these analyses is that the way in which the data were collected was acknowledged and respected when reporting the level of uncertainty in model results. In particular, these data were collected along transects over time and data collected this way tends to be more similar than data collected randomly from potentially very different parts of the survey area within some time window. This is akin to measuring the body weight of 10 human subjects, monthly for 10 consecutive months (N=100) compared with measuring the body weight of 100 different human subjects once throughout a 10-month period (also N=100). Traditional ways of reporting the uncertainty about model estimates (e.g., bird counts in any given location) often assumes the modelled data are either randomly sampled in some way, or the variables included in the model *fully* explain these patterns of similarity in these observations collected along transects (resulting in uncorrelated left-overs/residuals). This is far from guaranteed, and the approach used here was to simply measure the extent of similarity observed in model residuals (within transects – the correlated panels/blocks) and use this value to increase the uncertainty about model estimates so that the results can be interpreted in the usual way: e.g., "With 95 % confidence we estimate the number of birds in this location to be between five and eight birds, on average."

Spatial data specification

The transect lines were segmented into approximately 500m long blocks and the sightings allocated appropriately; if there were no sightings the segments were recorded as 0. For each species, models were fitted to each of the 11 surveys separately allowing for the distribution of birds to change in each one.

Spatial covariates

The response variable in each case was bird counts and thus the response was modelled using a quasi-Poisson framework, with estimated (over)dispersion. In this study, the (one-dimensional) covariates used for analysis were bathymetry and distance to coast (Figure) and to account for localized surface patterns (as a result of unmeasured covariates) a spatial surface was also fitted to each model. Specifically, a two-dimensional CReSS-based surface using a Gaussian radial basis function, was also included in the model terms.

The following equation represents an example of a model fitted with a one-dimensional smooth term (e.g., bathymetry) alongside a two-dimensional spatial smooth:

$$y_{ijt} = Poisson(\mu_{ijt})$$

$$\mu_{ijt} = e^{(\beta_0 + s_1(Bathymetry_{ijt}) + s_2(XPos_{ijt}, YPos_{ijt}))}$$

where y_{ijt} is the estimated count for transect *i* segment *j* and time point t. s_1 represents a quadratic *B*-spline smooth of bathymetry and s_2 is a two dimensional smooth of space (with coordinates XPos and YPos in UTMs). Implicit in this model are also coefficients for the intercept (β_0) and any coefficients associated with the smooth terms. The effort associated with each observation varied depending on the associated segment area and was included as an offset term (on the log scale).

In these models both a globally applicable "bathymetry" and/or distance to coast term and a more nuanced spatial term were trialed for inclusion in each model, in order to indicate how best to model spatial patterns in each case. In particular, this helped signal if any spatial patterns were sufficiently described by a (one-dimensional) depth metric (which applies the same across the surface determined solely on the depth) or if a more considered approach to spatial patterns was justified for each survey.

For example, if 'bathymetry' was selected and a two-dimensional spatial element was *not* deemed necessary (as determined by the model selection procedure governed by objective fit criteria) then this signals that any spatial patterns are primarily a function of the depth, regardless of the geographical location of this depth in the survey area.

If the two-dimensional spatial term was selected for inclusion in a model then the spatial density patterns (over and above any depth-related terms) were accommodated using a spatially adaptive term which permits different amounts of flexibility across the surface in a parsimonious way (relatively complex spatial patterns can be accommodated with very few parameters). If the spatial term was selected (as indicated by an improved fit under the objective 10-fold cross validation metric) then this replaced any distance to coast terms in a model. This was undertaken to allow the more flexible spatial term to instead represent any 'distance to coast' effects which are likely to change across the survey area, depending on location.

An objective fit criteria, based on a 10-fold cross validation procedure was used to govern the model selection process which attempts to balance the fit to data unseen by the model while minimising the number of parameters (parsimony).

The response data are collected along survey lines in sequence, and so consecutive observations are likely to be correlated in space and time (i.e., points close together in space and/or time are likely to be more similar that points distance in time and/or space). Further, the covariates included in the model are unlikely to explain these patterns in full and so some element of these patterns are likely to remain in model residuals. These patterns are a violation of residual independence (which underpin traditional model approaches such as Generalized Additive Models) and thus, robust standard errors were used as part of the modelling framework to account for residual auto-correlation.

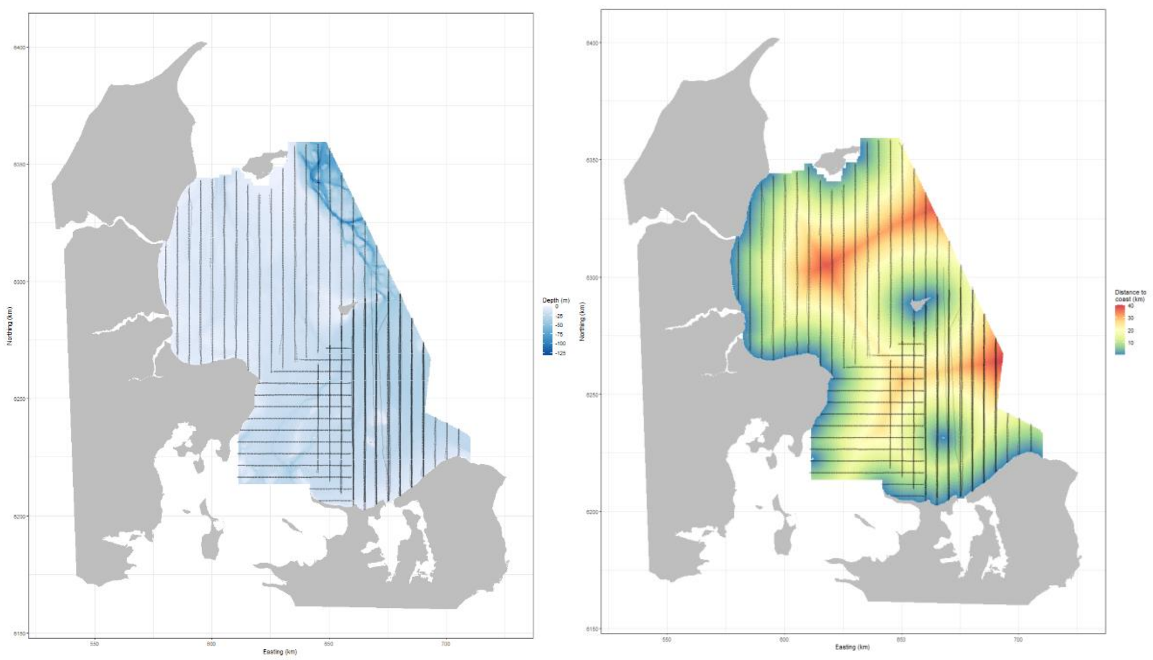

Figure 3: Visual representation of bathymetry (left) and distance to coast (right) for the large survey area. The grey polygons represent land and the black lines illustrated in the waters represent survey effort across all 11 surveys (transect lines).

Model specification, selection and fitting

CReSS-based spatially adaptive generalized additive models, with targeted flexibility, using a Spatially Adaptive Local Smoothing Algorithm (Walker et al. 2010, Scott-Hayward 2013, Scott-Hayward et al. 2014), were fitted to each set of survey data to allow for non-linear relationships between the one-dimensional and two-dimensional covariates and the response. The one-dimensional covariates were permitted to have a linear or nonlinear relationship with the response in each case, and when a smooth term was included in a model it was specified to be a quadratic (degree 2) *B*-spline and permitted to exhibit flexibility (dictated by the degrees of freedom) underpinned by objective fit criteria. The degrees of freedom for these terms determine the flexibility of these smooth (and nonlinear) relationships -- the more degrees of freedom, the more flexible the relationship can be. The location of this flexibility (along the x-axis) in these terms (e.g., bathymetry) was also determined as part of the model selection process using SALSA. This permitted the relationship in some areas of the covariate range to be relatively complex (e.g., in shallow waters) and the relationship in other areas (e.g., in deep waters) to be relatively simplistic.

The spatial patterns in each survey were permitted to be determined either by a one-dimensional distance from coast (including the central island feature) relationship or instead based on a two-dimensional spatial term (of variable complexity). The flexibility of the spatial element constituted part of the model selection procedure and for each survey was determined using SALSA. While this model selection element technically occurred between limits (*df*=[2,100]), the flexibility chosen in each case was not bounded in practice by those values since the selection procedure occurred well within the bounds of the specified range.

The MRSea R package, designed to fit both CReSS and SALSA type models, was used for model fitting and a 10-fold cross-validation (CV) procedure was used to govern all model selection elements (Scott-Hayward et al. 2019a, 2019b). The associated CV metric was used to determine which terms to include in each model and the extent of the flexibility exhibited by each term for those selected. Note, this cross validation was predicated on preserving correlated blocks of survey data (transect lines) so that any residual autocorrelation present was not disrupted when choosing folds. This was considered necessary to ensure independent sampling units under the scheme.

Parameter inference

Uncertainty about model parameter estimates proceeded via robust standard errors due to the nature of the survey procedure. The data were collected along transects and thus robust standard errors were used to account for any positive correlation (present after model fitting). These essentially work by inflating the standard errors (which would normally be obtained under traditional approaches) in relation to the positive correlation observed within pre-specified blocks of residuals. In cases, where this residual correlation is minimal, the adjustments are small, and when the correlation is more extreme, the inflation is larger.

A transect-based blocking structure was used to reflect potential correlation within blocks while independence between blocks was assumed. To ensure this assumption was realistic, the decay of any residual correlation to zero (i.e., independence) with the distance between points (within blocks along transects) was assessed visually. Specifically, transects in each survey were used as the blocking structure and an Auto Correlation Function (ACF) plot on this basis was used to check the suitability of this blocking structure, via a 'decay to zero' trend within blocks.

Modelling diagnostics

To assess the adequacy of model fit in each case, a range of diagnostic measures were used.

The assumed mean-variance relationship under the model was assessed visually using plots of the fitted values from the model against the variance of the residuals which is assumed to hold in each case. In this example, quasi-Poisson models were employed which assumes a proportional mean-variance relationship; $V(Y) = \varphi V(\mu) = \varphi\mu$, where φ is known as the dispersion parameter. The dispersion parameter was also estimated for each model and this estimate was used in the visual assessment of this mean-variance relationship assumed to hold under the model.

The Pearson's residuals for each model were also visualised spatially to ensure there were no areas of consistent bias across the survey area, which would be indicated by clusters of negative or positive residuals in spatially similar locations.

Residual independence was not assumed to hold under the model and instead model inference proceeded under robust standard errors. As described, Auto Correlation Function (ACF) plots were instead used to check the suitability of this blocking structure, via a 'decay to zero' trend within blocks and are presented for inspection.

Model Predictions and estimates of uncertainty

Predictions based on each model were made to a 500m^2 grid across the study region for each survey, and the uncertainty in these predictions was comprehensively quantified by cascading the uncertainty in both the detection function estimation and the spatially adaptive model fitted using a combination of one-dimensional and two-dimensional model terms.

The uncertainty in the detection function was reflected using non-parametric bootstrap estimates (*n*=250) of re-sampled distance sampling data (sampling unique transect ID's with replacement). Based on these resamples, new estimates for the probability of detection were found for each new dataset, which were then used to generate new estimated counts for each segment. The spatially adaptive generalized additive model was then fitted to each of the new datasets to obtain a new set of parameter estimates (based on the originally selected spatial model). The final output of this process was a parametric bootstrap process using the robust variance-covariance matrix from each non-parametric bootstrap model. These were used to calculate 250 sets of model predictions (one from each non-parametric model) which generated 95 % percentile-based intervals in addition to generating a coefficient of variation for each grid cell.

A calculation of 'persistence' was also undertaken across surveys using the geo-referenced estimates of density (abundance/associated area) across the survey area. Low persistence values indicate that a given area is less important to a given bird species, estimated across many surveys. High persistency values indicate areas frequently used by the species in question. Persistence scores were calculated for every 500m x 500m grid cell in the following way: Firstly, each (final) bootstrap replicate was allocated a binary value based on whether or not the estimate in each location was above the mean estimated density (1) throughout the survey area or below (0) this mean estimated density. This was performed for all 250 sets of plausible predictions in each grid cell (based on the bootstrap replicates) and the proportion of these bootstrap predictions in excess of the mean (indicated by the value of 1) was calculated for each grid cell to give a persistence score for that location. For example, a persistence score of 1 indicates that the density in that grid cell was estimated to be above average in every bootstrap replicate in every survey (so uniformly above the mean; high persistence) while a value of 0.1 indicates that just 10 % of the estimates were above the estimated mean, and thus indicates low persistence in that location.

Windfarm Area Assessment

Spatially Explicit Differences

Distributional changes over time were evaluated by comparing the estimated distributions from the large scale surveys of 2008, 2013 and 2016 to the estimated distribution in the most recent 2020 survey. Additionally, any changes during this time in and around the proposed Hesselø OWF area could be observed.

Difference plots were used to visualise any spatially explicit changes in the distribution of birds. The bootstraps from the modelling process described above were used to generate a 95- percentile interval for the difference in abundance in each grid cell. If the interval contained zero it was deemed not to indicate a statistically significant difference in abundance between the two comparison years. If the range of plausible values for the difference (indicated by the 95 % confidence interval) did not include zero, then the change was deemed to be significantly positive or negative.

Impact Scenarios

In order to assess the number of birds likely to be impacted by a wind farm development in the Hesselø OWF area, we have used the predicted density surface result from four species/species groups, which occur in the highest densities. It is known from previous studies that all or some of these species are likely to be attracted to or displaced elsewhere because of their attraction or reticence to approach the turbines, resulting in potentially higher or lower densities within the wind farm area post construction. In order to model the extent and magnitude of these changes in local abundance, we have used existing data on proportions of species/species groups observed during previous studies and reported in the literature.

The availability of empirical data documenting the attraction/displacement effect from offshore wind farms on the distribution of resting waterbirds remains limited (Dierschke et al. 2016, Fox & Petersen 2019). To estimate the numbers of potentially displaced birds from the construction of the Hesselø OWF we used information, retrieved from a literature survey, on displacement for the four avian species/species groups that were particularly relevant in relation to the Hesselø OWF. The information is summarized in Table 5.

For Red-throated Diver/Black-throated Divers we estimated displacement based on an 80 % reduction within the footprint and a gradually reduced effect out to a distance of 16 km from the site. This is based on studies from the German Bight (Mendel et al. 2019, Heinänen et al. 2020, Petersen et al. 2014).

Previous studies suggest Gannets show distributional effects from the construction of offshore wind farms. In the North Sea, several studies reported strong displacement effects. Around the island of Helgoland 89 % of pre-breeding and breeding Gannets avoided entering OWF’s (Pelchko et al. 2020). Other studies described 37 % fewer birds within the footprint of the wind farm area, with a gradually reduced effect out to a distance of 15 km (Vanermen et al. 2015, Welcker & Nehls 2016). In this analysis, we have adopted the 37 % value estimate displacement from the Hesselø OWF area.

Previous studies have reported that the Kittiwake has shown variable responses to the construction of offshore wind farms, ranging from attraction to avoidance (Dierschke et al. 2016). At the Alpha Ventus wind farm site in German North Sea, a displacement effect was observed (Welcker & Nehls 2013, Mendel et al. 2014), whereas an attraction was reported from the Kentish Flat and Gunfleet Sands sites in the UK (Dierschke et al. 2016). For this reason, in this report, we present the change in relative abundance before and after the construction of the turbines under two scenarios, namely i) a 20 % reduction in the footprint of the wind farm site and a reduced effect out to a distance of 2 km and ii) a 20 % increase in the footprint of the wind farm site and a reduced effect out to a distance of 2 km.

Displacement responses of Razorbill/Guillemot at sea to offshore wind farms have also been variable, not just between wind farm sites, but also between surveys (Zuur 2018). Given these conflicting results, we have used a precautionar "average" scenario and implemented a 50 % reduction of numbers within the footprint of the wind farm site and a gradually reduced effect out to a distance of 2 km.

The number of displaced or attracted birds was calculated for each survey, based on the observed abundance of each species within the footprint of the wind farm area adjusted by the percentage change values identified above (based on the literature values and summaries in Table 5) and also modified according to the linear changes in abundance with distance from the outer edge of the proposed wind farm out to the defined distance where the net effect was zero (again see above and Table 5 for definitions for each species).

In modelling the effect scenarios for post constructions distributions of birds from the 2020 large scale surveys, the displaced/attracted birds were re-located/taken from within the entire Kattegat Study Area. In the case of a decline in abundance, the displaced birds were "added" to the area outside of the footprint plus buffer following the estimated 2020 distribution of birds throughout the rest of the Kattegat Study Area. The scenario was imposed on every set of bootstrap predictions (250 sets) to calculate the mean number of birds lost in the footprint and footprint plus buffer area along with percentile-based 95 % confidence intervals.

Additionally, the abundance of birds was calculated in each of the six Special Protection Areas (SPAs) that are covered/part covered by the prediction area of this study. This allowed assessment of plausible changes in abundance in these SPAs, given the 2020 distribution and the scenario chosen for that species. The changes were modelled on the basis of the SPA extents in place prior to the 1st December 2021 revision of the SPA's.

Table 5: Table detailing the impact scenarios for each species. A negative percentage indicates a decline in abundance and a positive one indicates an increase in abundance.

Species	Percentage Change	Buffer
Diver spp.	-80	16 km
Gannet	-37	15 km
Kittiwake	-20	2 km
	+20	2 km
Razorbill/ Guillemot	-50	2 km

Results

During the 11 surveys a total of 50 bird species and four species groups were recorded (Table 6). The most numerically abundant bird species were Common Scoter *Melanitta nigra*, Common Eider *Somateria mollissima* and Razorbill/Guillemot, both in actual numbers (Table 6) and when weighed for survey coverage (Table 7).

In the area of the proposed Hesselø OWF and a buffer zone 5 km around this, the most numerically abundant bird species, summed across all 11 surveys, were Razorbill/Guillemot (4,386), Herring Gull *Larus argentatus* (572), Gull sp. (526), Kittiwake (131), Gannet (114) and Great Black-backed Gull *Larus marinus* (105).

Table 6. Total number of birds observed by species/species group and survey. Note that the winter surveys of 2008, 2013, 2016 and 2020 cover the larger Kattegat Study Area (columns shaded grey), while the remaining seven surveys cover the smaller Middelgrund Study Area.

Species	Winter 2008	Winter 2013	Winter 2016	17/12 2018	10/01 2019	01/03 2019	01/04 2019	17/04 2019	09/09 2019	06/11 2019	Winter 2020
Diver sp.	105	34	174	8	23	43	52	8	1		65
Red-throated Diver	159	258	162	56	4	37	2	1			52
Black-throated Diver	2	4	3	1	1		2				2
Great Northern Diver		2									
Yellow-billed Diver			1								
Slavonian Grebe		1									
Red-necked Grebe	6	2	33				4			2	6
Great Crested Grebe	1	6									2
Grebe sp.	1		2			6					2
Great Northern Diver		2									
Yellow-billed Diver			1								
Northern Fulmar	23		5		1		1				4
Northern Gannet	10	3	29	6	9	2	312	170	13	21	51
Great Cormorant	502	421	369	623	490	37	169	8	50	367	1372
Grey Heron							2				
Mute Swan	2	1	2			3	2			2	14
Whooper Swan	70		21							39	5

Greylag Goose	11		22				2	5			4
Brent Goose		65	33								24
Barnacle Goose							1				
Canada Goose		20								4	
Shelduck	208	5	1								22
Mallard	691	2	1483				30				35
Northern Pintail	15										
Eurasian Wigeon								15			38
Tufted Duck	135		2								
Greater Scaup			5000								
Goldeneye	32	186	89	1		3	2				57
Long-tailed Duck	249	124	248				5			9	171
Common Eider	8773	6826	7764	545	261	251	248	76	18	297	3711
Common Scoter	74289	15782	10812	1555	260	149	348	8		144	11114
Velvet Scoter	267	1477	643	8		46	48	7			2729
Goosander			8								
Red-breasted Merganser	50	50	86	32	21	26	21	14			94
Marsh Harrier								1			
White-tailed Eagle		2									
Peregrine Falcon	1										
Oystercatcher	23										101
Grey Plover											1
Curlew		1	5								
Dunlin			450								3
Great Skua							1		4		1
Common Gull	3	81	32				4		1	10	15
Herring Gull	1245	1851	1214	153	312	250	125	171	10	20	1032
Lesser black-backed Gull							5	8			
Great Black-backed Gull	173	121	132	34	58	38	31	67	15	9	173
Black-headed Gull	43	39	11	1			4	1			12
Little Gull	7		2								1
Black-legged Kittiwake	439	24	31	10	31	22	3			24	143
Arctic/ Common Tern								1			1
Sandwich Tern								1			

Razorbill	135	29	232	30	11		7		26	2	95
Razorbill/ Common Guillemot	3833	61	2985	278	1118	918	846	61	119	108	1662
Common Guillemot	50	5	351		8	13	3	5	111		8
Black Guillemot	9	11	3				1		1		5

Because the length of transect line covered varied between surveys, a relative number was calculated as number of observed individuals by 100 km of transect line coverage. The values are given for a subset of species/species groups (Table 6).

Table 7. The relative number of recorded birds by species/species group and data. The relative numbers was calculated as number of birds observed / survey effort (100 km transect covered). Species with a predominantly coastal occurrence have been omitted.

Species	**Winter 2008**	**Winter 2013**	**Winter 2016**	**17/12 2018**	**10/01 2019**	**01/03 2019**	**01/04 2019**	**17/04 2019**	**09/09 2019**	**06/11 2019**	**Winter 2020**
Diver sp.	2,15	0,82	3,56	0,54	1,56	2,93	4,51	0,54	0,09	0,00	1,36
Red-throated Diver	3,25	6,19	3,31	3,80	0,27	2,52	0,17	0,07	0,00	0,00	1,09
Black-throated Diver	0,04	0,10	0,06	0,07	0,07	0,00	0,17	0,00	0,00	0,00	0,04
Great Northern Diver	0,00	0,05	0,00	0,00	0,00	0,00	0,00	0,00	0,00	0,00	0,00
Yellow-billed Diver	0,00	0,00	0,02	0,00	0,00	0,00	0,00	0,00	0,00	0,00	0,00
Red-necked Grebe	0,12	0,05	0,67	0,00	0,00	0,00	0,35	0,00	0,00	0,15	0,13
Great Crested Grebe	0,02	0,14	0,00	0,00	0,00	0,00	0,00	0,00	0,00	0,00	0,04
Grebe sp.	0,02	0,00	0,04	0,00	0,00	0,41	0,00	0,00	0,00	0,00	0,04
Northern Fulmar	0,47	0,00	0,10	0,00	0,07	0,00	0,09	0,00	0,00	0,00	0,08
Northern Gannet	0,20	0,07	0,59	0,41	0,61	0,14	27,09	11,57	1,13	1,61	1,07
Great Cormorant	10,27	10,10	7,55	42,31	33,14	2,52	14,67	0,54	4,34	28,16	28,77
Tufted Duck	2,76	0,00	0,04	0,00	0,00	0,00	0,00	0,00	0,00	0,00	0,00
Greater Scaup	0,00	0,00	102,24	0,00	0,00	0,00	0,00	0,00	0,00	0,00	0,00
Golden-eye	0,65	4,46	1,82	0,07	0,00	0,20	0,17	0,00	0,00	0,00	1,20
Long-tailed Duck	5,09	2,97	5,07	0,00	0,00	0,00	0,43	0,00	0,00	0,69	3,59

Common Eider	179,46	163,73	158,76	37,01	17,65	17,08	21,53	5,17	1,56	22,79	77,82
Common Scoter	1519,67	378,55	221,08	105,60	17,58	10,14	30,21	0,54	0,00	11,05	233,06
Velvet Scoter	5,46	35,43	13,15	0,54	0,00	3,13	4,17	0,48	0,00	0,00	57,23
Goosander	0,00	0,00	0,16	0,00	0,00	0,00	0,00	0,00	0,00	0,00	0,00
Red-breasted Merganser	1,02	1,20	1,76	2,17	1,42	1,77	1,82	0,95	0,00	0,00	1,97
Great Skua	0,00	0,00	0,00	0,00	0,00	0,00	0,09	0,00	0,35	0,00	0,02
Common Gull	0,06	1,94	0,65	0,00	0,00	0,00	0,35	0,00	0,09	0,77	0,31
Herring Gull	25,47	44,40	24,82	10,39	21,10	17,01	10,85	11,64	0,87	1,53	21,64
Lesser Black-backed Gull	0,00	0,00	0,00	0,00	0,00	0,00	0,43	0,54	0,00	0,00	0,00
Great Black-backed Gull	3,54	2,90	2,70	2,31	3,92	2,59	2,69	4,56	1,30	0,69	3,63
Black-headed Gull	0,88	0,94	0,22	0,07	0,00	0,00	0,35	0,07	0,00	0,00	0,25
Little Gull	0,14	0,00	0,04	0,00	0,00	0,00	0,00	0,00	0,00	0,00	0,02
Black-legged Kittiwake	8,98	0,58	0,63	0,68	2,10	1,50	0,26	0,00	0,00	1,84	3,00
Arctic/ Common Tern	0,00	0,00	0,00	0,00	0,00	0,00	0,00	0,07	0,00	0,00	0,02
Sandwich Tern	0,00	0,00	0,00	0,00	0,00	0,00	0,00	0,07	0,00	0,00	0,00
Razorbill	2,76	0,70	4,74	2,04	0,74	0,00	0,61	0,00	2,26	0,15	1,99
Razorbill/ Common Guillemot	78,41	1,46	61,04	18,88	75,61	62,47	73,44	4,15	10,33	8,29	34,85
Common Guillemot	1,02	0,12	7,18	0,00	0,54	0,88	0,26	0,34	9,64	0,00	0,17
Black Guillemot	0,18	0,26	0,06	0,00	0,00	0,00	0,09	0,00	0,09	0,00	0,10

Species account

In this section the abundance and the distribution of selected bird species or species groups are described, along with data on their phenology and depth preferences. For four species/species groups spatial models are presented. For other species the distribution of observed birds are presented.

Red-throated Diver/Black-throated Diver *Gavia stellata/Gavia arctica*

Divers were present in high numbers in the Kattegat study area, especially in winter and spring. A total of ca. 6,000 divers were estimated to winter in the inner Danish waters in 2008 (Petersen & Nielsen 2011), with the majority of the birds in Kattegat.

In the Kattegat study area both Red-throated Diver and Black-throated Diver occur. Red-throated Divers account for ca. 90 % of these (Dierschke 2002). The two species are difficult to distinguish during aerial surveys, and most of the observed divers were not identified to species.

Within the Kattegat and Middelgrund Study Area divers primarily occurred in offshore areas between Djursland, Læsø and Anholt and along the north coast of Sjælland (Figure 4). In total, sightings of 1,259 Red-throated/Black-throated Divers appeared in this data set (Table 6). Of these, 666 appeared within the Middelgrund Study Area and 157 appeared within 16 km of the proposed wind farm area.

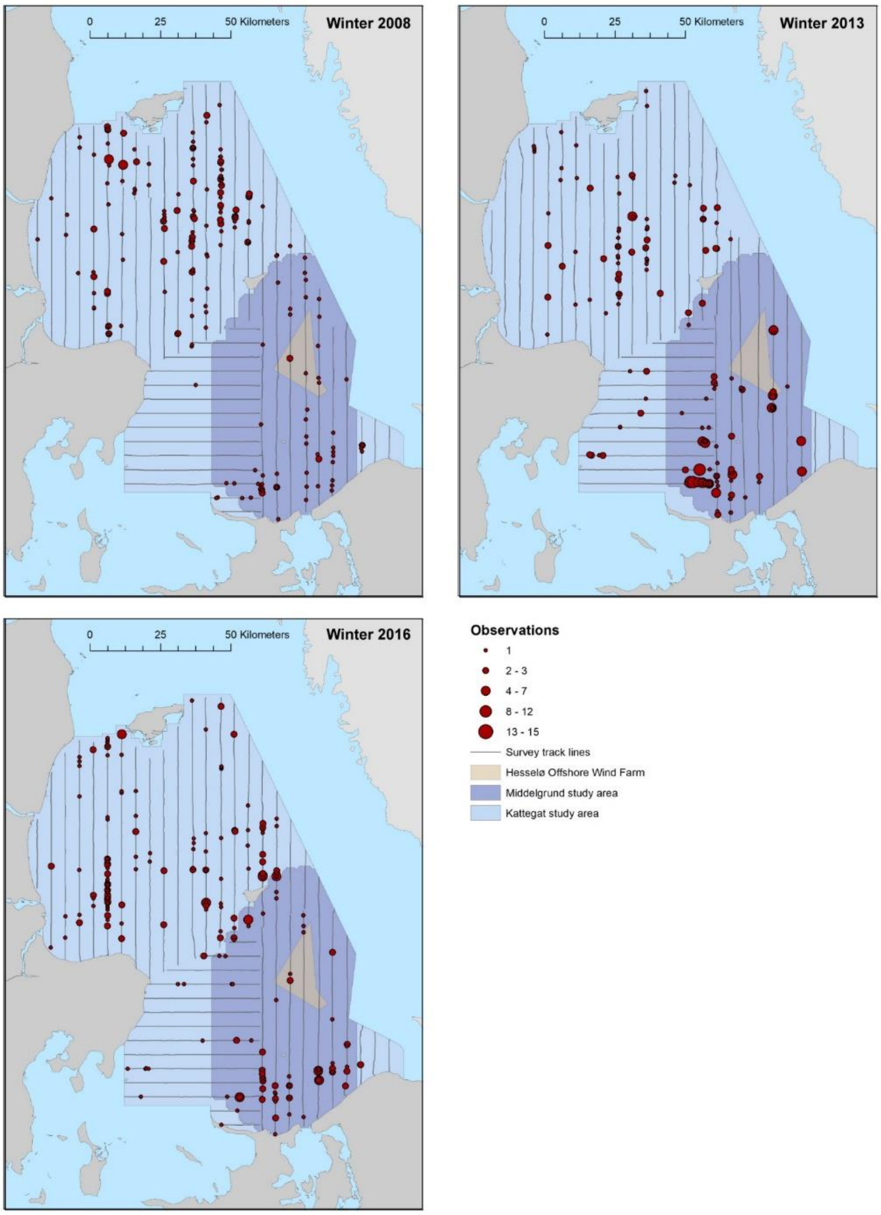

Figure 4. The spatial distribution of observed Red-throated Diver/Black-throated Diver from 11 surveys of birds in the study area between winter 2008 and winter 2020. Survey timing for the individual surveys are given in upper right corner of each map. The survey track lines covered for each survey is given.

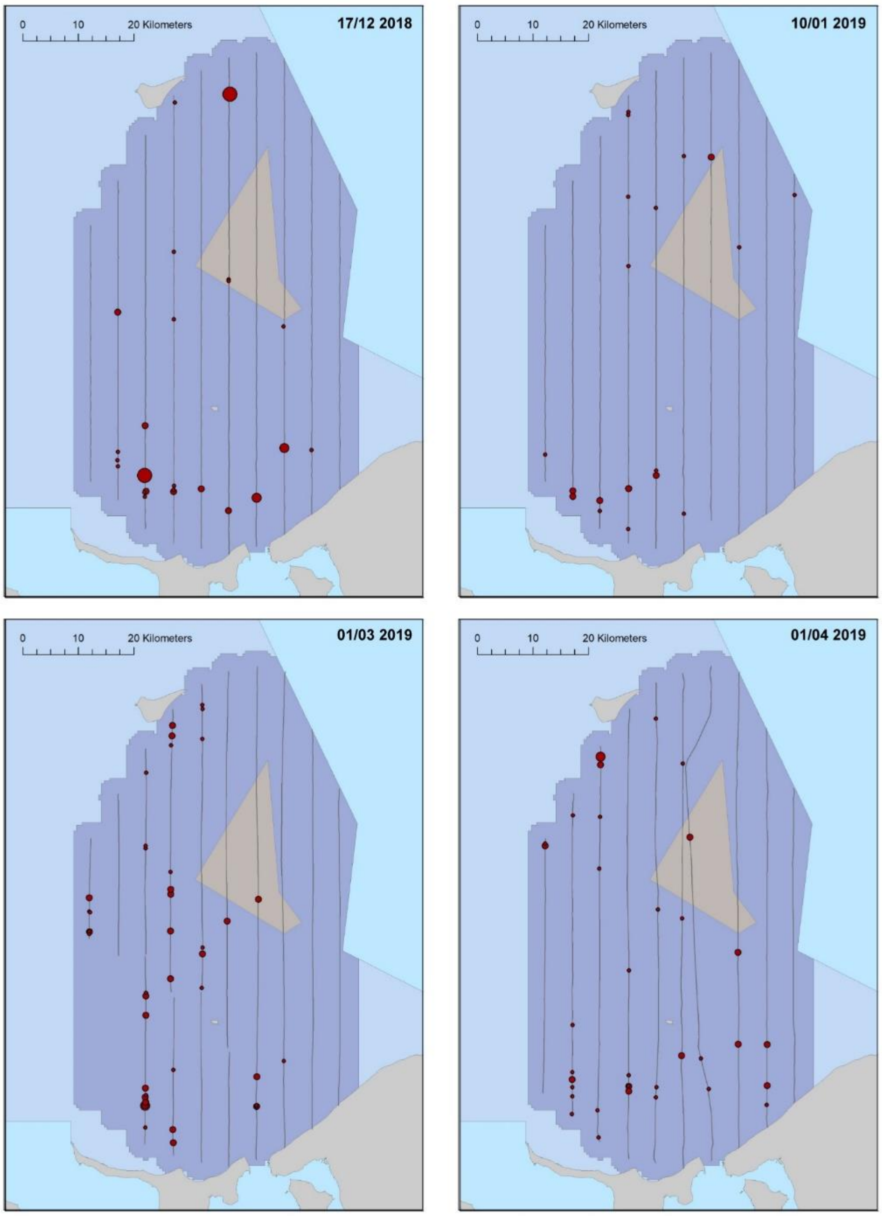

Figure 4. Red-throated Diver/Black-throated Diver, continued

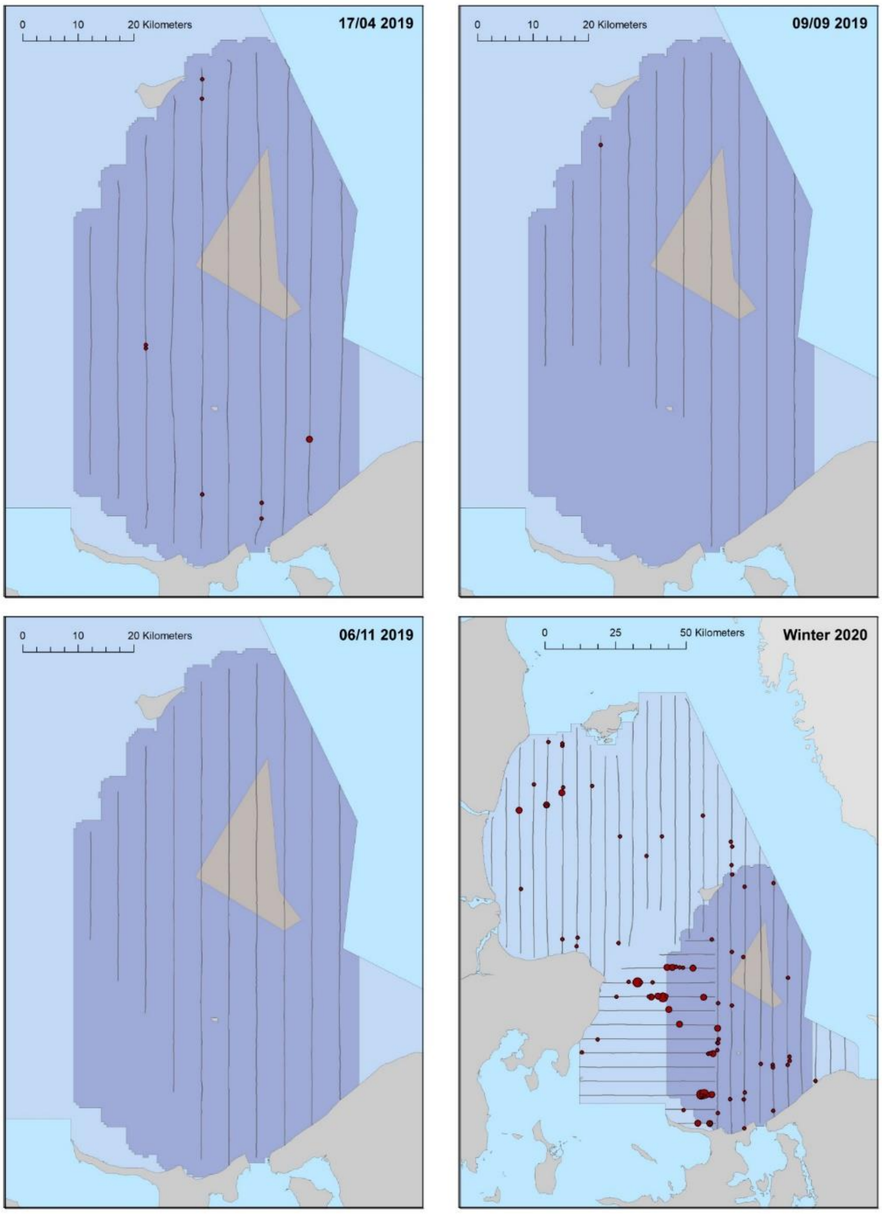

Figure 4. Red-throated Diver/Black-throated Diver, continued

The divers generally appear in the area from November until April (Figure 5). Highest numbers were observed from February to April. This annual pattern corresponds with the annual pattern found in Kattegat as recorded during 15 surveys in that area from 1999 until 2001 (Petersen et al. 2003).

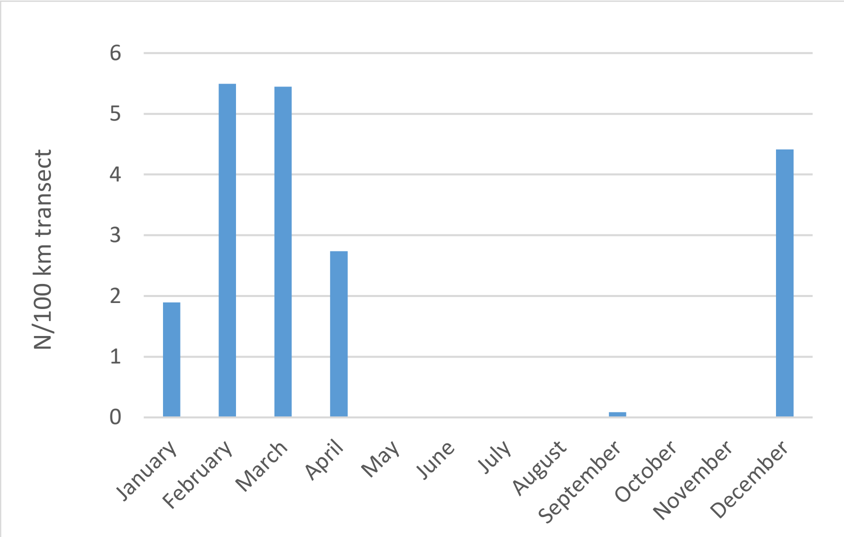

Figure 5. The annual variation in the relative density of Red-throated Diver/Black-throated Diver in the Kattegat survey area from 11 surveys included in this report.

Divers are found on a wide range of water depths, mainly from 10 to 26 meters. Most birds (almost 20 %) were found in the depth interval 20-22 meters (Figure 6).

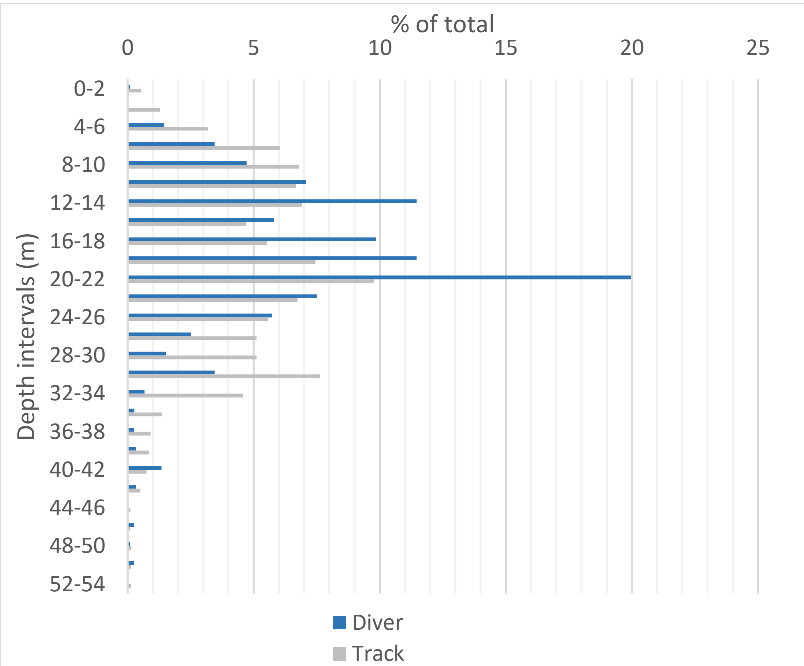

Figure 6. The depth frequency distribution of Red-throated Diver/Black-throated Diver in the Kattegat study area in 2 m depth intervals and expressed as % of total numbers observed. The depth frequency distribution of the covered survey track lines is given for comparison.

Distance Analysis

The average probability of sighting divers was estimated to be 0.22 (CV=0.046). This probability was estimated using a hazard rate detection function that varied with observer, behaviour, cluster size and glare (Figure & Figure 83). As there was only one sighting in band D, this detection was excluded and the strip half width set to be 956m.

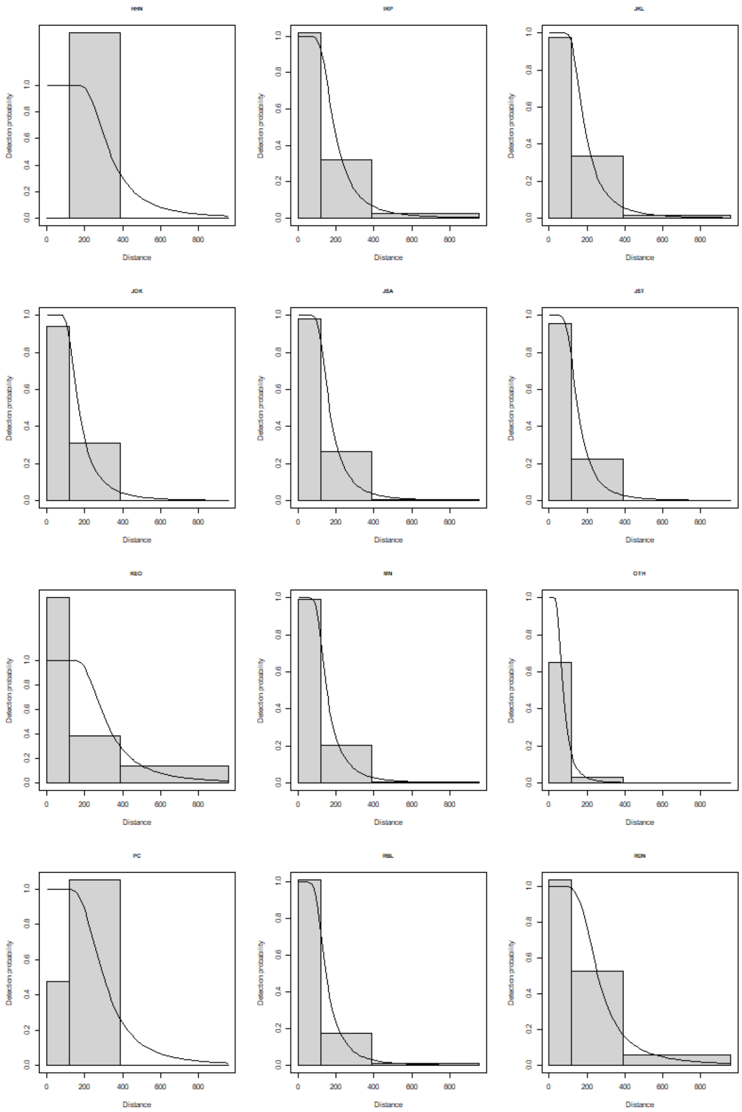

Figure 7: Figure showing the estimated detection function for each of the observers. The histograms are the distances of the observed sightings.

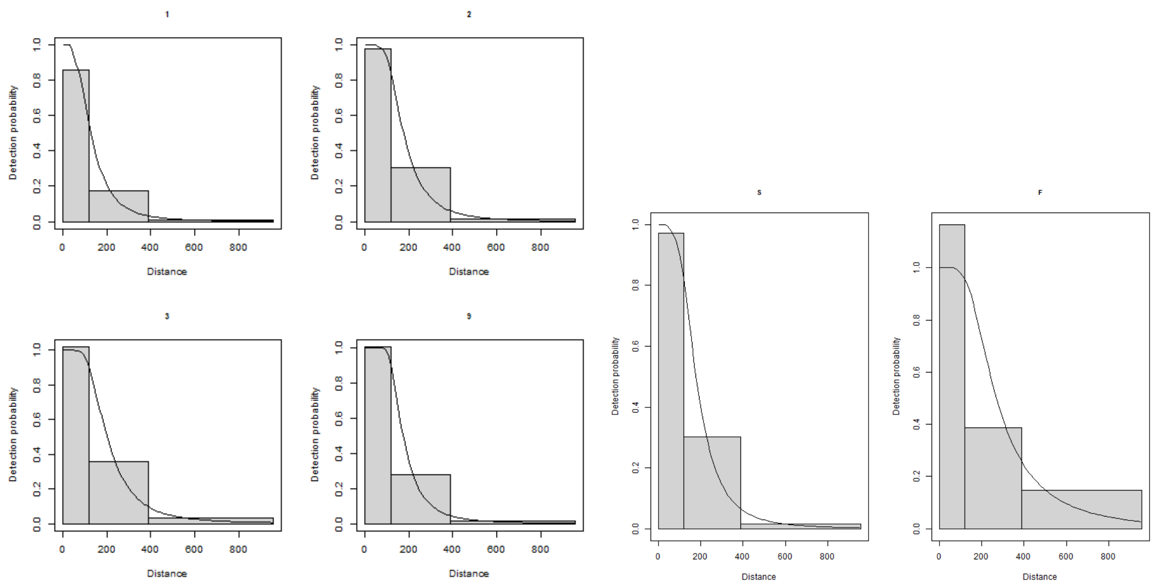

Figure 83: Figure showing the estimated detection function for each of the glare levels (left) and behaviours (right). The histograms are the distances of the observed sightings.

The dataset for the spatial analysis comprised 26,656 segments, 2.3 % of which were segments containing diver sightings. Table shows the breakdown of survey effort within each of the 11 surveys and Figure shows the distribution of the distance corrected counts. As there were no diver sightings in surveys MG07 and only one in MG06, these were not included in the spatial analysis.

Table 8: Table showing a summary of the survey effort for the diver spp. in each of the 11 surveys.

Survey	Number of Segments	
	With Sightings	Total
W08	176	4930
W13	127	4805
W16	177	4920
MG01	23	1481
MG02	19	1469
MG03	39	1368
MG04	33	1484
MG05	8	1477
MG06	1	1160
MG07	0	1313
W20	81	4886

Figure 9: Distance-corrected counts for the diver species across nine surveys. The red circles indicate the distance-corrected counts along the transect lines while the grey polygons represent land. The blue line denotes the MG study area.

Model Selection results

There was compelling evidence for spatial patterns in diver density across all nine surveys (two surveys in September and November 2019 had too few observations to conduct this analysis, and are therefore omitted here), with variable complexity. Specifically, between two and ten degrees of freedom were selected for the spatial terms across these survey-specific models (Table). A water depth relationship was not selected in any of the models suggesting there was no compelling signal for a depth-based term for any survey.

All models estimated a dispersion parameter larger than one, indicating an over-dispersed approach was justified in these models (Table).

Table 9: Model selection results for the nine surveys. "N/S" indicates the term was not selected as part of the 10-fold cross validation procedure and df=degrees of freedom for that selected relationship.

Survey	Depth	s(xpos, y.pos)	Dispersion parameter estimate
W08	N/S	$p < 0.0001$ (df=10)	8.4
W13	N/S	$p < 0.0001$ (df=8)	11.7
W16	N/S	$p < 0.0001$ (df=4)	10.8
MG01	N/S	$p < 0.0001$ (df=8)	9.2
MG02	N/S	$p < 0.0001$ (df=8)	4.0
MG03	N/S	$p < 0.0001$ (df=5)	7.8
MG04	N/S	$p < 0.0001$ (df=8)	6.3
MG05	N/S	$p < 0.0001$ (df=2)	4.7
W20	N/S	$p < 0.0001$ (df=7)	6.9

The estimated abundances within the Middelgrund Study Area and for each survey are given in Table . Survey MG03 had the largest estimated abundance but also the largest uncertainty associated with this estimate (in line with the estimated mean-variance relationship). Of the W surveys, W13 had the largest estimated abundance but its confidence interval overlapped substantially with the other W surveys, indicating that the underlying abundance in this survey may not genuinely differ with other W labelled surveys.

Table 10: Table of estimated counts of divers for the Middelgrund Study Area and for each survey. The 95 % CI are percentile-based confidence intervals from the 250 bootstraps generated which incorporate the uncertainty from both the detection function estimation and the subsequent spatial analyses.

Survey	Estimated Count	95 % CI
W08	797.1	(415.4, 1807.1)
W13	1377.8	(774.0, 2793.6)
W16	1161.4	(631.5, 2133.0)
MG01	763.8	(380.5, 1999.5)
MG02	440.2	(195.6, 1190.6)
MG03	2098.6	(984.5, 5054.9)
MG04	691.7	(342.6, 1600.1)
MG05	126.4	(53.4, 405.5)
W20	711.9	(379.1, 1410.1)

For further details on model selection, please see refer to MacKenzie & Scott-Hayward (2021).

Spatial Results

When a common scale was chosen to display the model predictions across all nine surveys, the surfaces were largely dominated by survey MG03 which has a relatively high (but relatively low in absolute terms) prediction in the extrapolated area to the west of the survey area (Figure). Notably, this area was not surveyed in MG03 and thus, the predictions in this area are speculative at best.

When all surveys were displayed separately, clearer patterns were evident indicating that diver density was somewhat mobile across surveys. Notably, there was a consistently high diver density in the southern edge of the survey area near the coast in some surveys (W13,Figure ; W16, Figure ; W20, Figure) while these relatively high numbers were shifted to the southern western edge in others (MG02, Figure ; MG04, Figure). There was also evidence of higher numbers in the central or northern part of the survey area in surveys W08 (Figure), W13 (Figure) and W16 (Figure).

There were relatively low numbers of divers around the existing windfarm footprint in the W-labelled surveys and also relatively low number of divers estimated to inside the proposed Hesselø OWF footprint, with the exception of MG01 where there are some slightly elevated estimated counts in the lower section of the proposed footprint. Please note that these areas (represented as polygons on the figures) did not form part of the analysis but were merely overlaid after analysis for reference.

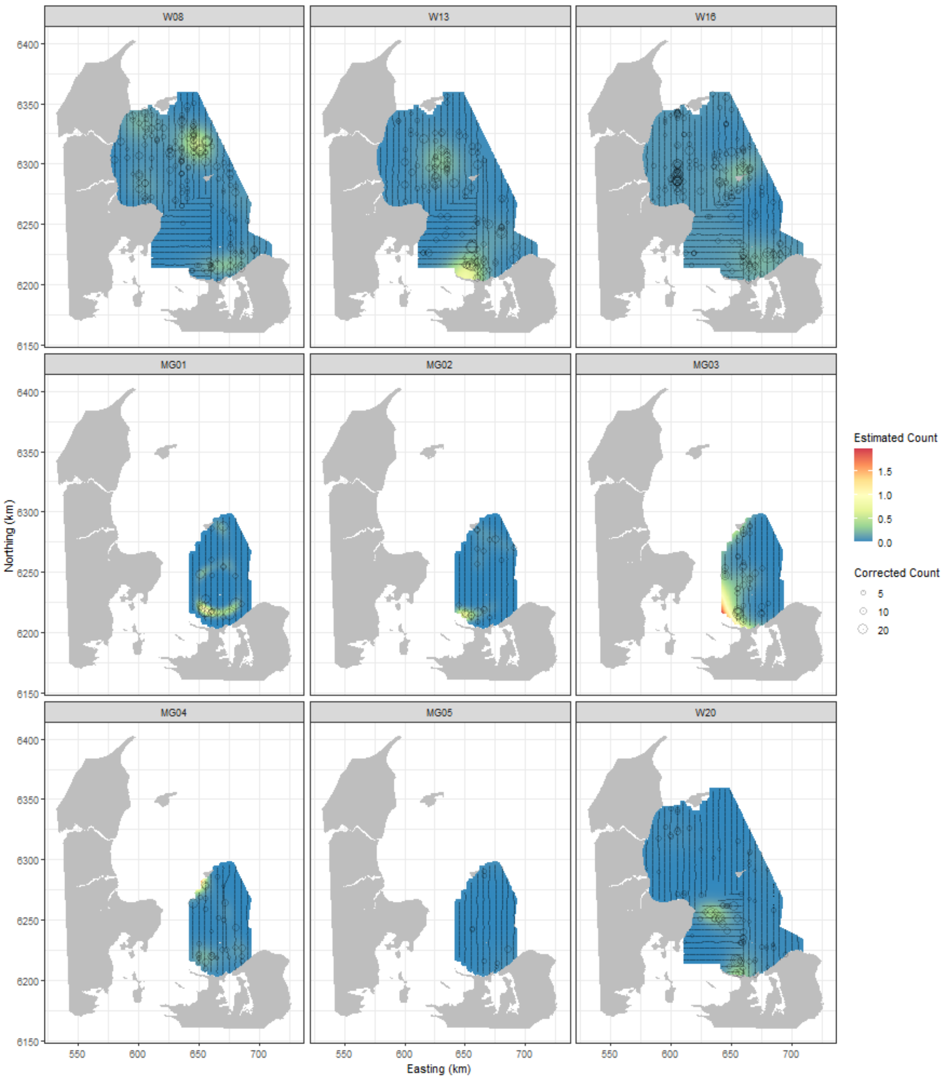

Figure 10: Figure showing the average Diver count across the study site for each of the nine surveys. The counts are per 500x500m grid cell. The open circles show the observed, distance corrected count while the coloured graphics represent the predicted values in each location.

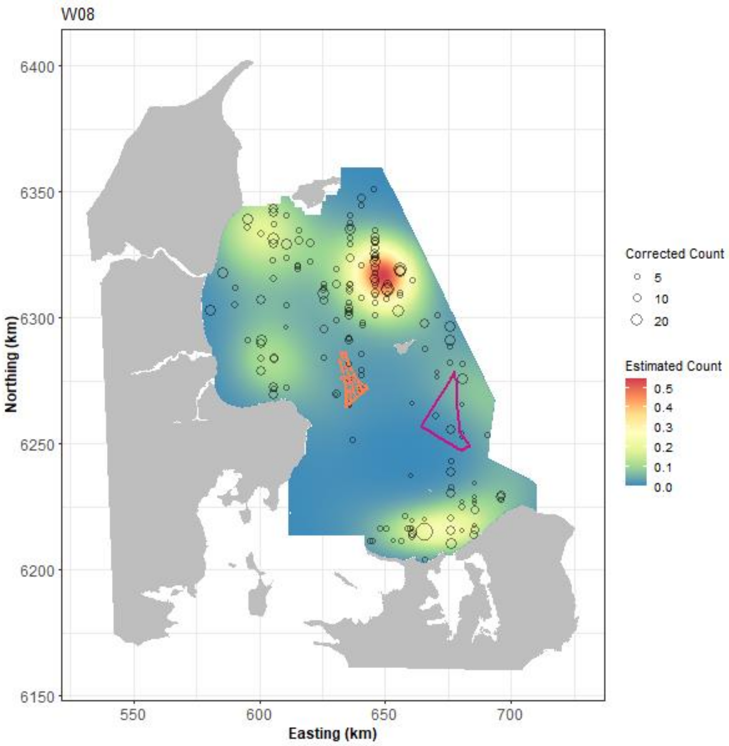

Figure 11: Figure showing the average diver count across the study site for the W08 survey. The counts are per 500x500m grid cell. The open circles show the observed, distance corrected count while the coloured graphics represent the predicted values in each location.

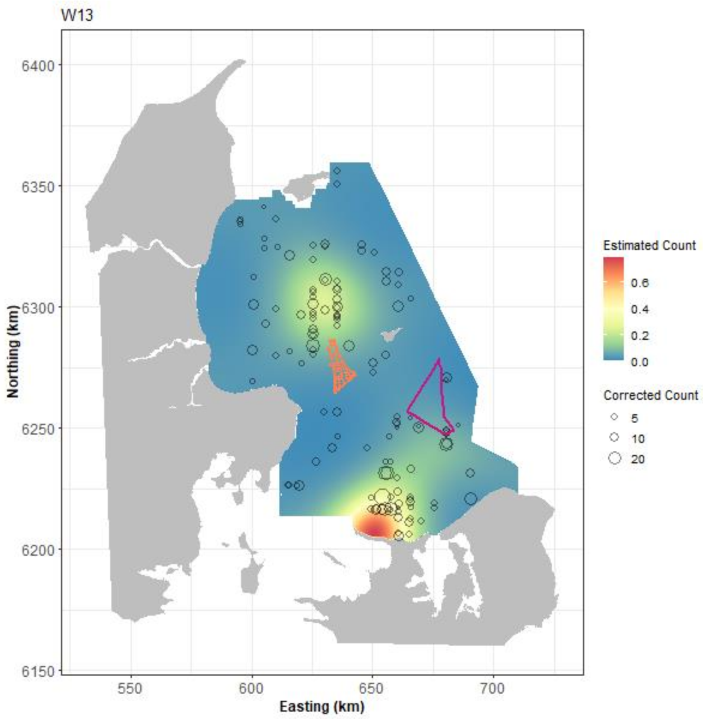

Figure 12: Figure showing the average diver count across the study site for the W13 survey. The counts are per 500x500m grid cell. The open circles show the observed, distance corrected count while the coloured graphics represent the predicted values in each location.

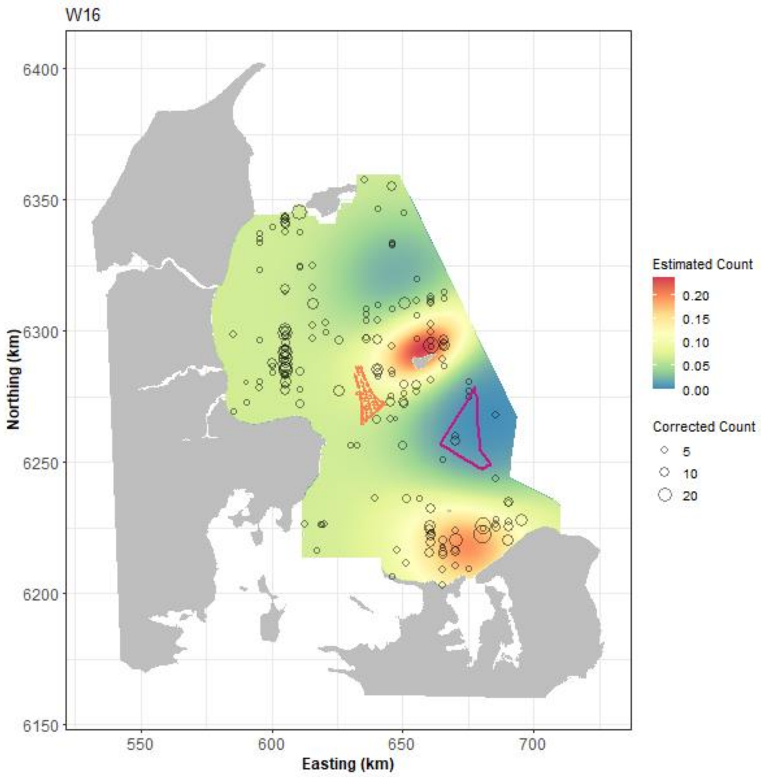

Figure 13: Figure showing the average diver count across the study site for the W16 survey. The counts are per 500x500m grid cell. The open circles show the observed, distance corrected count while the coloured graphics represent the predicted values in each location.

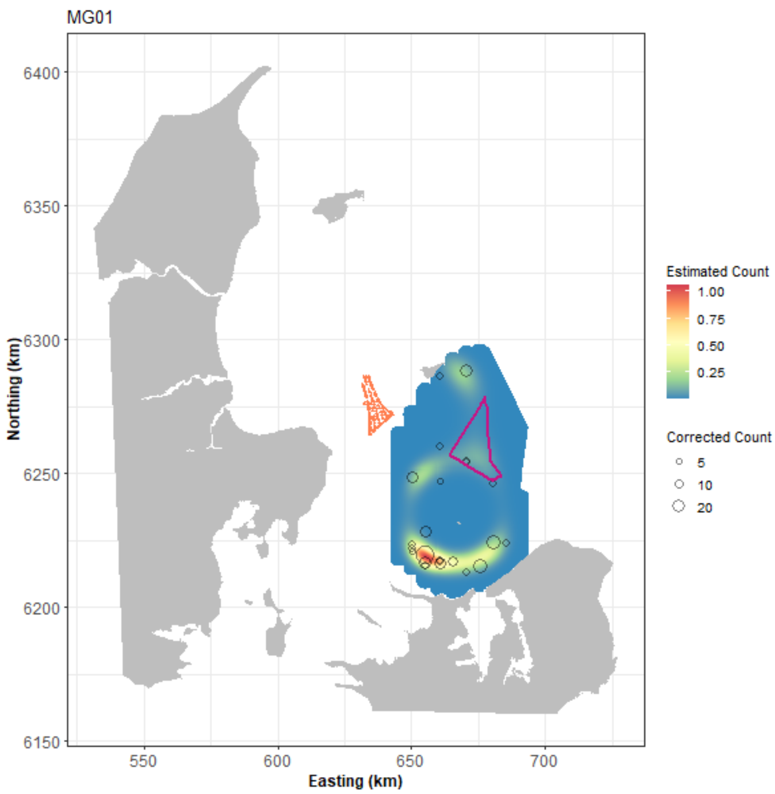

Figure 14: Figure showing the average diver count across the study site for the MG01 survey. The counts are per 500x500m grid cell. The open circles show the observed, distance corrected count while the coloured graphics represent the predicted values in each location.

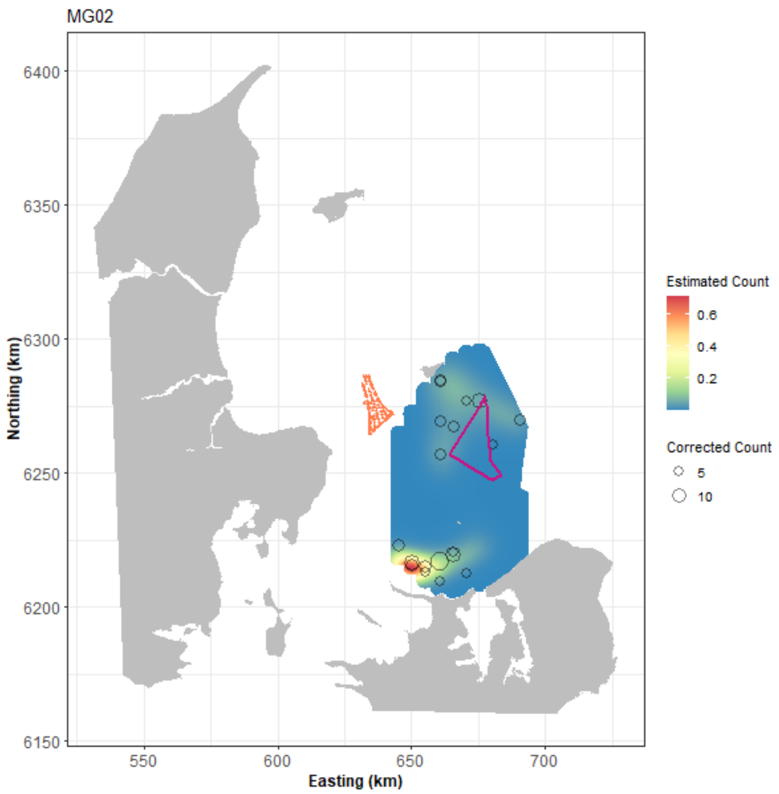

Figure 15: Figure showing the average diver count across the study site for the MG02 survey. The counts are per 500x500m grid cell. The open circles show the observed, distance corrected count while the coloured graphics represent the predicted values in each location.

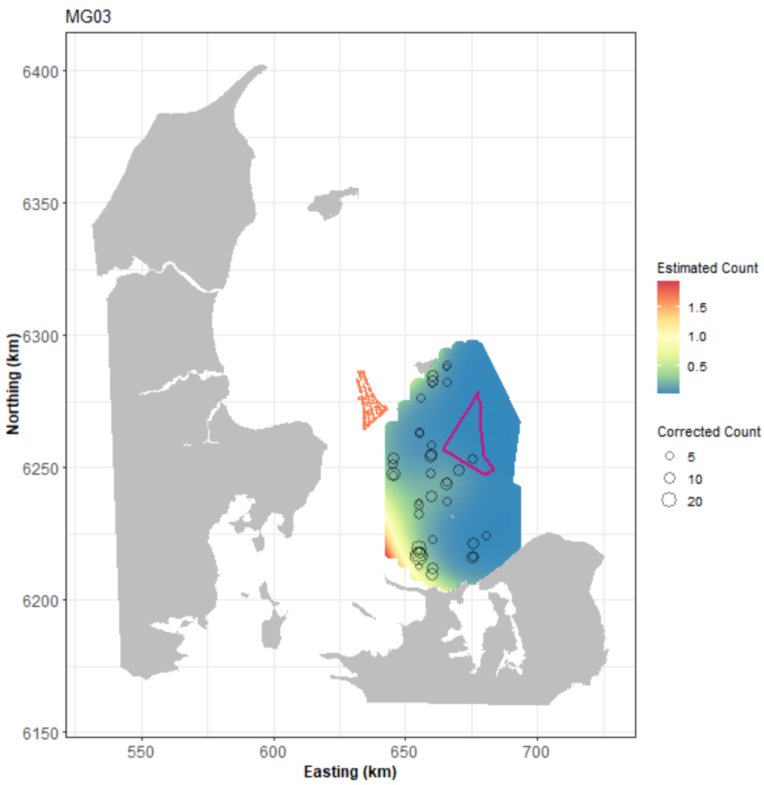

Figure 16: Figure showing the average diver count across the study site for the MG03 survey. The counts are per 500x500m grid cell. The open circles show the observed, distance corrected count while the coloured graphics represent the predicted values in each location.

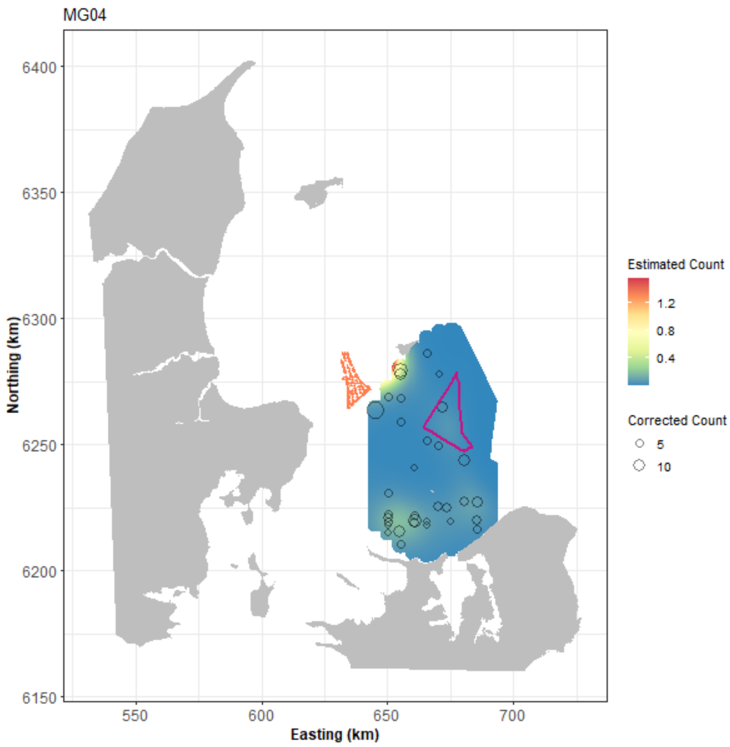

Figure 17: Figure showing the average diver count across the study site for the MG04 survey. The counts are per 500x500m grid cell. The open circles show the observed, distance corrected count while the coloured graphics represent the predicted values in each location.

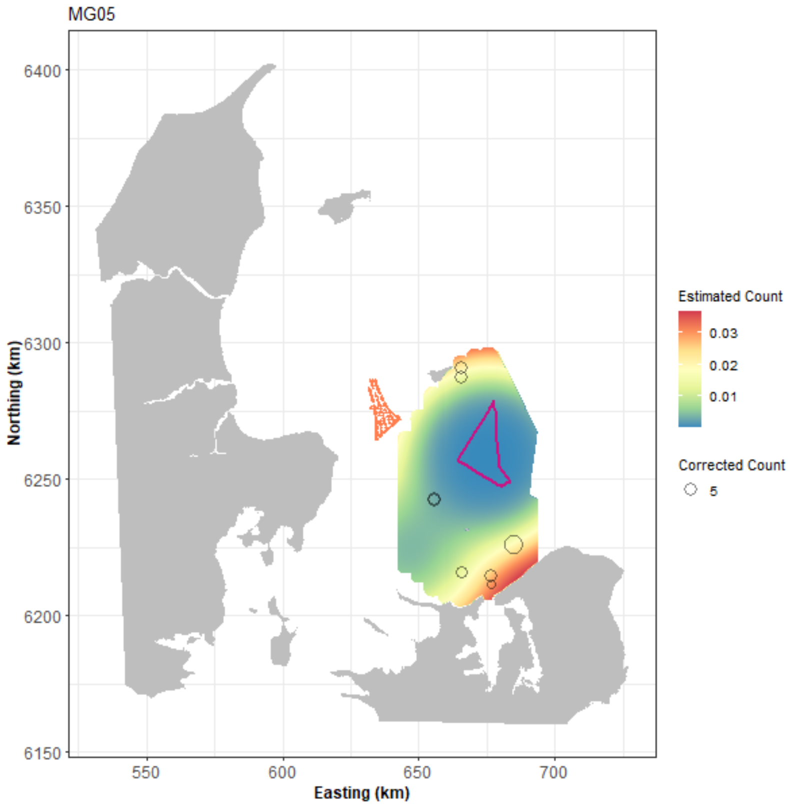

Figure 18: Figure showing the average diver count across the study site for the MG05 survey. The counts are per 500x500m grid cell. The open circles show the observed, distance corrected count while the coloured graphics represent the predicted values in each location.

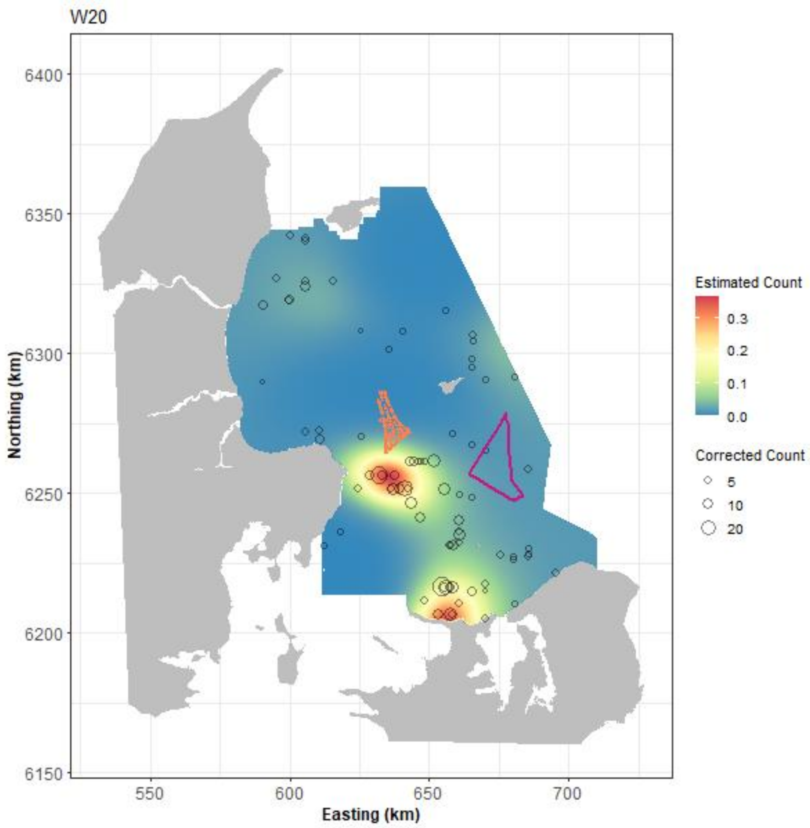

Figure 19: Figure showing the average diver count across the study site for the W20 survey. The counts are per 500x500m grid cell. The open circles show the observed, distance corrected count while the coloured graphics represent the predicted values in each location.

Uncertainty in the spatial predictions

There were no concerns regarding unreasonable uncertainties about the estimated spatial patterns across these surveys. The highest CV scores were associated with the very smallest predictions, which is to be expected given the sensitivity to this with the CV metric (Figure & Figure).

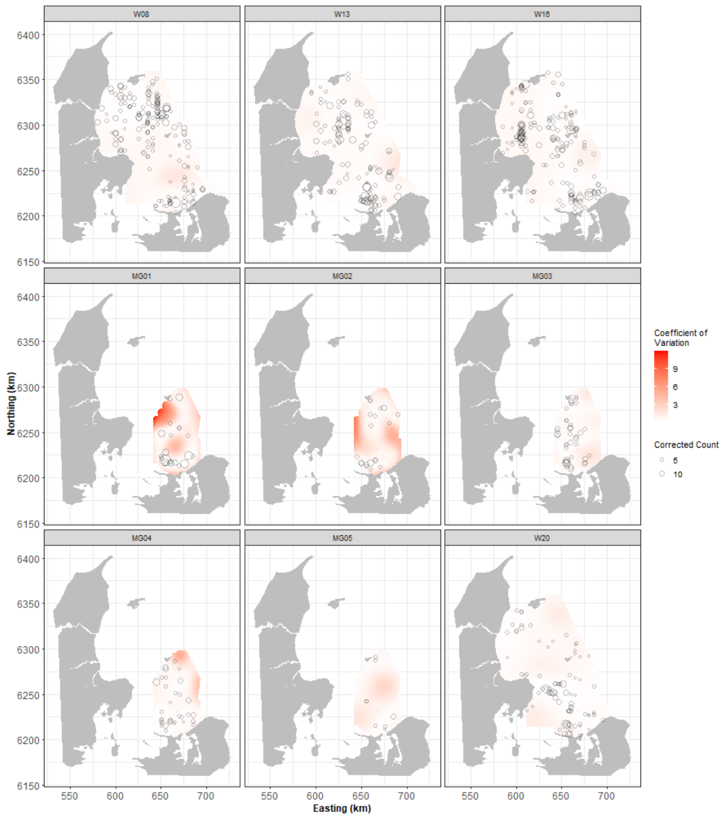

Figure 20: Figure showing the coefficient of variation (untruncated) across the study region for each of the surveys. The open circles show the observed, distance corrected counts.

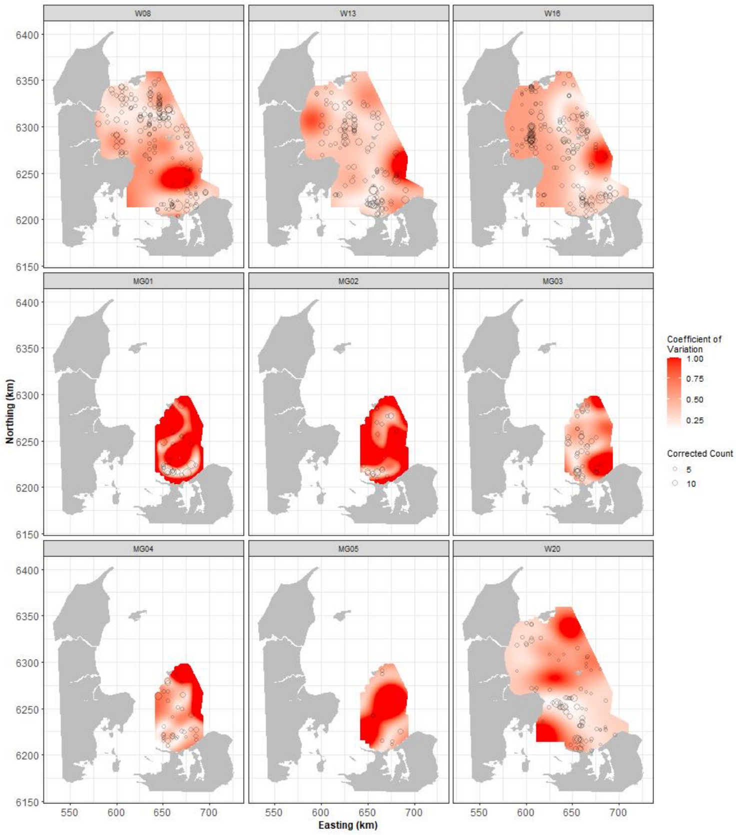

Figure 21: Figure showing the coefficient of variation across the study region for each of the surveys, capped at one. The open circles show the observed, distance corrected counts.

For further information on uncertainty in the spatial predictions, please refer to MacKenzie & Scott-Hayward (2021).

Areas of Persistence

There is evidence of relatively high persistence in the southwestern region of the (reduced survey) area, and very low persistence towards the centre and north eastern region of the survey area (Figure). There is, for the most part, low persistence inside the proposed windfarm footprint but low-to-moderate persistence in the southern part of this proposed footprint – largely based on the MG01 survey. These patterns collectively align well with the survey results which show these patterns in these areas (Figure - Figure).

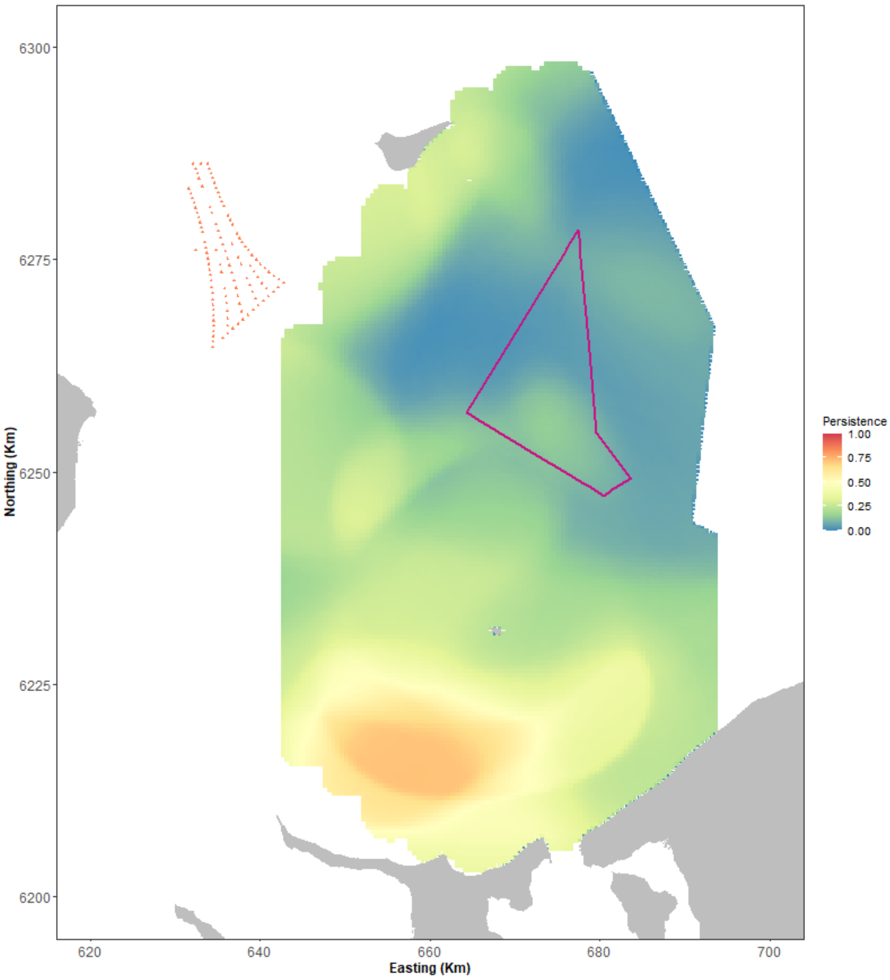

Figure 22: Persistence scores for red-throated/black-throated divers across the MG survey area (reduced survey area with consistent overlap).

Gannet *Morus bassanus*

Gannets have increased markedly in the study area over the period from 2008 until 2020.

The numbers fluctuated markedly between surveys, and of the 11 surveys in this data set, three surveys have higher numbers, namely the Middelgrund surveys of 1 April 2019 (312) and 17 April 2019 (170) as well as the Kattegat winter survey of 2020 (51, Table 5, Figure 23).

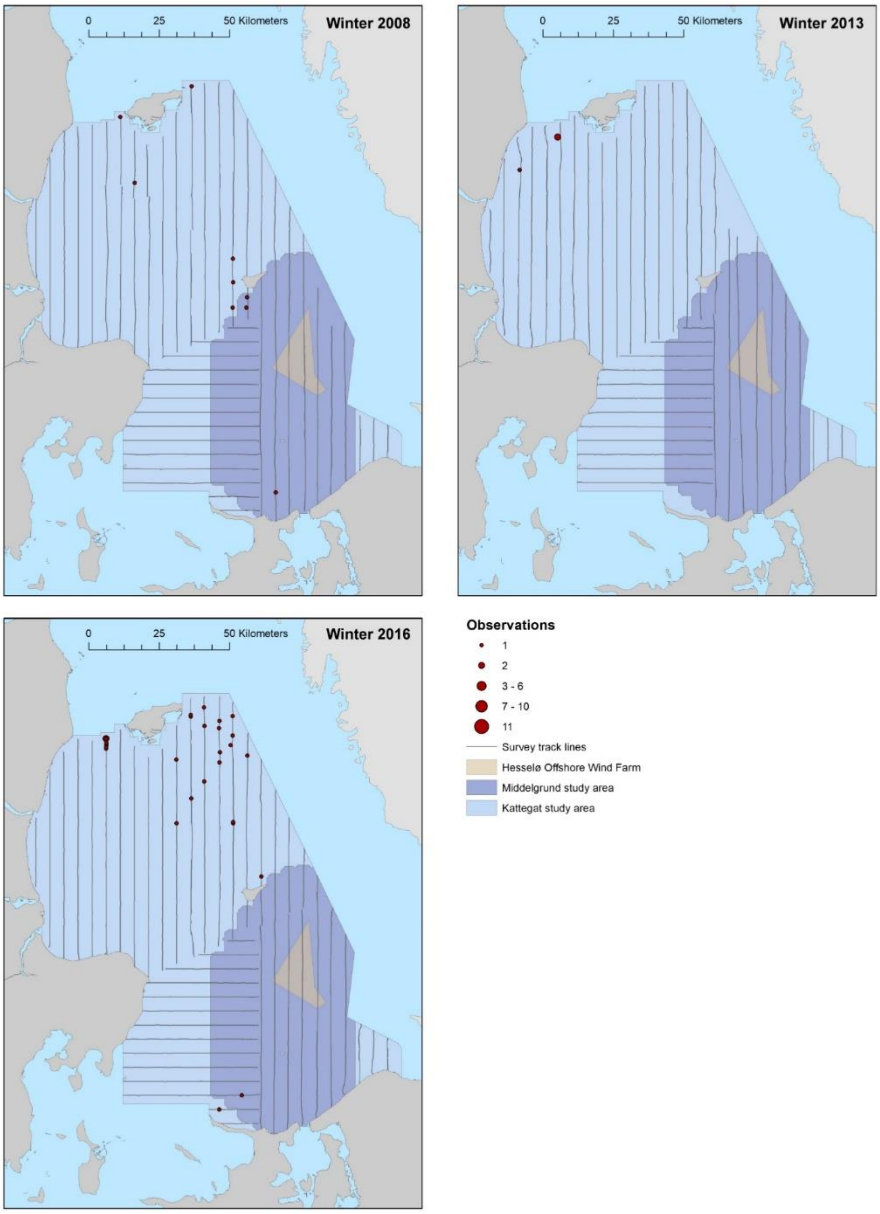

Figure 23. The spatial distribution of observed Gannets from 11 surveys of birds in the study area between winter 2008 and winter 2020. Survey timing for the individual surveys are given in upper right corner of each map. The survey track lines covered for each survey is given.

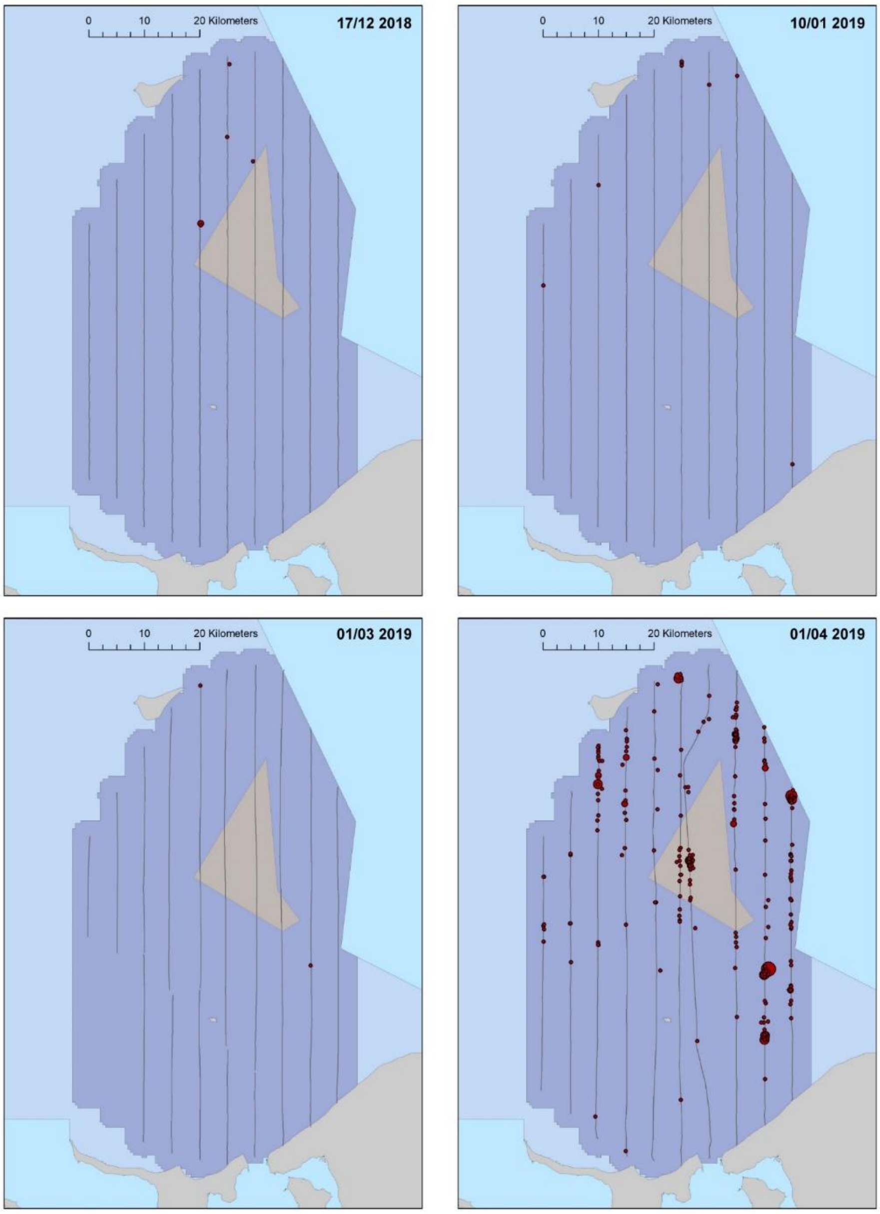

Figure 23. Gannet, continued

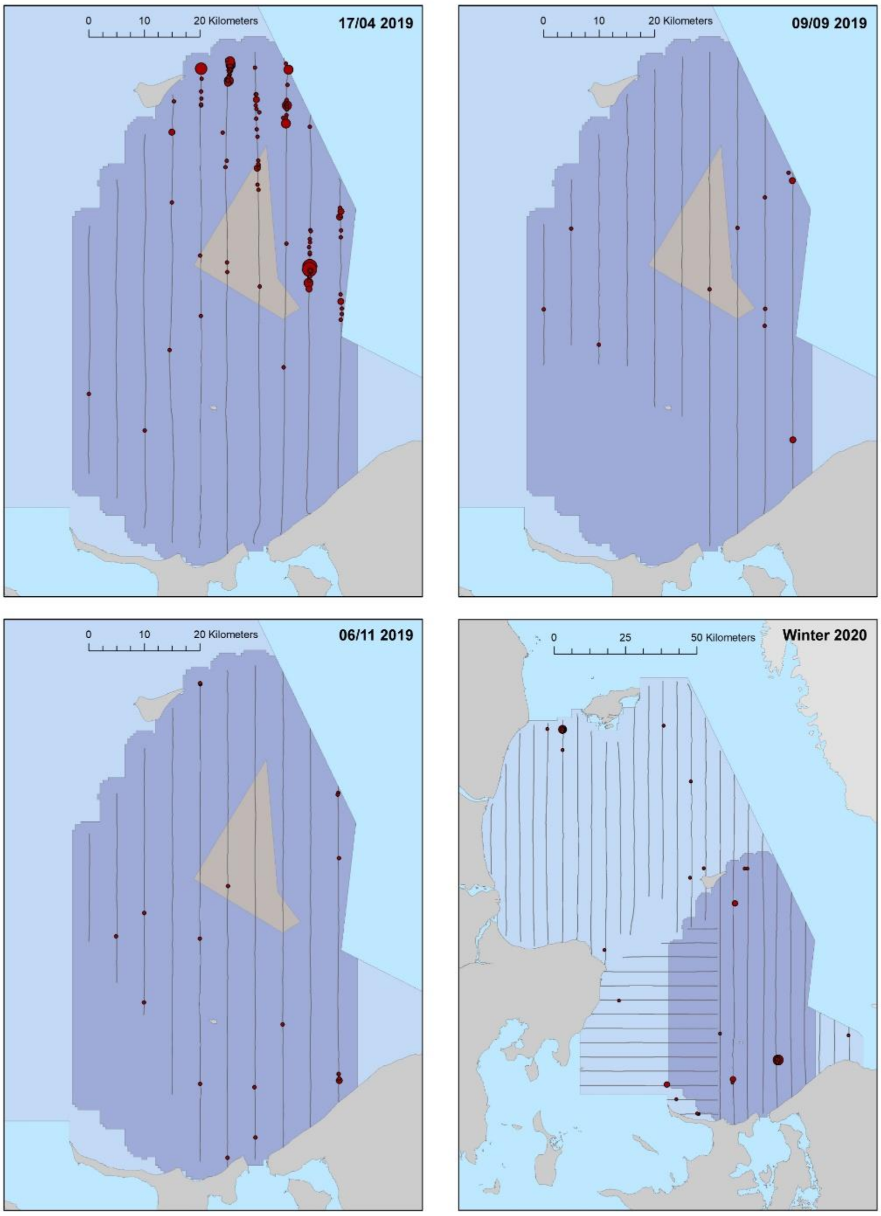

Figure 23. Gannet, continued

Gannets were most abundant in the Kattegat study area in April, while much lower relative density was found during the rest of the year (Figure 24).

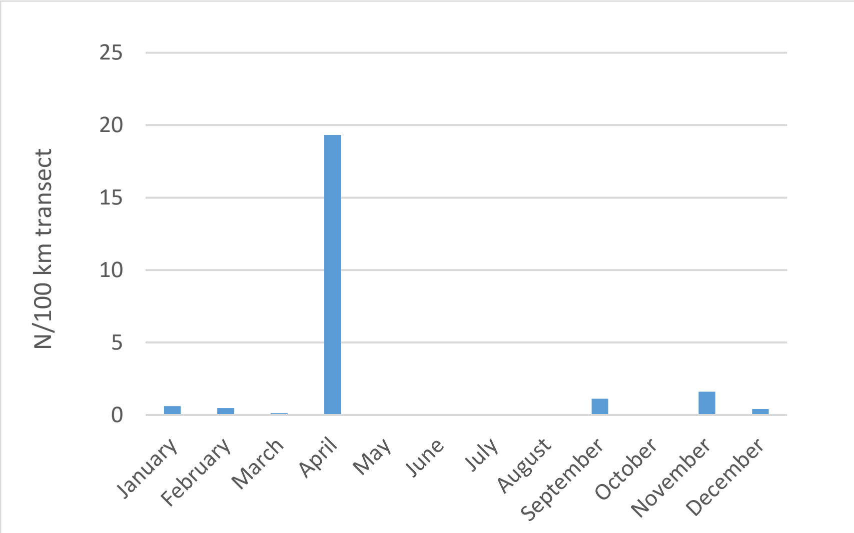

Figure 24. The annual variation in the relative density of Gannets in the Kattegat Study Area from 11 surveys included in this report.

Within the study area Gannets were mainly observed in the deeper, eastern parts of the area. In the Middelgrund study area the Gannets were mainly found in the deep north-eastern parts (Figure 23). Of the 626 observed Gannets in the general study area 563 (90 %) were observed in the Middelgrund Study Area, and 389 were observed within a distance of 15 km from the proposed wind farm site.

Most Gannets (17 %) were recorded in the depth interval 28-34 meters, and more than 70 % were recorded on water depths between 20 and 32 meters (Figure 25).

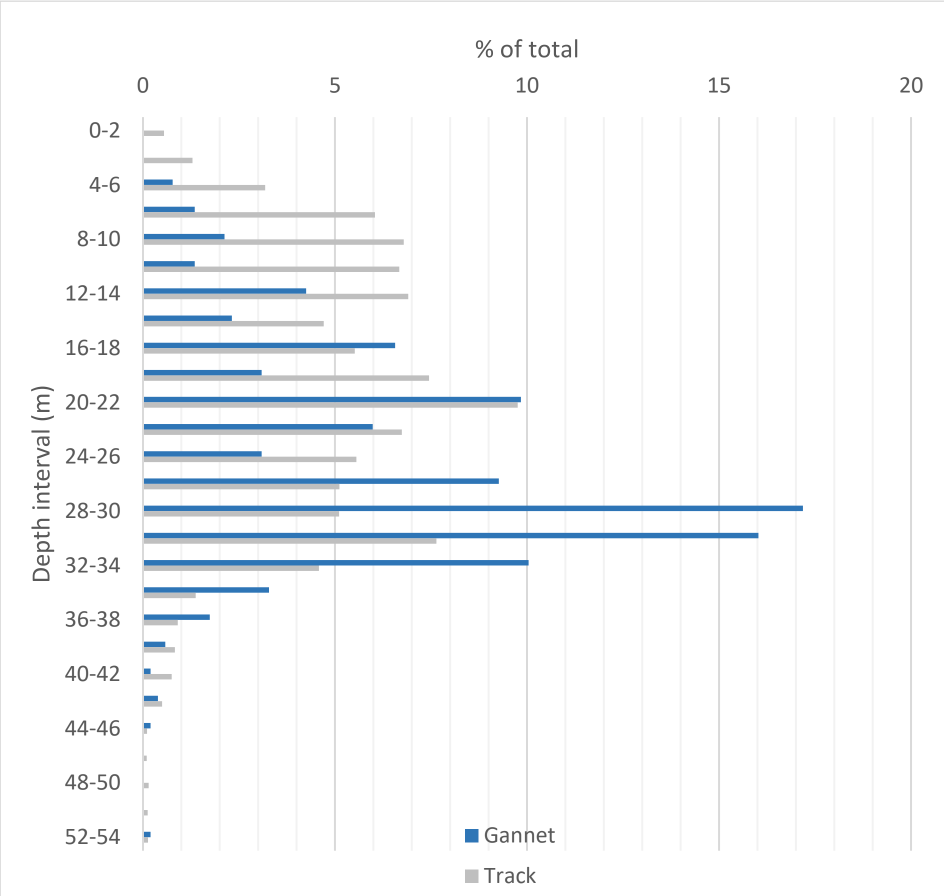

Figure 25. The depth frequency distribution of Gannet in the Kattegat Study Area in 2 m depth intervals and expressed as % of total numbers observed. The depth frequency distribution of the covered survey track lines is given for comparison.

Distance Analysis

The average probability of sighting gannets was estimated to be 0.42 (CV=0.052). This probability was estimated using a hazard rate detection function that varied with observer, glare and behaviour (Figure and Figure).

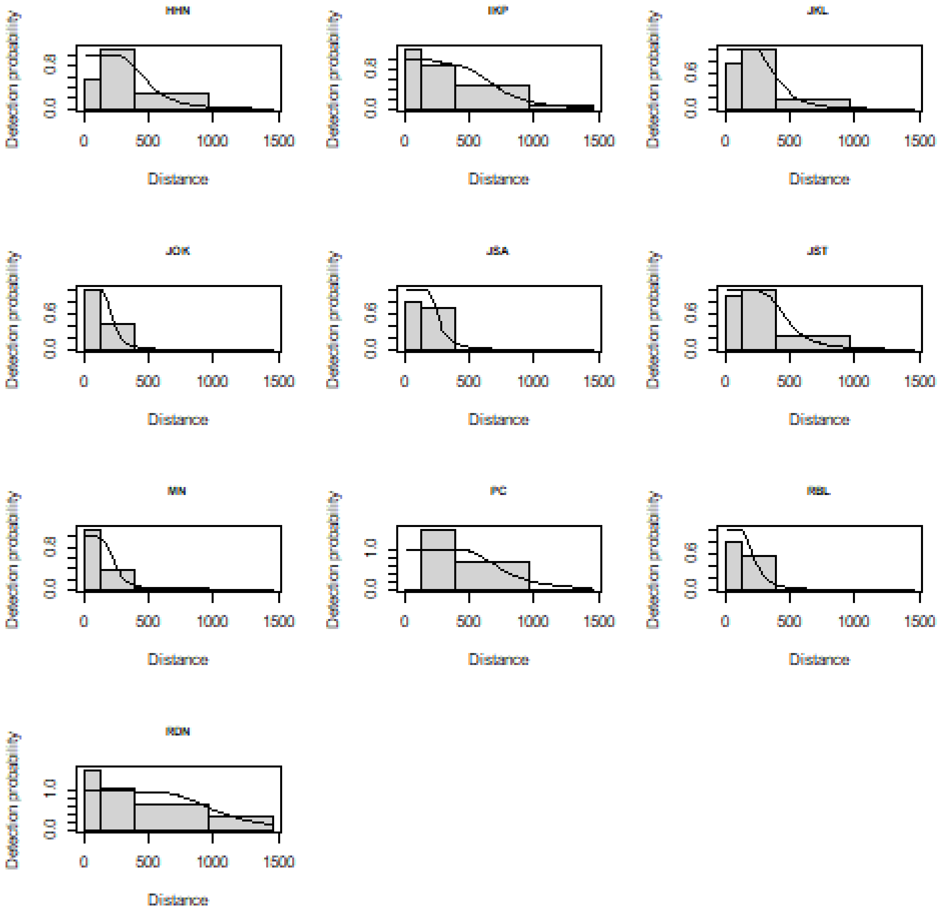

Figure 26: Figure showing the estimated detection function for each of the observers. The histograms are the distances of the observed sightings.

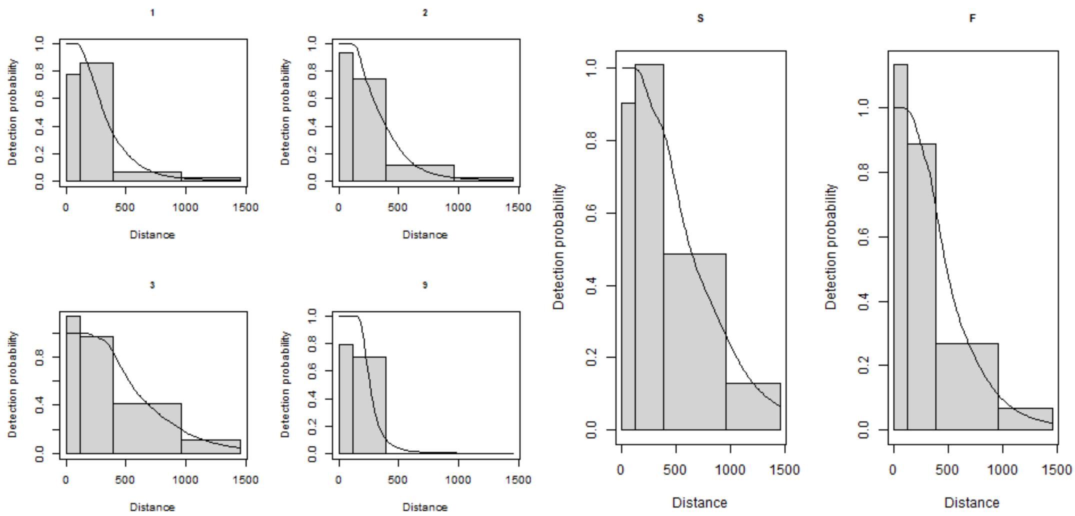

Figure 27: Figure showing the estimated detection function for each of the levels of glare (left) and behaviour (right). The histograms are the distances of the observed sightings.

The dataset for the spatial analysis comprised 29,293 segments, however just 1.2 % of these segments contained Gannet sightings. Table shows the breakdown of survey effort within each of the 11 surveys and Figure shows the distribution of the distance corrected counts.

Table 11: Table showing a summary of the survey effort for the Gannet species in each of the 11 surveys.

Survey	Number of Segments	
	With Sightings	Total
W08	9	4930
W13	2	4805
W16	26	4920
MG01	4	1481
MG02	7	1469
MG03	2	1368
MG04	169	1484
MG05	79	1477
MG06	11	1160
MG07	16	1313
W20	23	4886

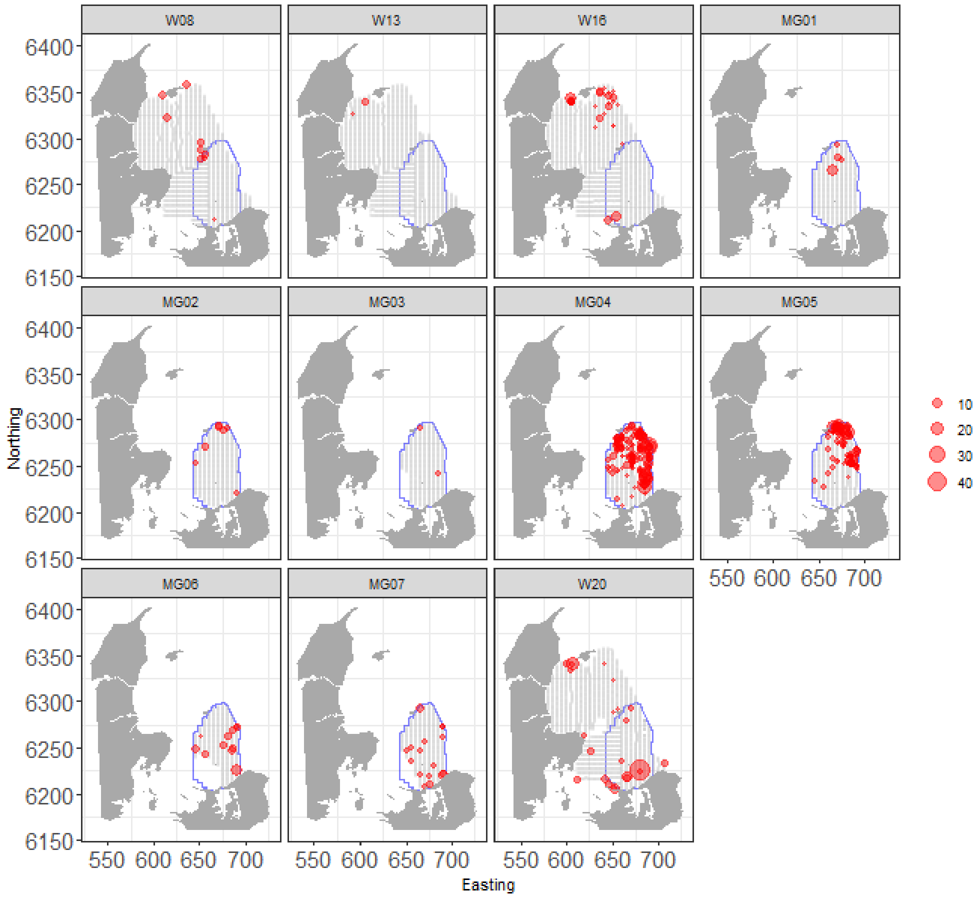

Figure 28: Distance-corrected counts for the Gannet species across the 11 surveys. The red circles indicate the distance-corrected counts along the transect lines while the grey polygons represent land. The blue line denotes the MG study area.

Model Selection results

There was compelling evidence for spatial patterns in Gannet density across nine of the 11 surveys (of variable complexity) and no compelling evidence for a water depth relationship in any survey. While in 9 surveys, localized spatial patterns were justified (using objective fit criteria) an intercept only model was selected for two of the 11 surveys (W13 and MG03; Table). These models return just one predicted value across the survey area.

Due to the very low numbers of non-zero counts in these surveys, the spatial surfaces selected were very low dimensional (with between two and five degrees of freedom) and all models estimated a dispersion parameter larger than one, indicating an over-dispersed approach was justified in these models (Table).

Table 12: Model selection results for the 11 surveys. "N/S" indicates the term was not selected as part of the 10-fold cross validation procedure and df=degrees of freedom for that relationship.

Survey	Depth	s(xpos, y.pos)	Dispersion parameter estimate
W08	N/S	$p < 0.0001$ (df=5)	3.8
W13	N/S	N/S	5.7
W16	N/S	$p = 0.0003$ (df=2)	2.1
MG01	N/S	$p = 0.1759$ (df=2)	2.5
MG02	N/S	$p < 0.0001$ (df=3)	2.9
MG03	N/S	N/S	2.7
MG04	N/S	$p < 0.0001$ (df=5)	6.5
MG05	N/S	$p < 0.0001$ (df=5)	5.8
MG06	N/S	$p < 0.0001$ (df=2)	5.4
MG07	N/S	$p < 0.0001$ (df=3)	4.1
W20	N/S	$p < 0.0001$ (df=3)	9.7

The estimated abundances for the Middelgrund Stury Area and for each survey are given in Table . Survey MG03 reported the lowest estimated abundance but the uncertainty associated with all of the estimates for the MG surveys meant no conclusions could be drawn about any genuine differences between them. Of the W surveys, W20 had the largest estimated abundance (significantly higher than numbers estimated in W13), but the remaining W surveys each had sufficient uncertainty to render them indistinct from each other, or W20.

Table 13: Table of estimated counts the Middelgrund Study Area and for each survey. The 95 % CI are percentile-based confidence intervals from the 250 bootstraps generated which incorporate the uncertainty from both the detection function estimation and the subsequent spatial analyses.

Survey	Estimated Count	95 % CI
W08	13.1	(3, 63.8)
W13	3.5	(0.5, 21.8)
W16	9.2	(2.6, 60.1)
MG01	41.3	(16.7, 49209)
MG02	70.5	(22.8, 756)
MG03	11.7	(3.6, 48.7)
MG04	1120	(680, 2120)
MG05	722.5	(399, 1557)
MG06	162.8	(62.8, 423)
MG07	195	(93.2, 478)
W20	119.9	(57.1, 282)

For further details on model selection, please see refer to MacKenzie & Scott-Hayward (2021).

Spatial Results

When a common scale was chosen to display the model predictions across all 11 surveys, the surfaces were largely dominated by surveys MG04 and MG05 (Figure) where significantly more Gannets were seen. When all surveys are plotted on potentially different scales however, clearer patterns are evident across surveys.

The spatial pattern concentrated near the island of Hesselø is evident in survey W08 (Figure), while the intercept (mean only) model is represented spatially in Figure . The Gannet distribution moved towards the (largely northern) edge of the survey area in surveys W16, MG02 and MG05 (Figure -Figure) while MG04 exhibited elevated numbers in the northern and eastern edges of the area (Figure). The relatively high values in the southern edges of the fitted surfaces for MG06 and MG07 (Figure and Figure) are to be treated with caution, since these areas were lacking in survey data in this case (Figure). The highest density area (though the overall density predictions are small) in survey W20 was also in the south (Figure).

There were only very low numbers of Gannets estimated to occur in the northwestern area of the Middelgrund Study Area, near the existing Anholt OWF in any of the surveys, but there were very small numbers of Gannets estimated to be present on the edge of the proposed wind farm site in MG01 (Figure). These were estimated to be more widespread in MG04 (though still in relatively low numbers; Figure) but otherwise there was no discernible coincidence between the proposed windfarm site and the estimated Gannet distribution.

Figure 29: Figure showing the average Gannet count across the study site for each of the 11 surveys. The counts are per 500x500m grid cell. The open circles show the observed, distance corrected count while the coloured graphics represent the predicted values in each location.

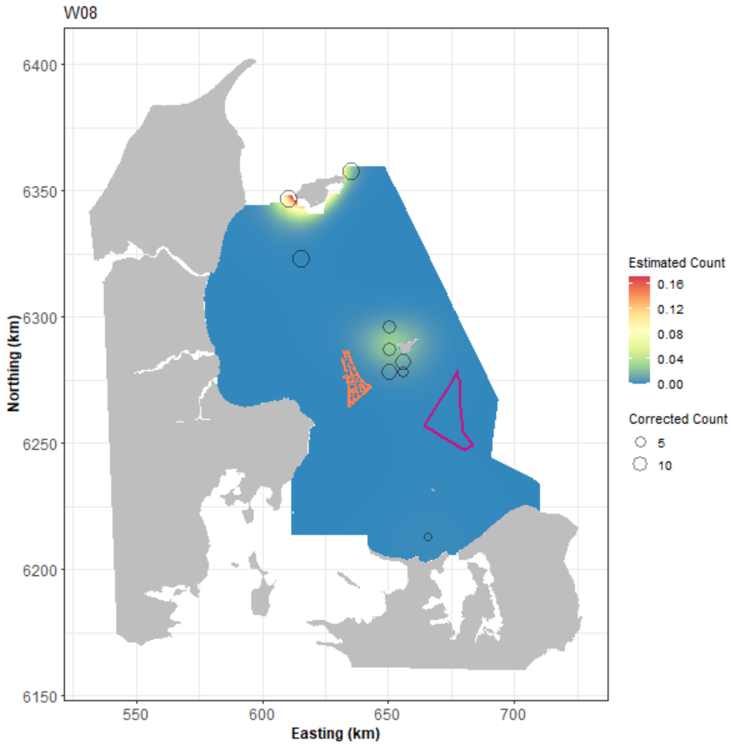

Figure 30: Figure showing the average Gannet count across the study site for the W08 survey. The counts are per 500x500m grid cell. The open circles show the observed, distance corrected count while the coloured graphics represent the predicted values in each location.

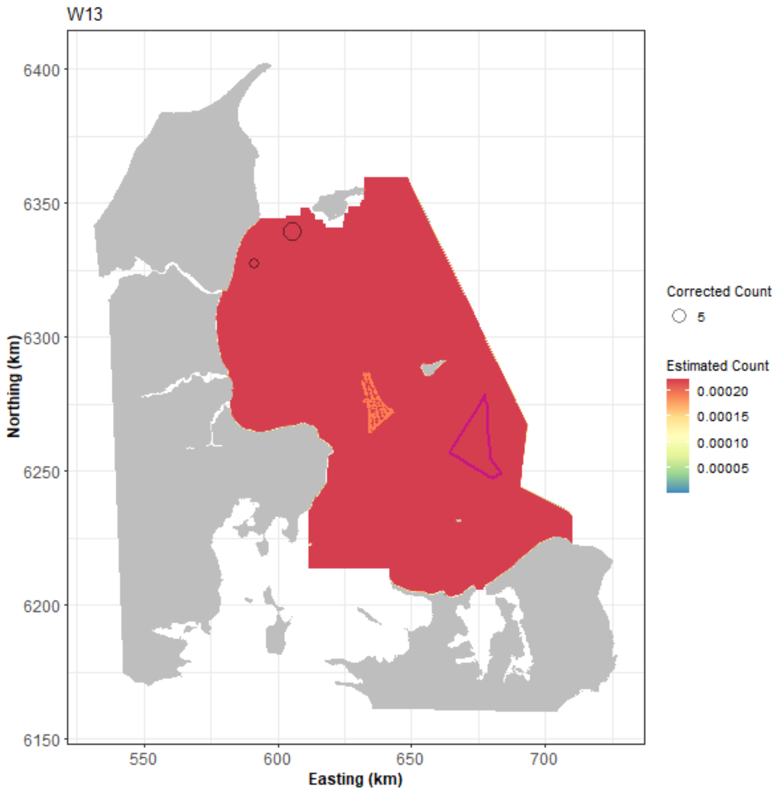

Figure 31: Figure showing the average Gannet count across the study site for the W13 survey. The counts are per 500x500m grid cell. The open circles show the observed, distance corrected count while the coloured graphics represent the predicted values in each location.

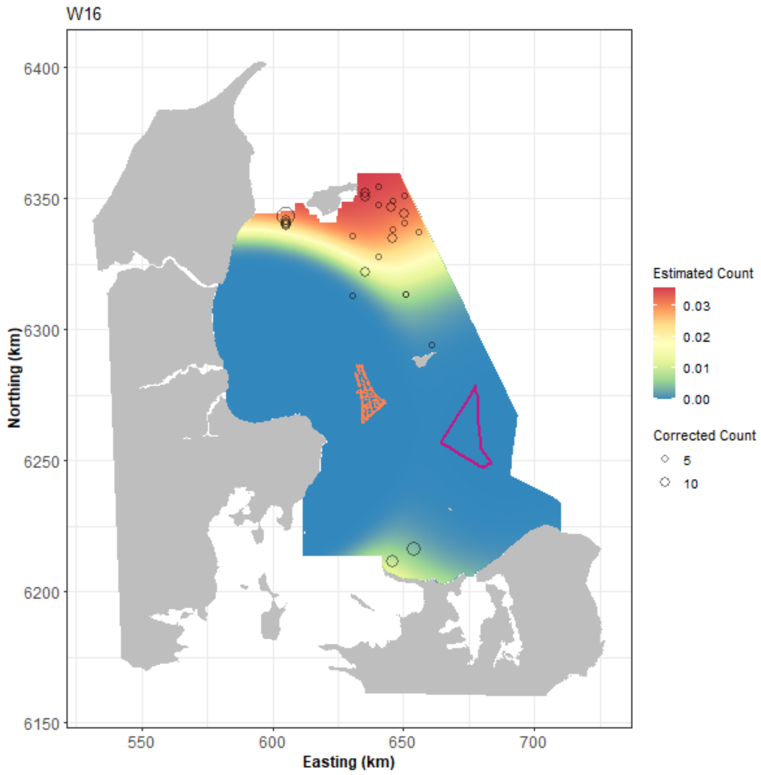

Figure 32: Figure showing the average Gannet count across the study site for the W16 survey. The counts are per 500x500m grid cell. The open circles show the observed, distance corrected count while the coloured graphics represent the predicted values in each location.

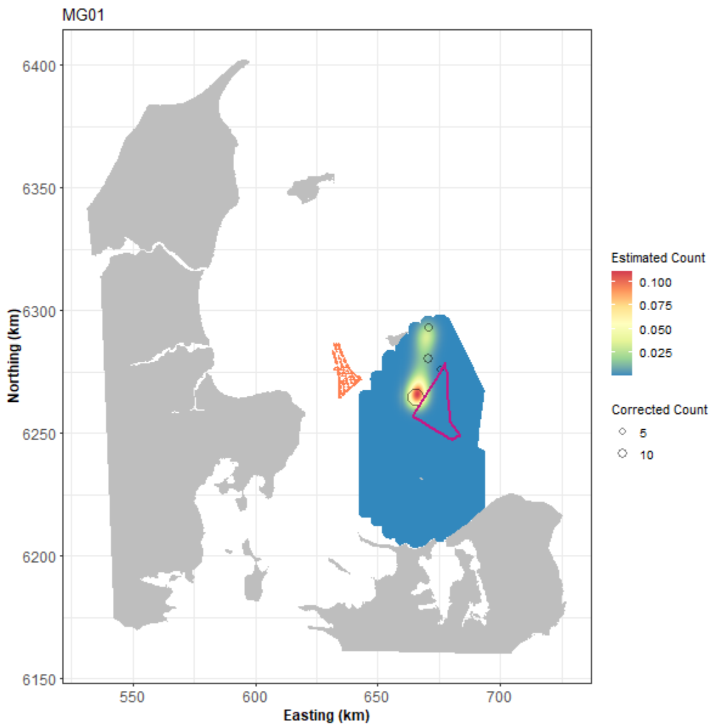

Figure 33: Figure showing the average Gannet count across the study site for the MG01 survey. The counts are per 500x500m grid cell. The open circles show the observed, distance corrected count while the coloured graphics represent the predicted values in each location.

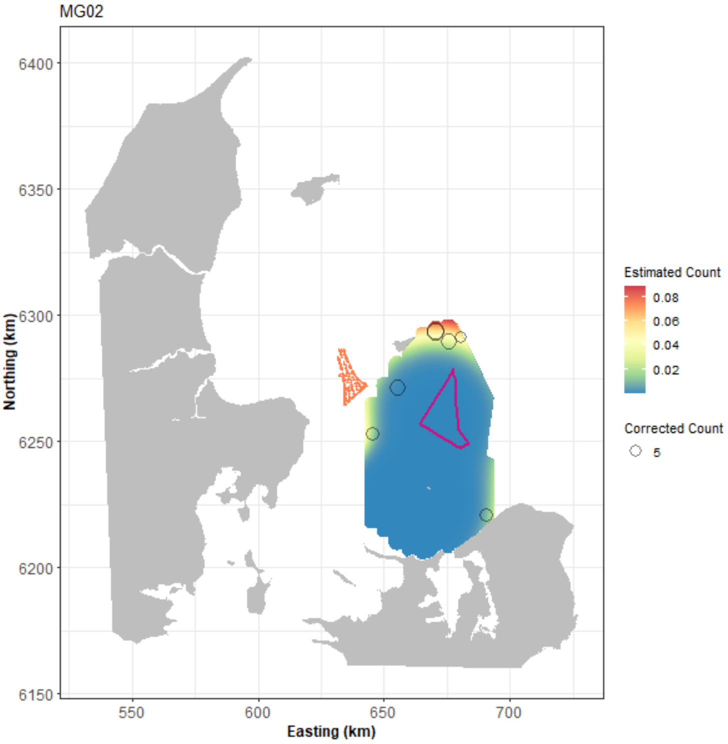

Figure 34: Figure showing the average Gannet count across the study site for the MG02 survey. The counts are per 500x500m grid cell. The open circles show the observed, distance corrected count while the coloured graphics represent the predicted values in each location.

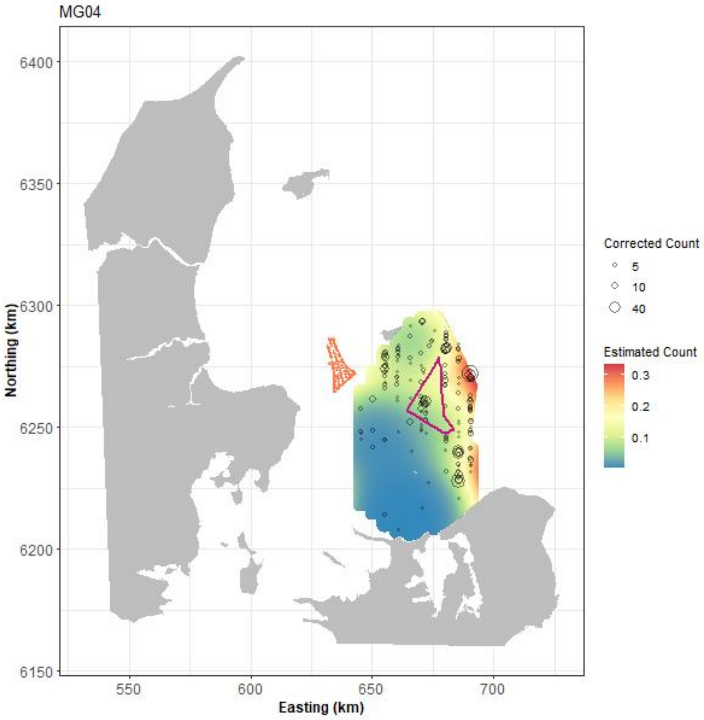

Figure 35: Figure showing the average Gannet count across the study site for the MG04 survey. The counts are per 500x500m grid cell. The open circles show the observed, distance corrected count while the coloured graphics represent the predicted values in each location.

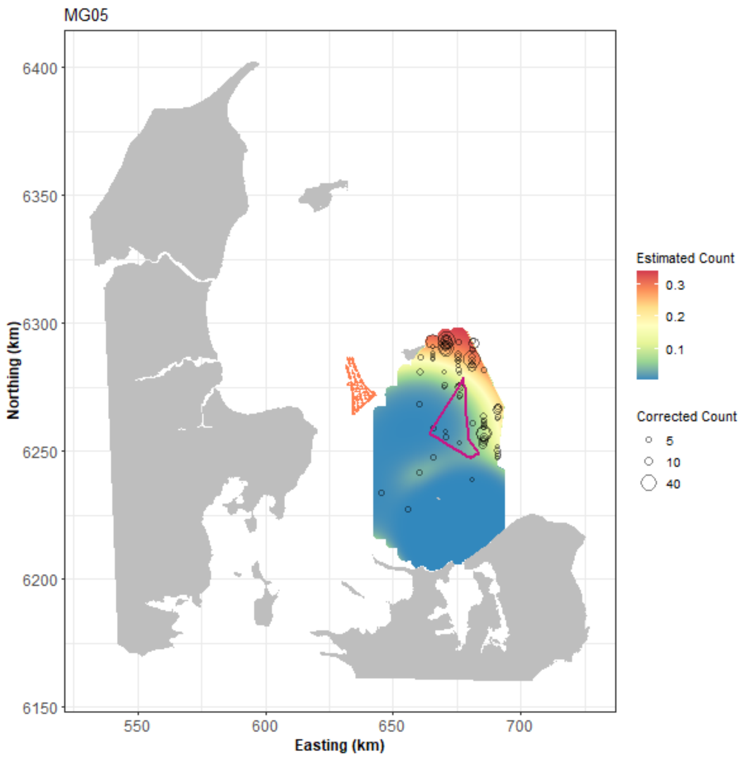

Figure 36: Figure showing the average Gannet count across the study site for the MG05 survey. The counts are per 500x500m grid cell. The open circles show the observed, distance corrected count while the coloured graphics represent the predicted values in each location.

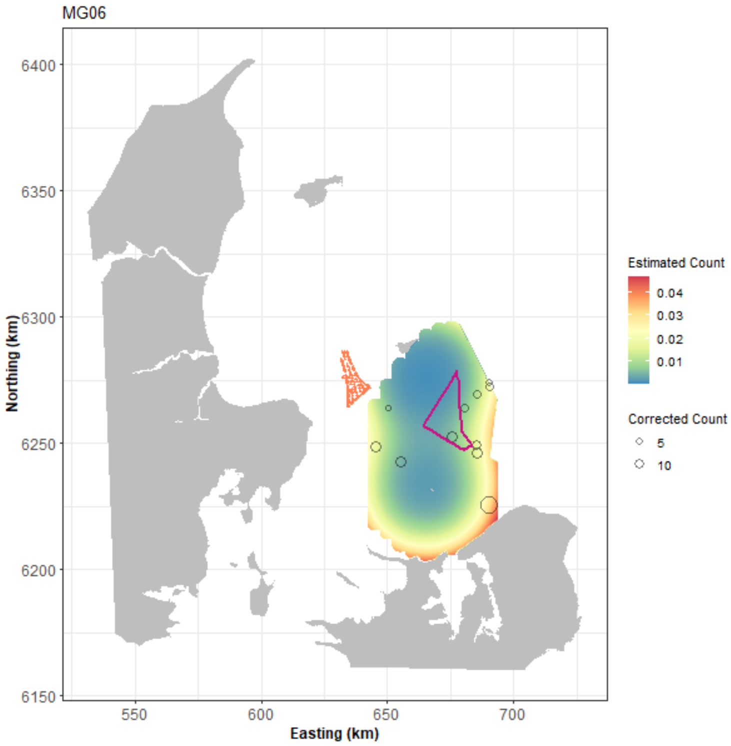

Figure 37: Figure showing the average Gannet count across the study site for the MG06 survey. The counts are per 500x500m grid cell. The open circles show the observed, distance corrected count while the coloured graphics represent the predicted values in each location.

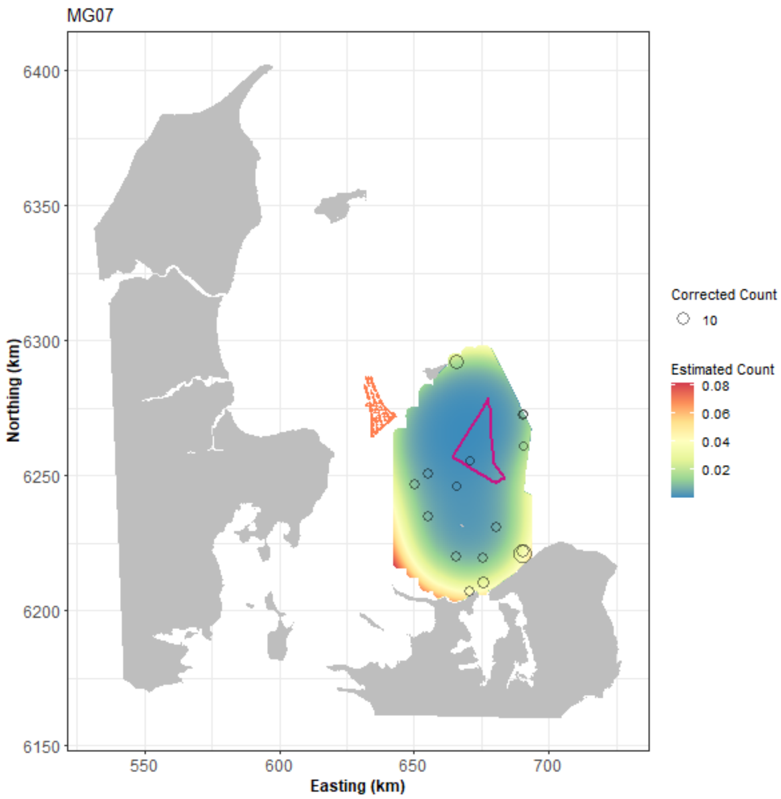

Figure 38: Figure showing the average Gannet count across the study site for the MG07 survey. The counts are per 500x500m grid cell. The open circles show the observed, distance corrected count while the coloured graphics represent the predicted values in each location.

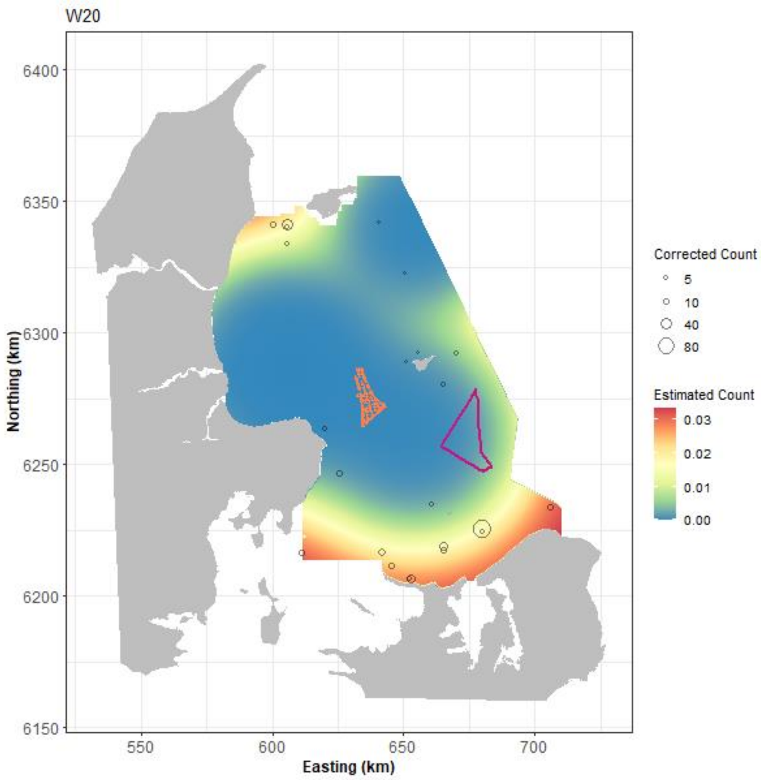

Figure 39: Figure showing the average Gannet count across the study site for the W20 survey. The counts are per 500x500m grid cell. The open circles show the observed, distance corrected count while the coloured graphics represent the predicted values in each location.

Uncertainty in the spatial predictions

The highest CV scores were associated with the very smallest predictions, however it is well-known that the CV metric is highly sensitive to any uncertainty for very small predictions and therefore results in no concerns in this case (Figure). There was no material overlap between the CV metric and the transect lines/locations with non-zero counts.

Upon closer inspection, when the CV is capped at one (Figure), no concerns were revealed and further demonstrate the relationship between large CV values when there are predictions very close to zero.

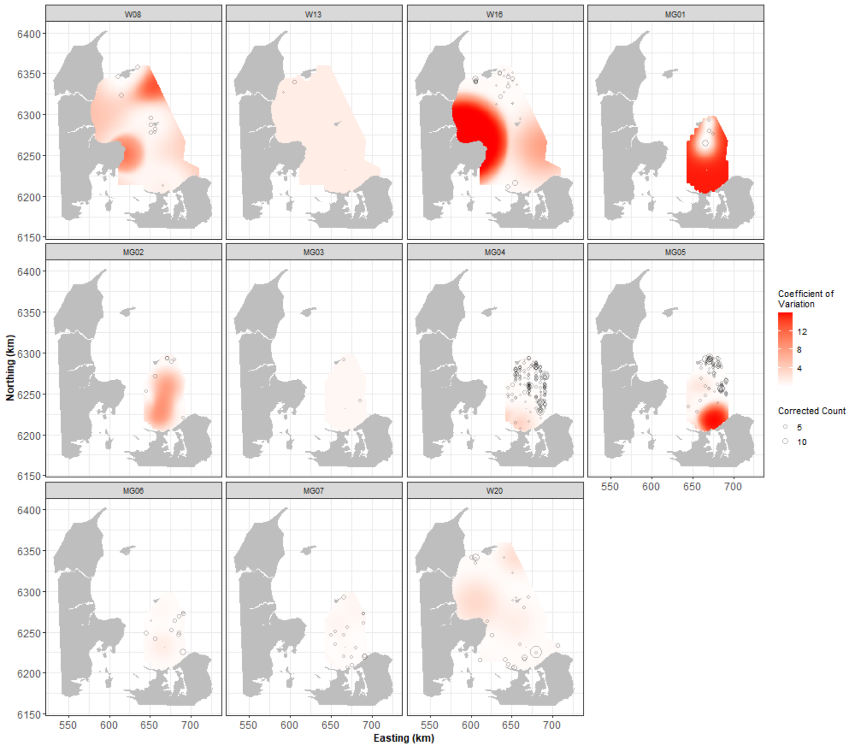

Figure 40: Figure showing the coefficient of variation (untruncated) across the study region for each of the surveys. The open circles show the observed, distance corrected counts.

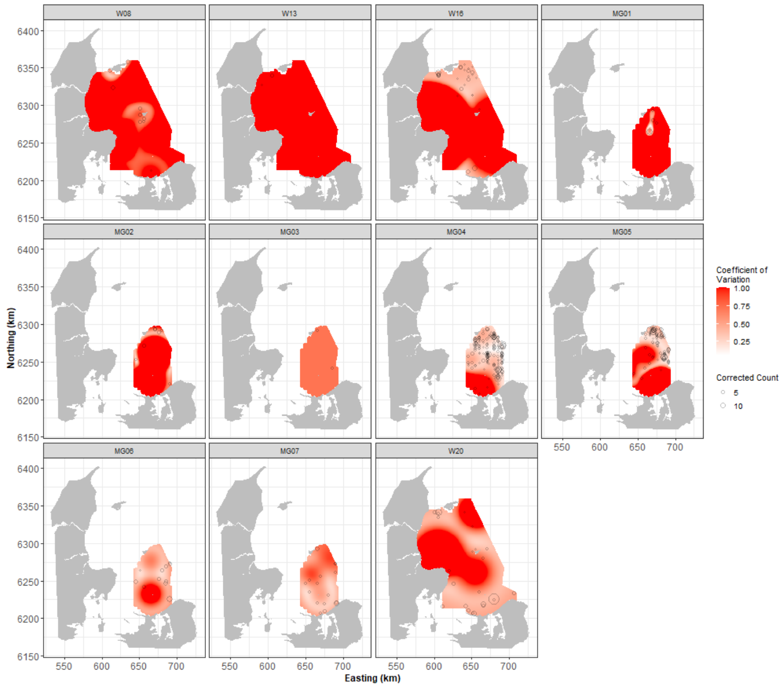

Figure 41: Figure showing the coefficient of variation across the study region for each of the surveys, capped at one. The open circles show the observed, distance corrected counts.

For further information on uncertainty in the spatial predictions, please refer to MacKenzie & Scott-Hayward (2021).

Areas of Persistence

There is evidence of relatively high persistence at the edges of the (reduced survey) area, and very low persistence towards the centre of the survey area (Figure). This aligns well with most of the survey results, excepting survey W08 (Figure) which exhibited spatial patterns around the island of Hesselø. Notably, there was low-to-moderate levels of persistence in the proposed wind farm area, however the very low numbers of Gannets observed across the surveys should be borne in mind.

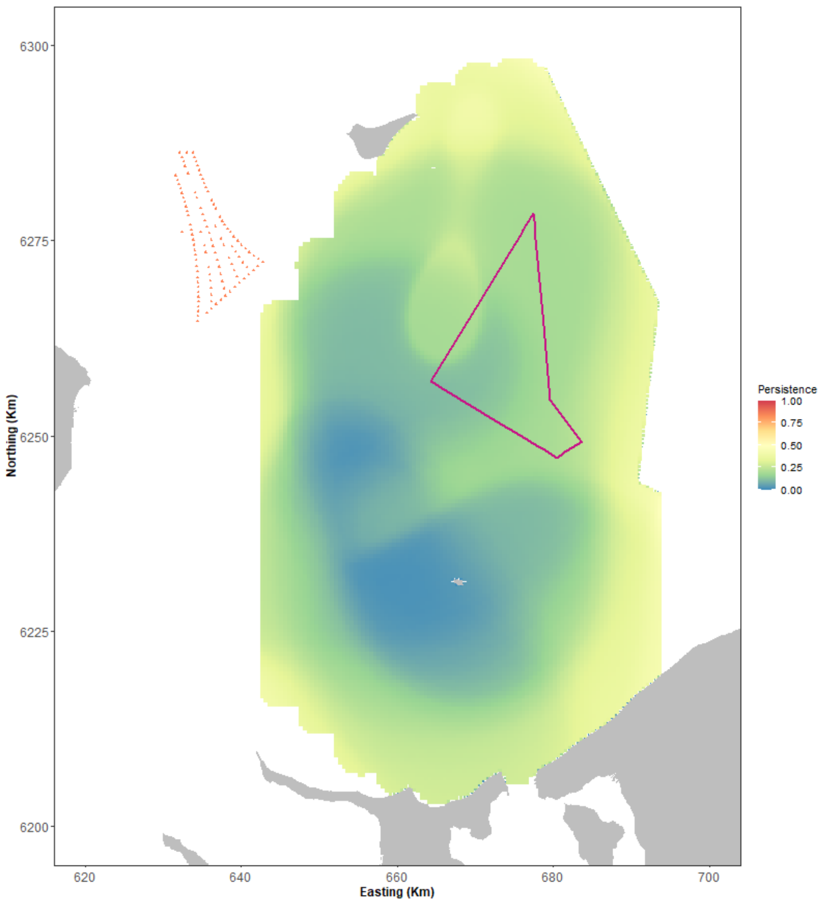

Figure 42: Persistence scores for Gannet across the MG survey area (reduced survey area with consistent overlap).

Common Eider *Somateria mollissima*

Common Eiders are found in Danish waters all year, and both breed, moult and winter here. Both the mid-summer and the winter population size was modelled from 2008 data, revealing a total number of 503,000 wintering birds and 110,000 in summer. The last figure cover only the main parts of the inner Danish waters, while the winter estimate covers all the Waddensee and greater parts of the inner Danish waters (Petersen & Nielsen 2011) and seemed stable over the winters of 2013 and 2016 (Holm et al. 2021).

Common Eiders were present in the study area in high numbers. A total of 28,770 birds was observed across all surveys (Table 5). Of these, most birds were recorded in Ålborg Bugt, around Læsø and Anholt as well as along the north coast of Sjælland (Figure 43). A total of 6,484 of the Common Eiders were observed in the Middelgrund study area, while only 18 individuals were observed within a distance of 2 km from the proposed wind farm area. The species was observed around the island of Hesselø, and occasionally in higher numbers at the Store Lysegrund, between the proposed wind farm site and the island of Hesselø.

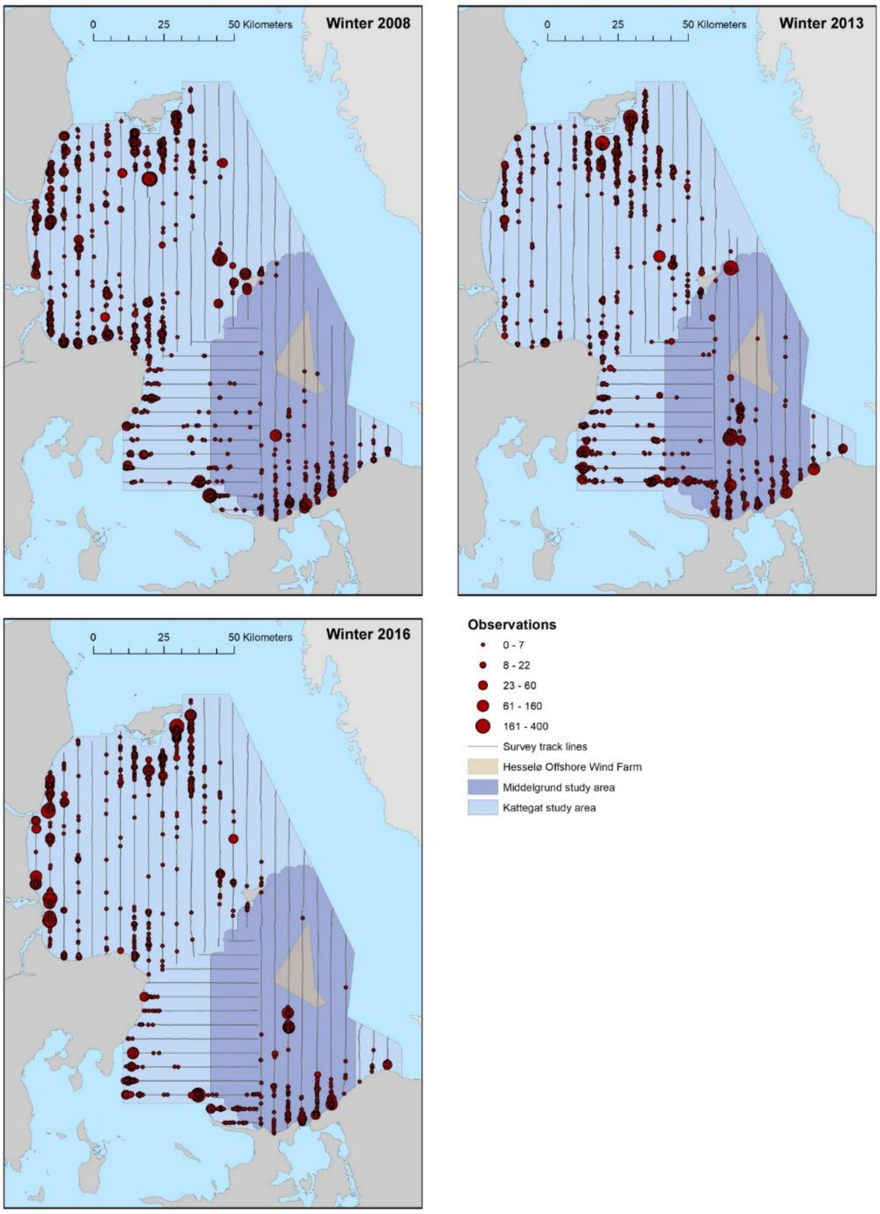

Figure 43. The spatial distribution of observed Common Eider from 11 surveys of birds in the study area between winter 2008 and winter 2020. Survey timing for the individual surveys are given in upper right corner of each map. The survey track lines covered for each survey is also given.

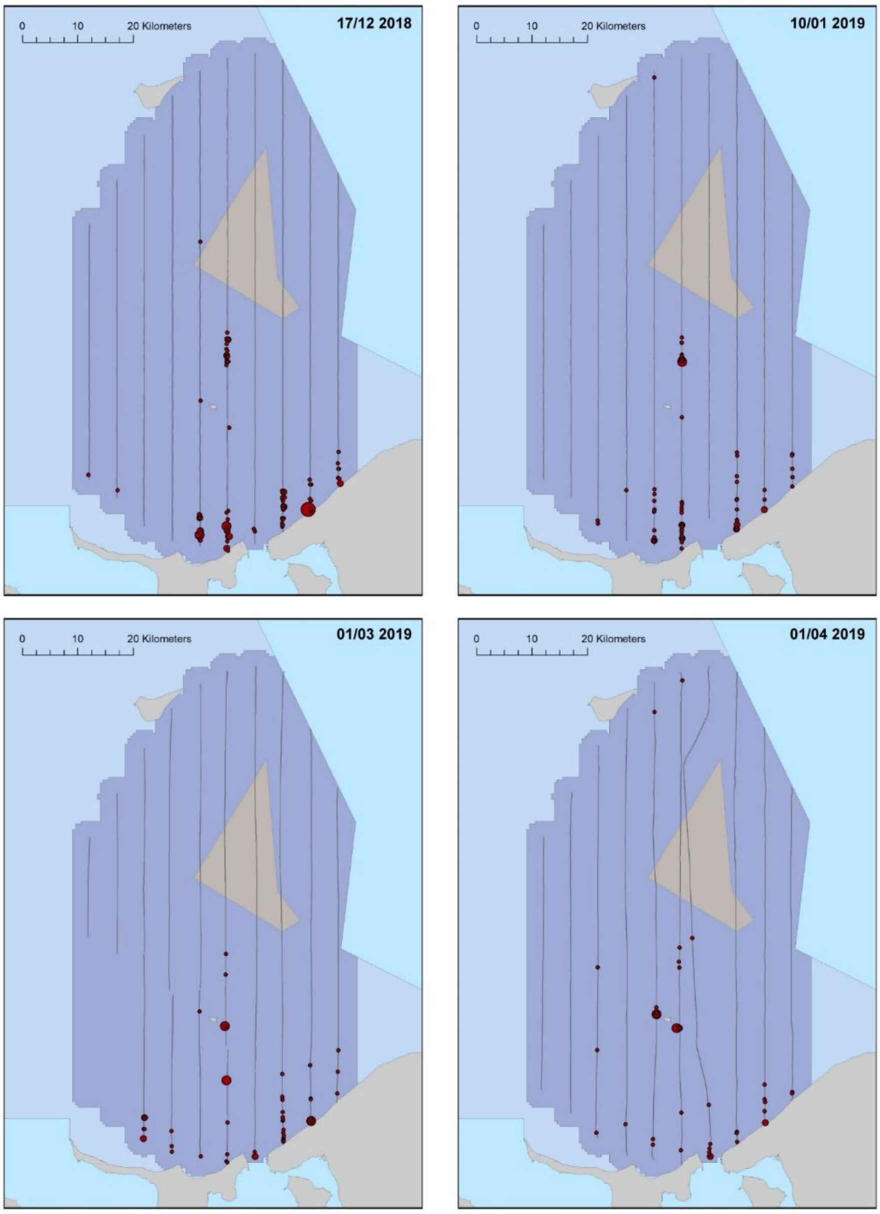

Figure 43. Common Eider, continued

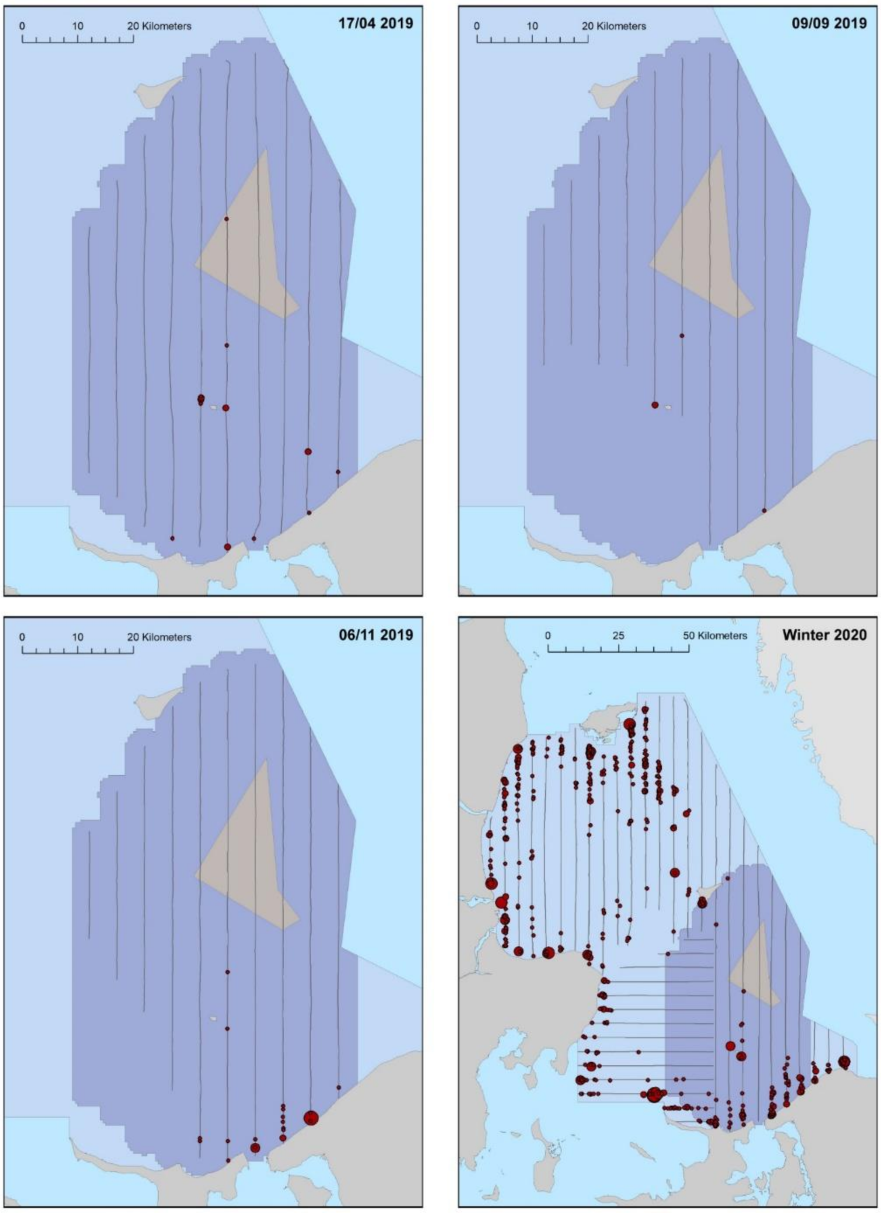

Figure 43. Common Eider, continued

Common Eider was most abundant in the study area in autumn and winter (Figure 44).

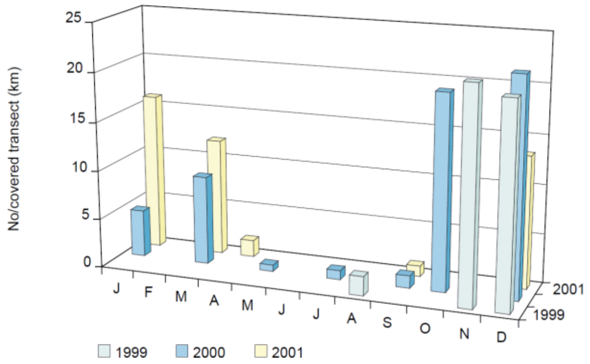

Figure 44. The annual variation in the relative density of Common Eider in the northern Kattegat area from 15 surveys. Conducted between 1999 and 2001 (From: Petersen et al. 2003).

Common Eider forage on benthic organisms, and therefore primarily in shallow to moderate water depths. More than 74 % of the Common Eiders was recorded on water depths between two and ten meters. Most birds were recorded (25 %) in the 6-8 meter depth interval (Figure 45).

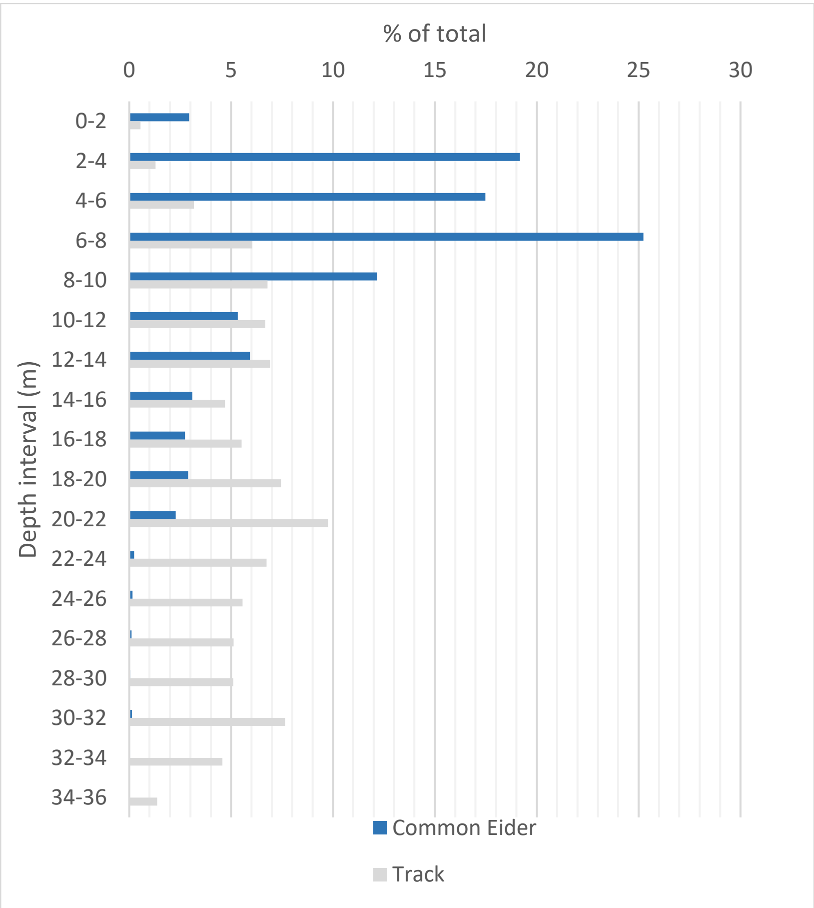

Figure 45. The depth frequency distribution of Common eider in the Kattegat Study Area in 2 m depth intervals and expressed as % of total numbers observed. The depth frequency distribution of the covered survey track lines is given for comparison.

Common Scoter *Melanitta nigra*

Common Scoters are present in Danish waters most of the year. They do not breed in Denmark, but both winter, migrate and moult here. The Common Scoter abundance in Danish waters was modelled from 2008 winter data, estimating a total winter abundance of more than 400,000 birds in the inner Danish waters (Petersen & Nielsen 2011). The numbers of wintering Common Scoters seems to have declined between 2008 and the winters of 2013 (194,000 to 258,000) and 2016 (184,000 to 371,000, Holm et al. 2021).

Common Scoter was most abundant in the Ålborg Bugt area and in the shallow waters between Læsø and Anholt (Figure 46). Smaller numbers was recorded along the north coast of Sjælland. A total of more than 114,000 Common Scoters was observed during the surveys (Table 5). Of these 9,718 individuals were recorded within the Middelgrund Study Area, and only five birds were recorded within a distance of 5 km from the proposed wind farm area.

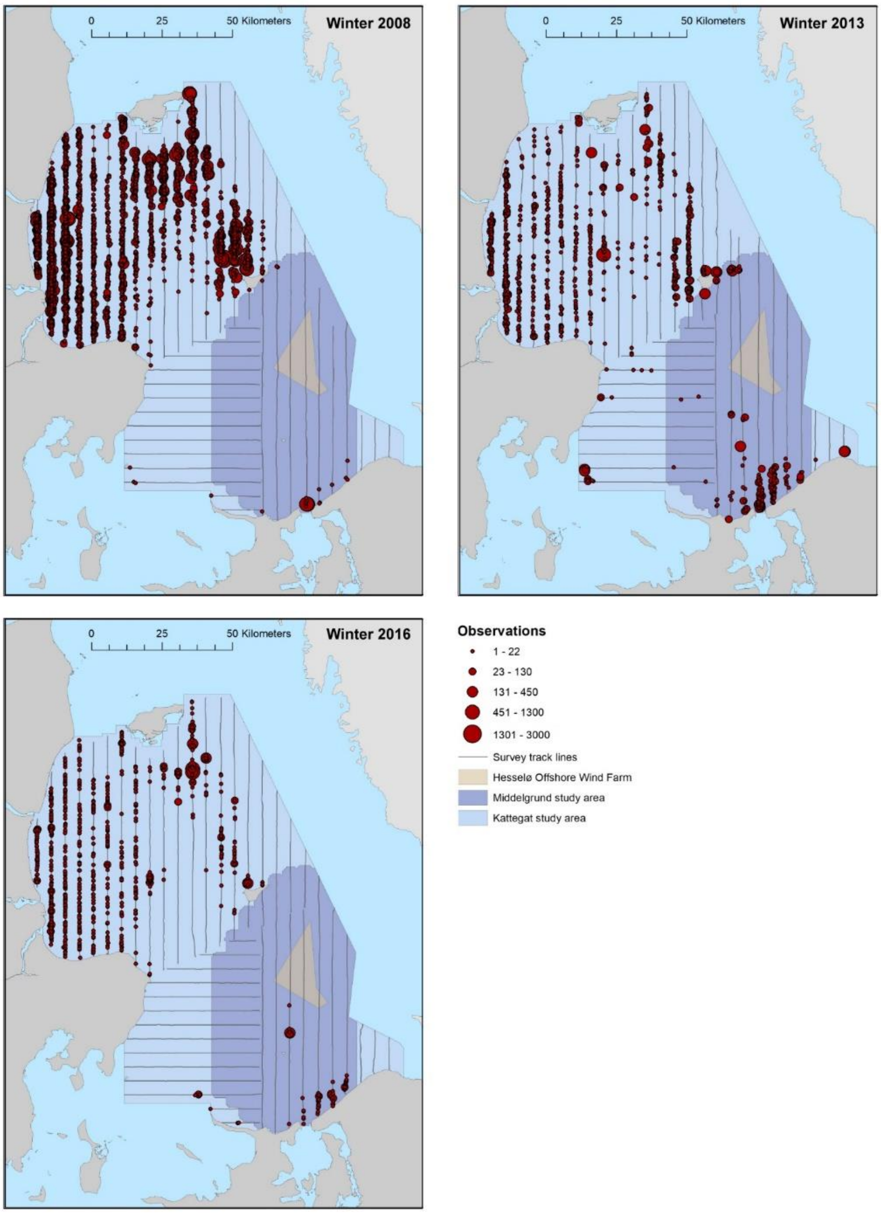

Figure 46. The spatial distribution of observed Common Scoter from 11 surveys of birds in the Kattegat Study Area between winter 2008 and winter 2020. Survey timing for the individual surveys are given in upper right corner of each map. The survey track lines covered for each survey is also given.

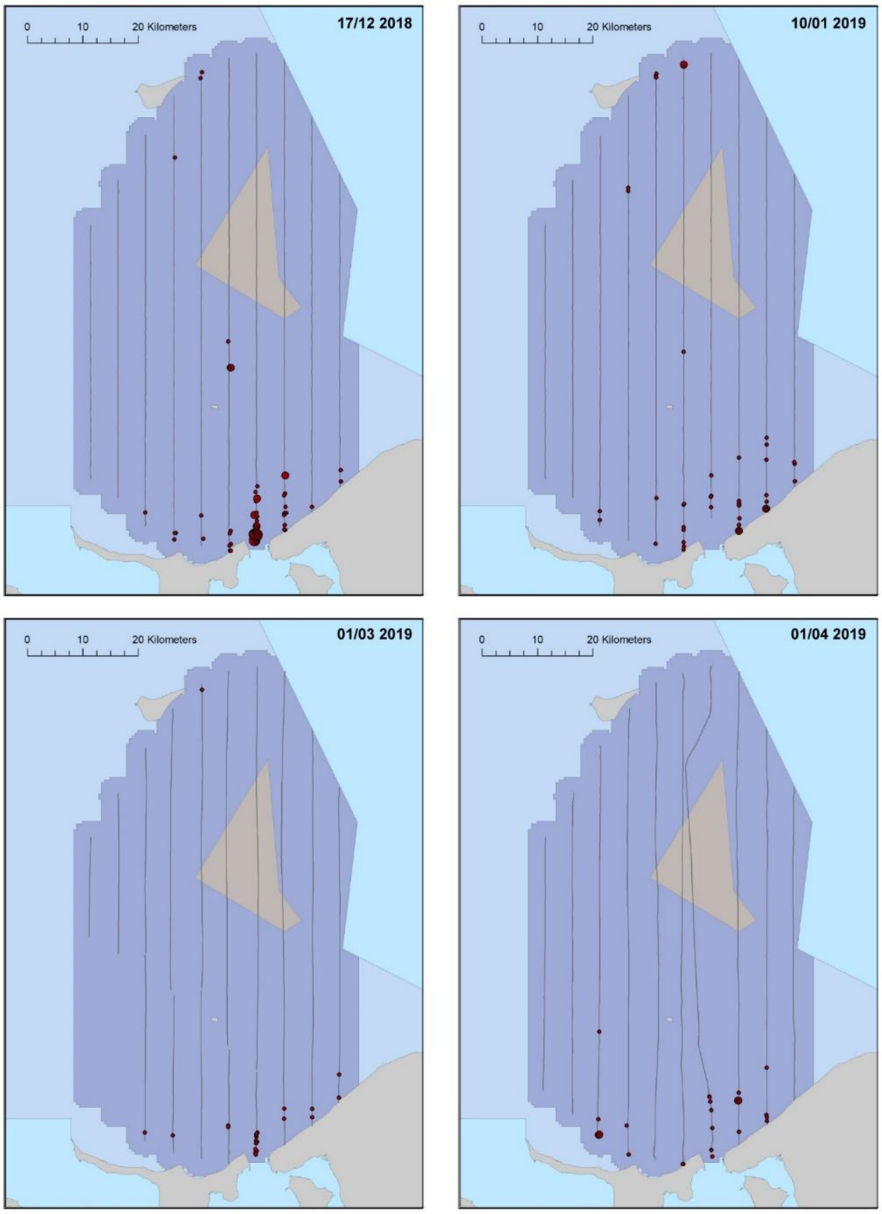

Figure 46. Common Scoter, continued.

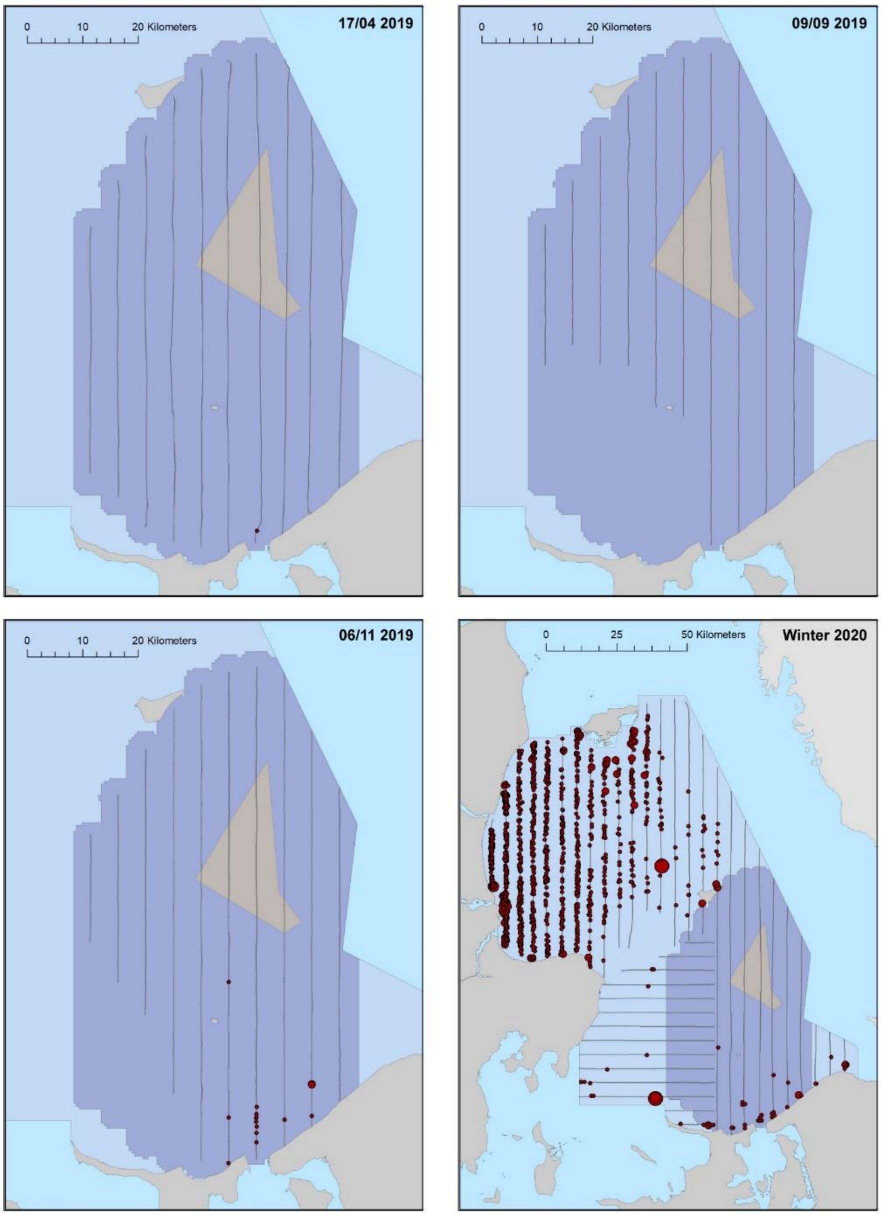

Figure 46. Common Scoter, continued.

Common Scoters migrate towards the breeding grounds in March to May, and by the end of May most birds have left the study area. Already in late June and July birds return from the breeding grounds (Figure 47), primarily males. They undergo moult in the study area (primarily in Ålborg Bugt) from late June until early September (Petersen & Fox 2009).

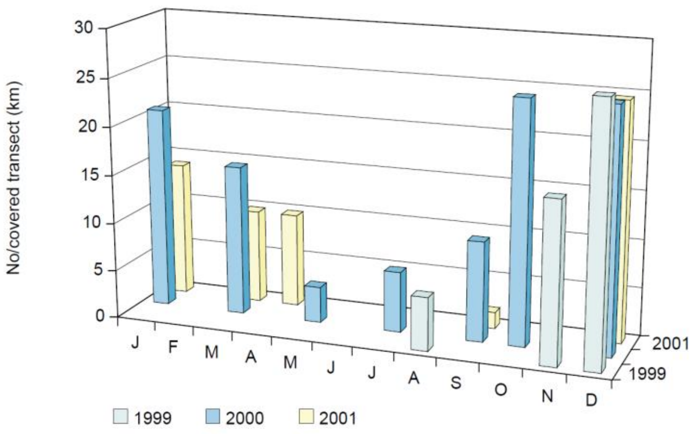

Figure 47. The annual variation in the relative density of Common Scoter in the northern Kattegat area from 15 surveys, conducted between 1999 and 2001 (From: Petersen et al. 2003).

Common Scoters forage on benthic organisms, and was therefore primarily found on shallow or medium water depths. Eighty-eight percent of the birds were recorded within the depth interval of 4-14 meters, and most birds (ca. 26 %) was recorded in the 6-8 meter depth interval (Figure 48).

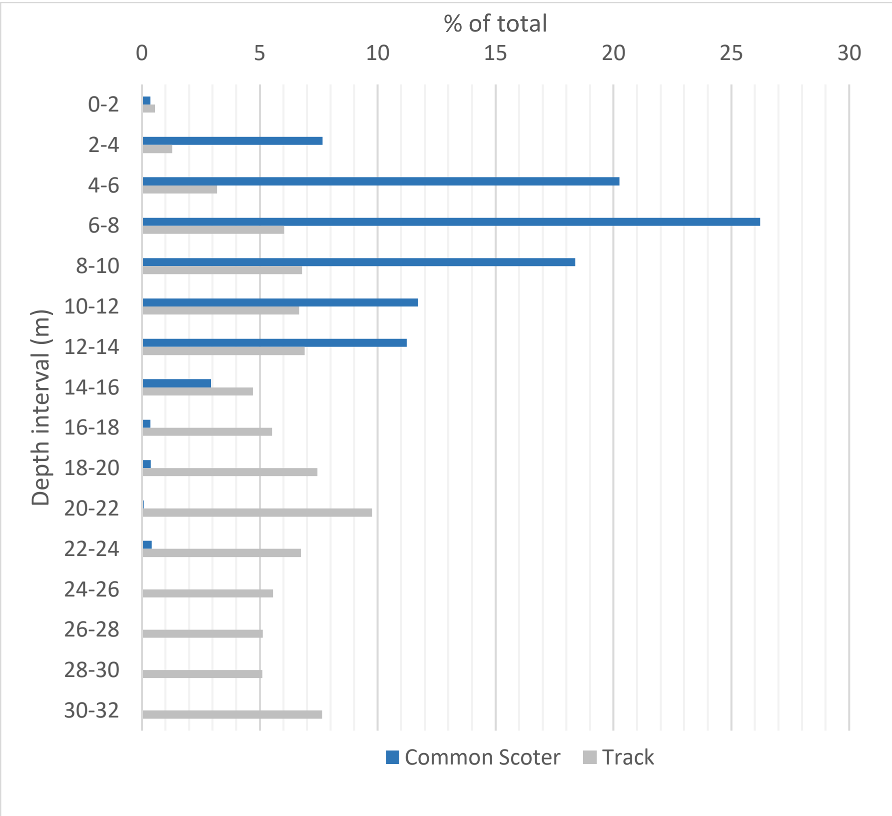

Figure 48. The depth frequency distribution of Common Scoter in the Kattegat study area in 2 m depth intervals and expressed as % of total numbers observed. The depth frequency distribution of the covered survey track lines is given for comparison.

Velvet Scoter *Melanitta fusca*

Velvet scoters are present in Danish marine watersthroughout most of the year. They do not breed in Denmark, but winter, migrate and moult here. Numbers have fluctuated hugely between years. The two most recent estimates are from the 2013 and 2016 winter surveys, when numbers between 26,000 and 65,000 and 10,000 to 24,000 was estimated which was considered an increasing trend as calculated over the period from 2004 to 2016 (Holm et al. 2021). Common Scoter and Velvet Scoter are often found in mixed flocks and due to their similarity this can potentially result in underestimation of the number of Velvet Scoter.

More than 5,200 Velvet Scoters was observed during the 11 surveys (Table 5). The majority of these were found in the Ålborg Bugt area, around Læsø and Anholt and smaller numbers along the north coast of Sjælland. A total of 425 individuals were recorded in the Middelgrund Survey Area, while no birds were recorded within 5 km from the proposed wind farm area (Figure 49).

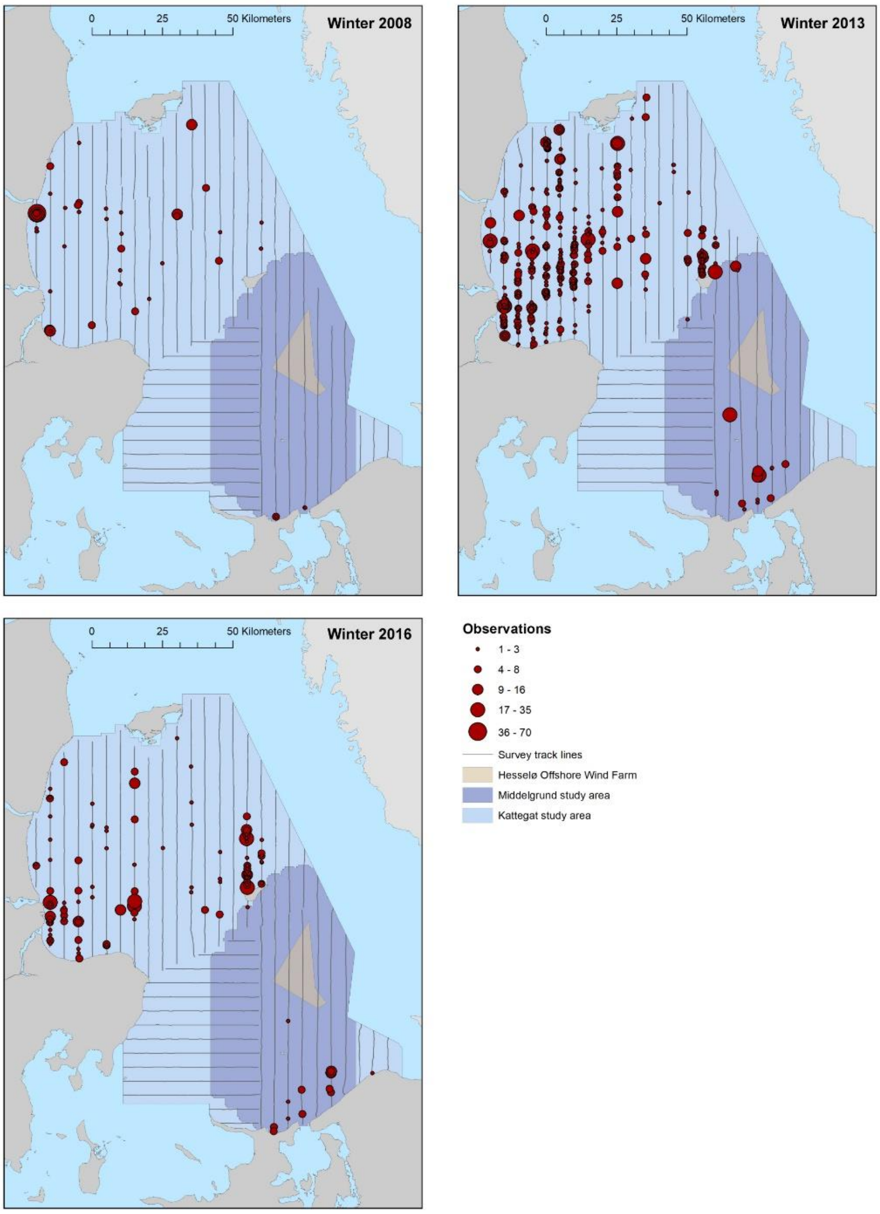

Figure 49. The spatial distribution of observed Velvet Scoter from 11 surveys of birds in the study area between winter 2008 and winter 2020. Survey timing for the individual surveys are given in upper right corner of each map. The survey track lines covered for each survey is also given.

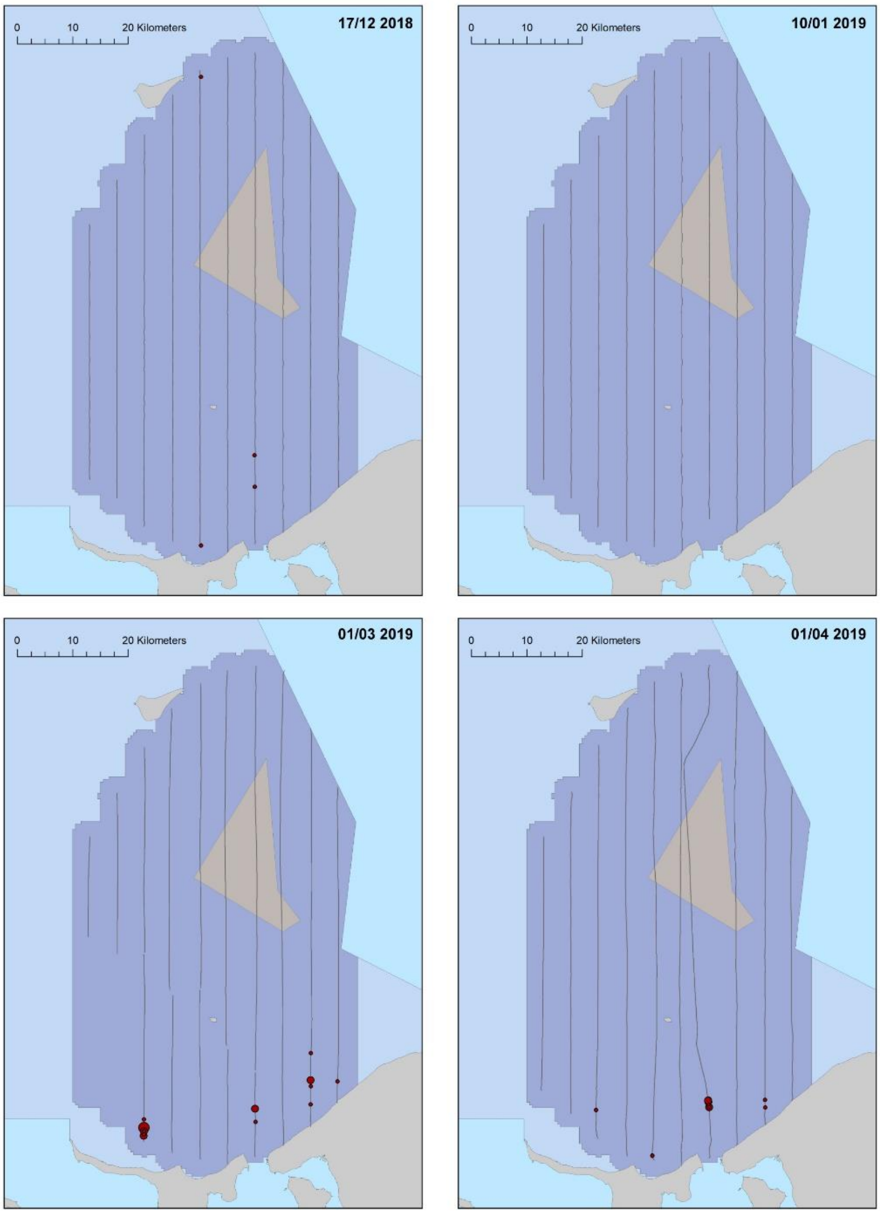

Figure 49. Velvet Scoter, continued.

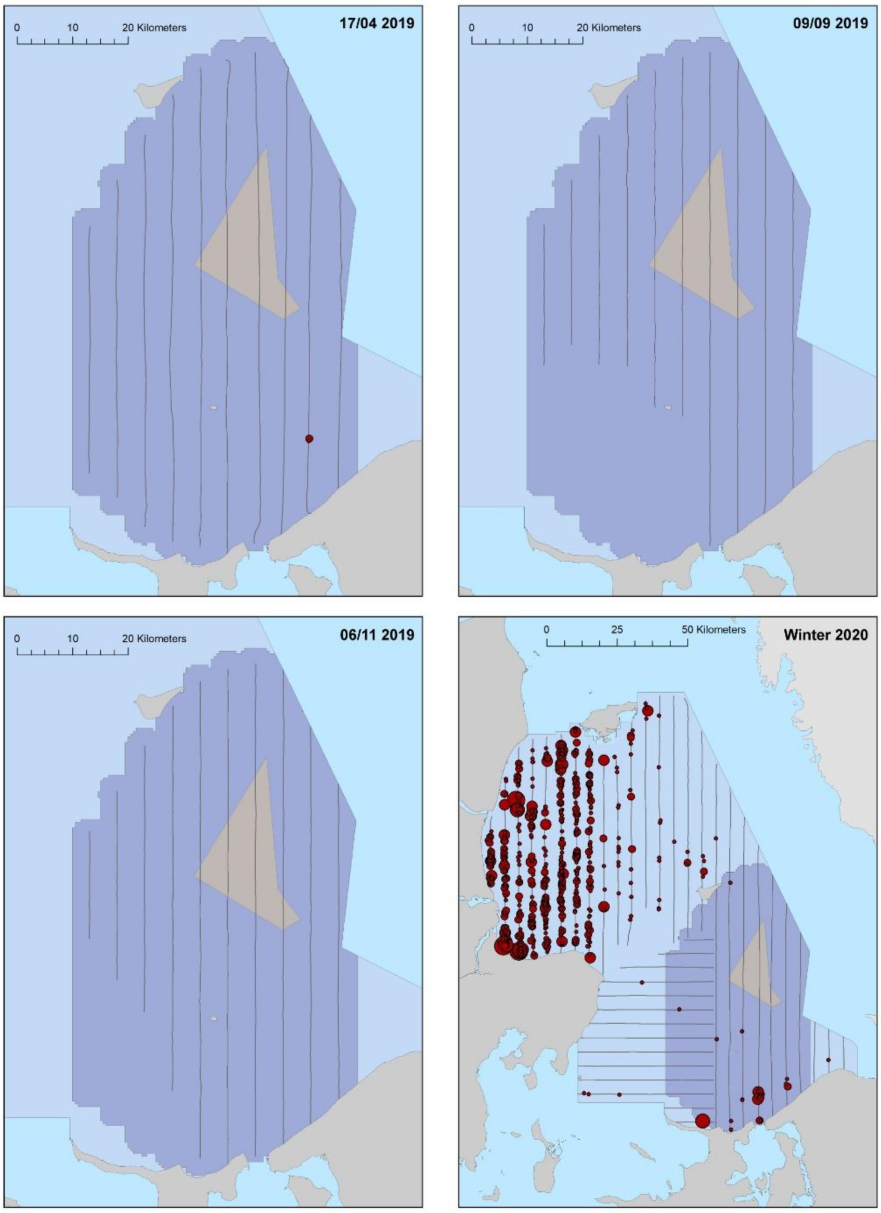

Figure 49. Velvet Scoter, continued.

Velvet Scoters migrate towards their breeding grounds in the inner Baltic, Scandinavia and Russia, and are generally away from Denmark by April/May. In July, birds already start to return from the breeding grounds, mainly males, which undergo moult in Danish waters. Numbers increase during the autumn, and reach highest numbers in the winter (Figure 50).

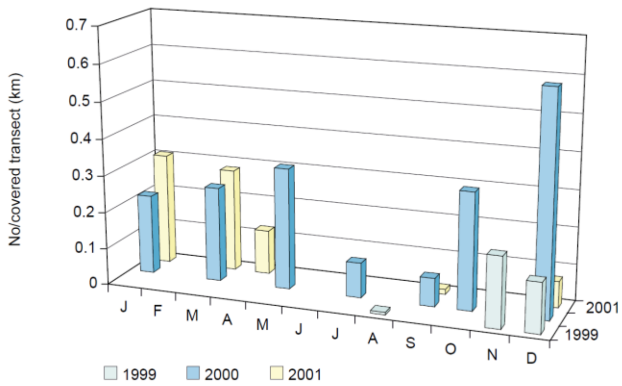

Figure 50. The annual variation in the relative density of Velvet Scoter in the northern Kattegat area from 15 surveys, conducted between 1999 and 2001 (From: Petersen et al. 2003).

Gulls *Laridae spp.*

Gulls were recorded across the entire study area. Under this heading, we present data on all other gull species but Kittiwake, which is described below. A total of almost 8,400 gulls (other than Kittiwake) was observed, covering the following gull species: Common Gull *Larus canus* (2 %), Herring Gull (76 %), Great Black-backed Gull (10 %), Lesser Black-backed Gull *Larus fuscus*, Black-headed Gull *Chroicocephalus ridibundus* (1 %), Little Gull *Hydrocoloeus minutus*, and unidentified gulls (10 %, Table 5). The percentage of Common Gull may be underestimated due to challenges separating the species from Herring Gull by the aerial surveys method.

The gull species are found across the entire study area, with some coastal concentrations (Figure 51). Marked fluctuations in distribution between surveys of the same time of year was found, as for instance seen when comparing the winter surveys of 2008, 2013, 2016 and 2020 (Figure 51).

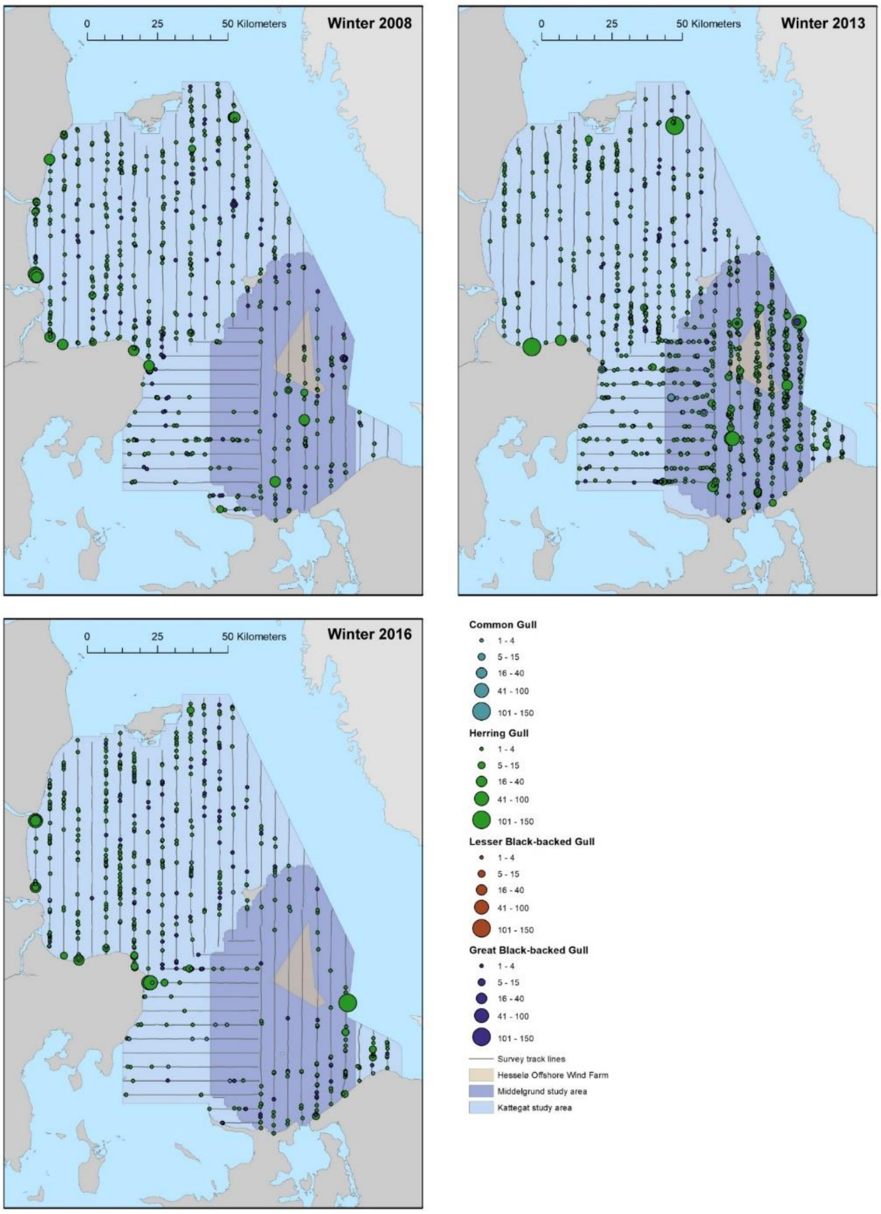

Figure 51. The spatial distribution of observed Common Gulls, Herring Gulls, Lesser Black-backed Gulls and Great Black-backed Gulls from 11 surveys of birds in the study area between winter 2008 and winter 2020. Survey timing for the individual surveys are given in upper right corner of each map. The survey track lines covered for each survey is also given.

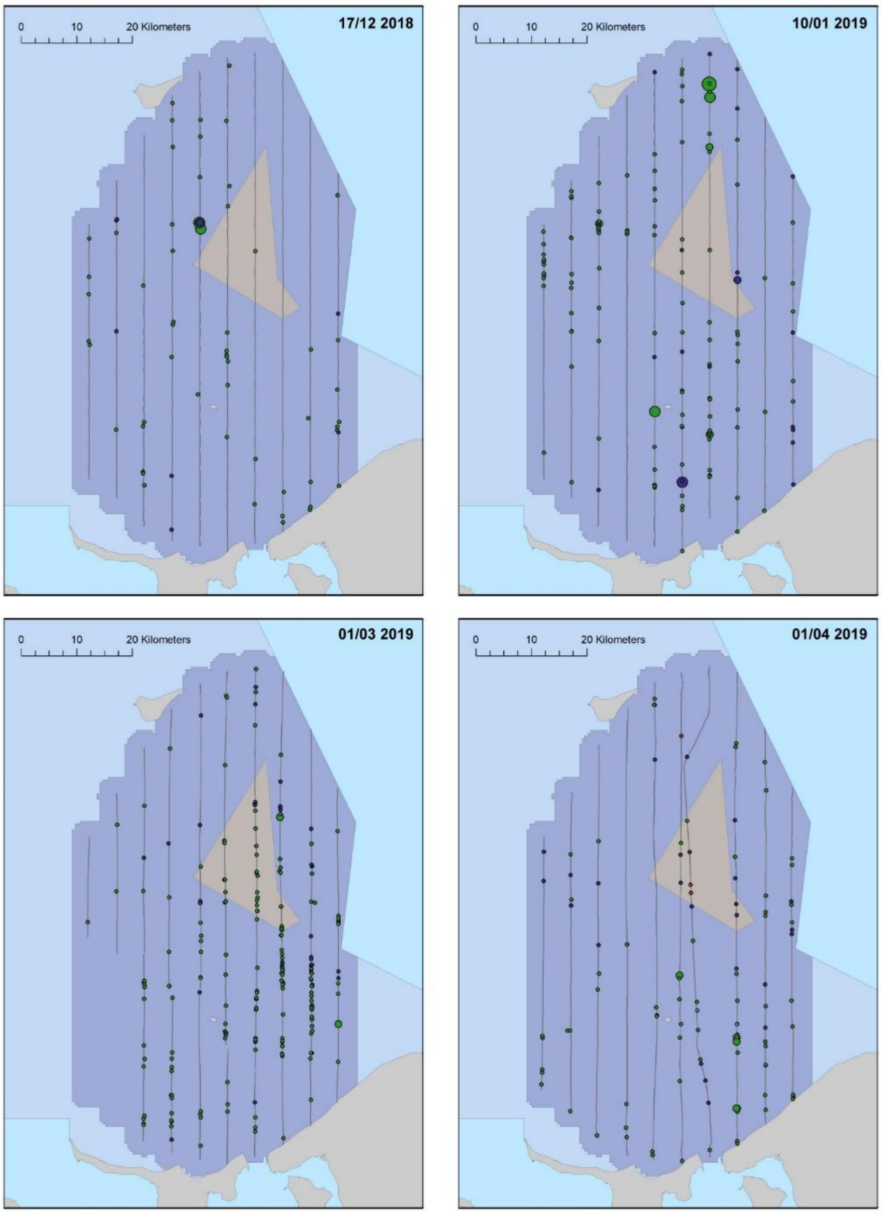

Figure 51. Common Gulls, Herring Gulls, Lesser Black-backed Gulls and Great Black-backed Gulls, continued.

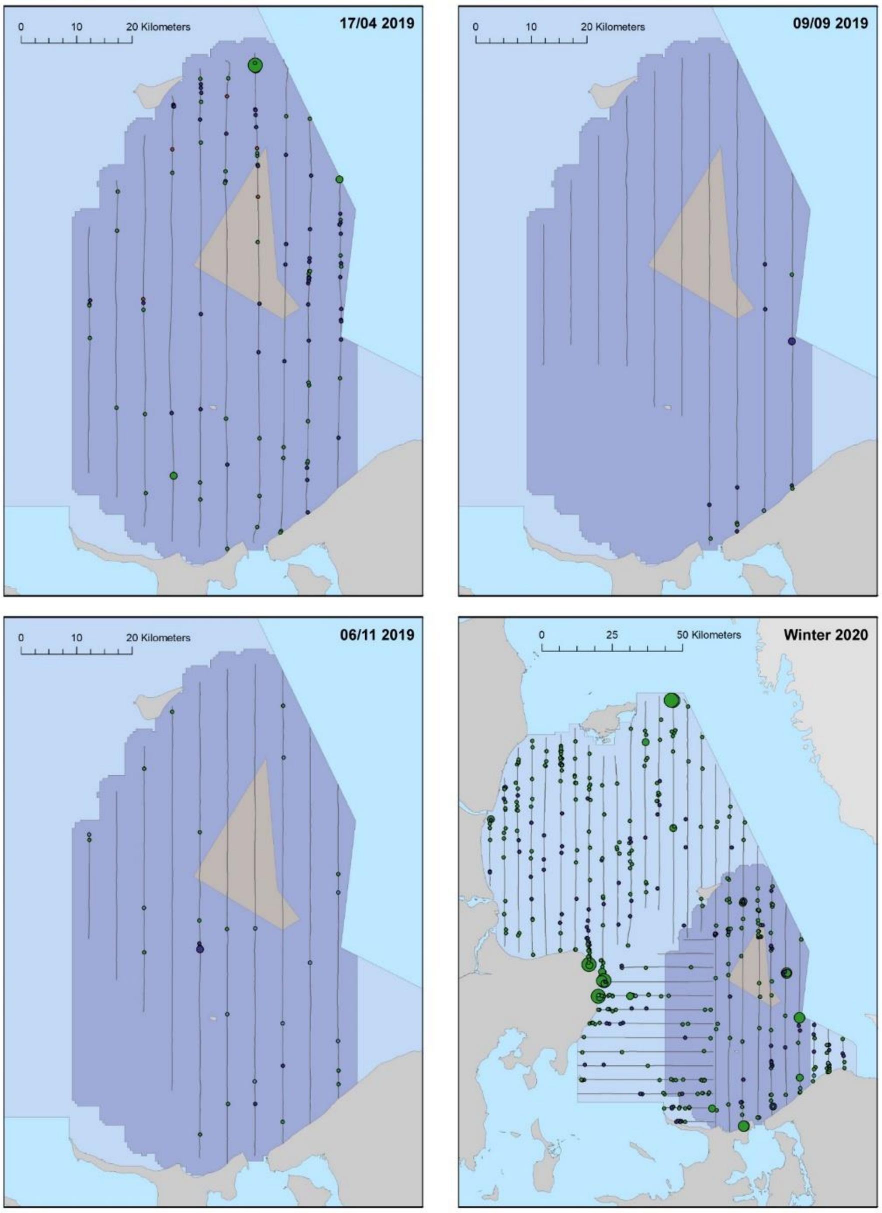

Figure 51. Common Gulls, Herring Gulls, Lesser Black-backed Gulls and Great Black-backed Gulls, continued.

Black-legged Kittiwake *Rissa tridactyla*

In Danish waters Kittiwakes are most abundant in the North Sea, but are also present in significant numbers in Kattegat. There is no recent estimate of total numbers in the non-breeding season in Denmark.

Within the study area a total of 727 Kittiwakes was recorded during all aerial surveys (Table 5). The majority of these were seen in the eastern and southeastern parts (Figure 52). A total of 571 Kittiwakes were observed within the Middelgrund Study Area, and 68 individuals were recorded within a distance of 2 km from the proposed wind farm area (Figure 52).

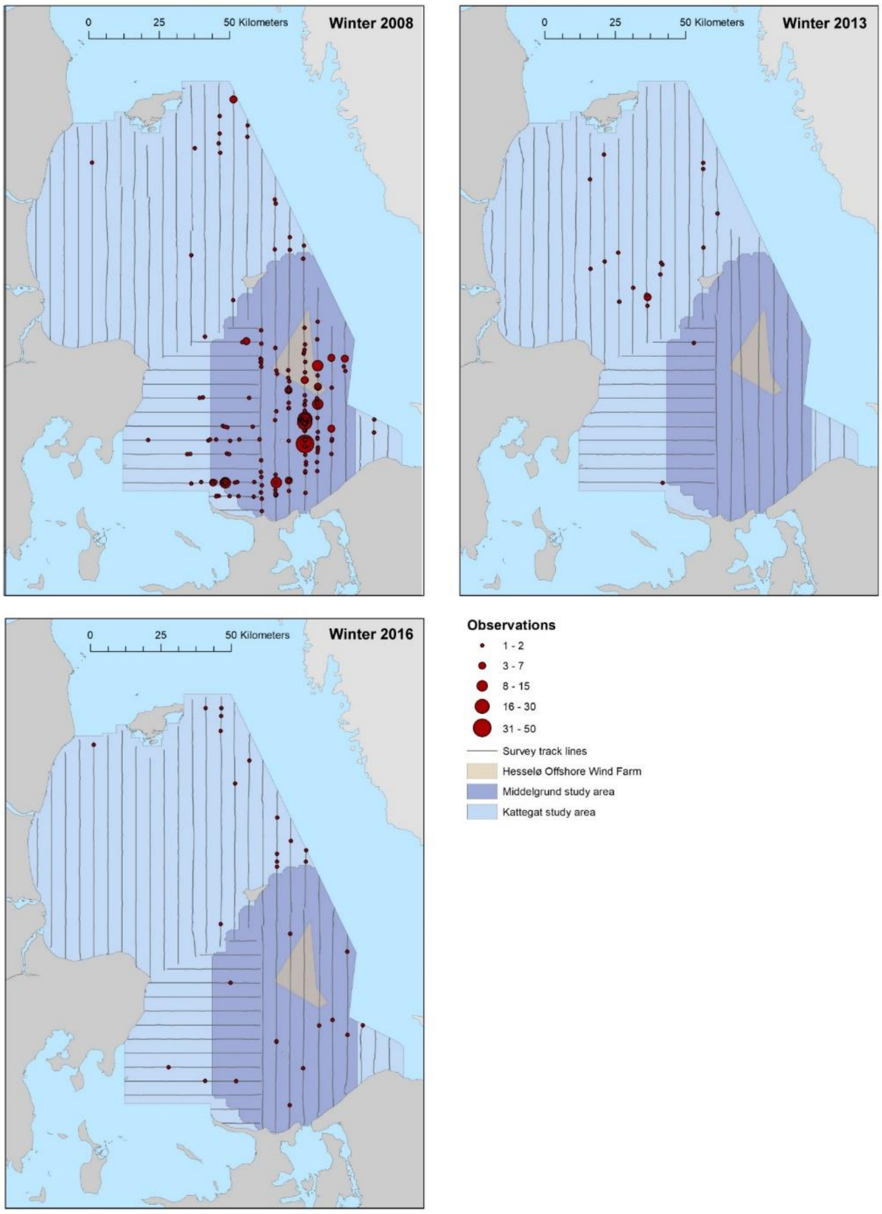

Figure 52. The spatial distribution of observed Kittiwake from 11 surveys of birds in the study area between winter 2008 and winter 2020. Survey timing for the individual surveys are given in upper right corner of each map. The survey track lines covered for each survey is also given.

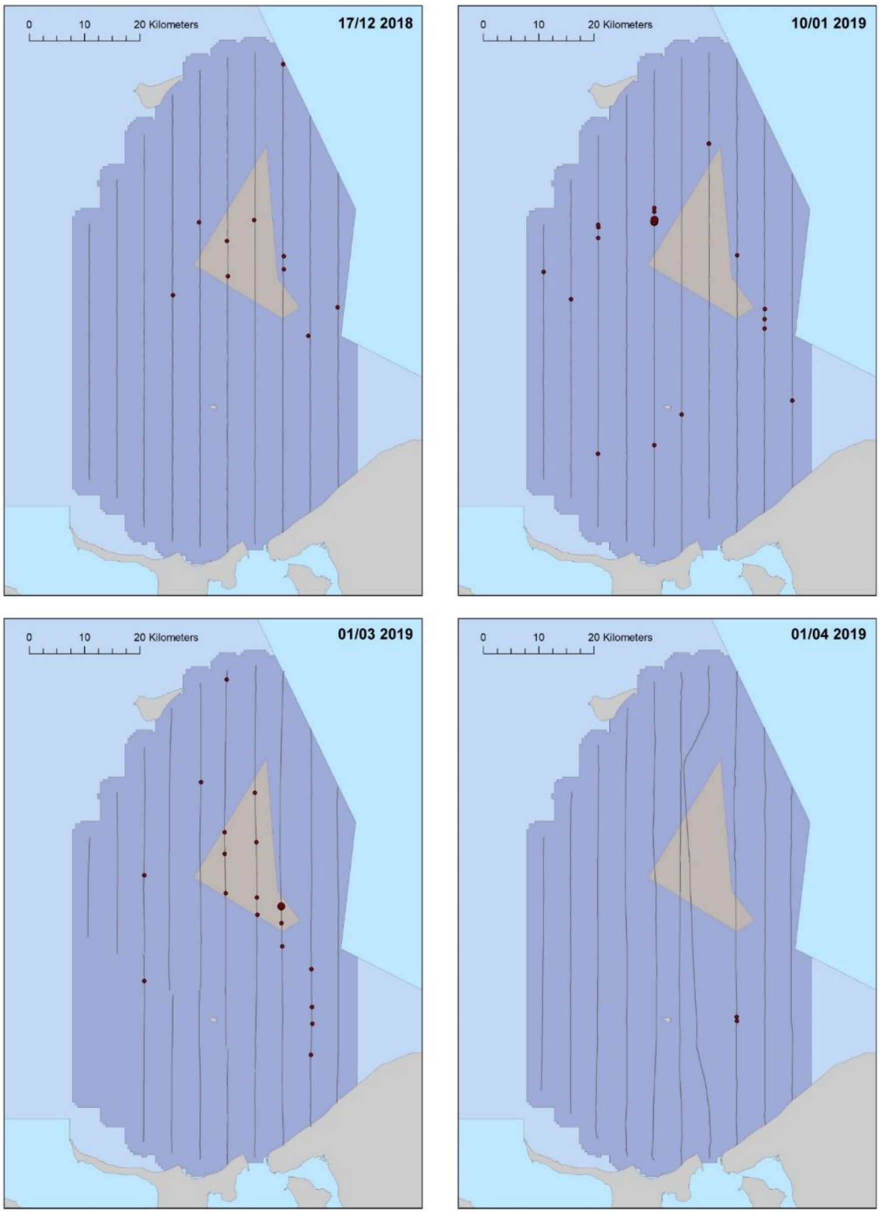

Figure 52. Kittiwake, continued.

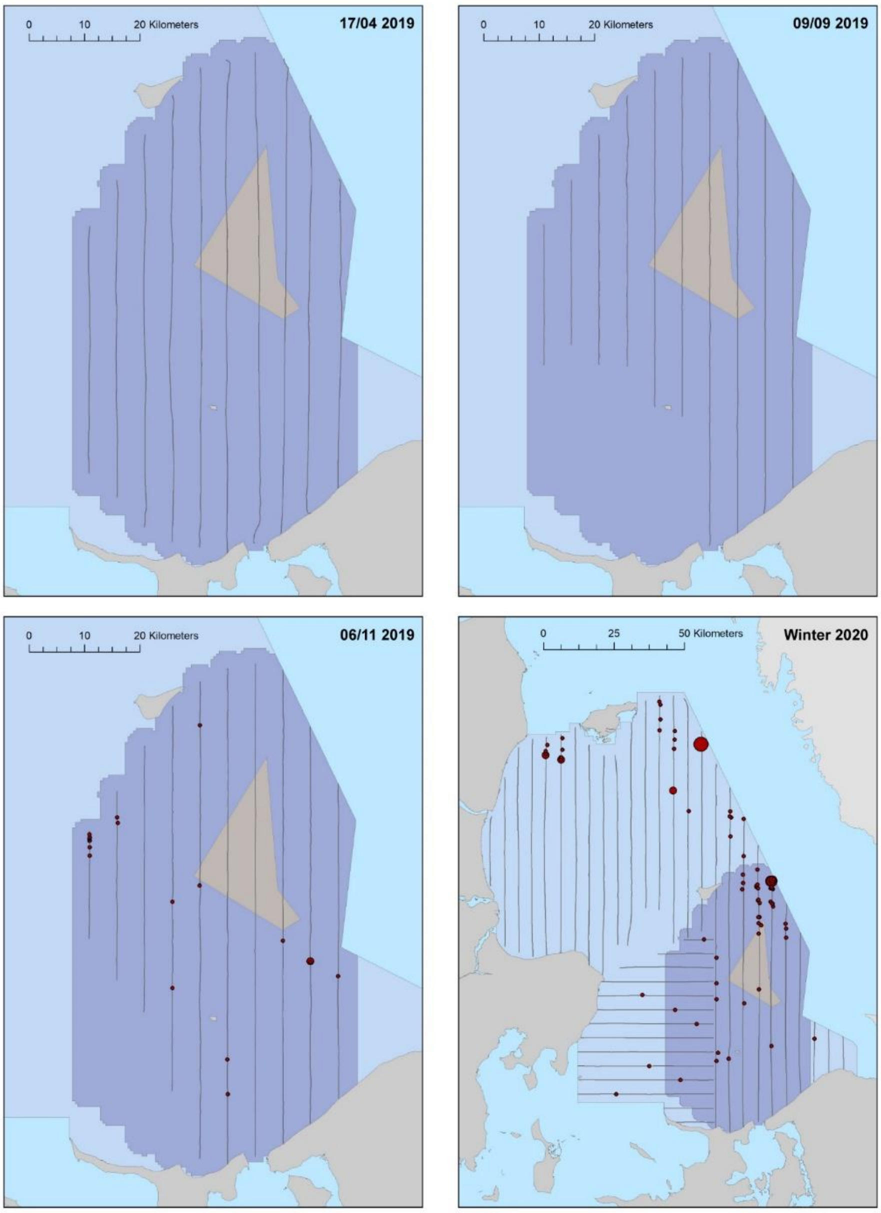

Figure 52. Kittiwake, continued.

Kittiwakes are most abundant in the study area over the winter, from November until March (Figure 53).

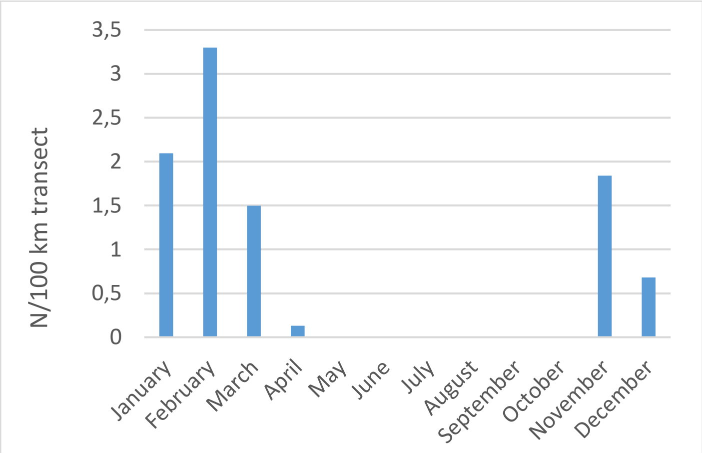

Figure 53. The annual variation in the relative density of Kittiwake in the Kattegat Study Area from 11 surveys included in this report.

Kittiwakes were observed in the deeper parts of the study area. Seventy-nine percent of the birds were recorded within the depth interval 18-36 meters, while 3 % occurred in shallower waters and 11 % in deeper waters than those intervals (Figure 54).

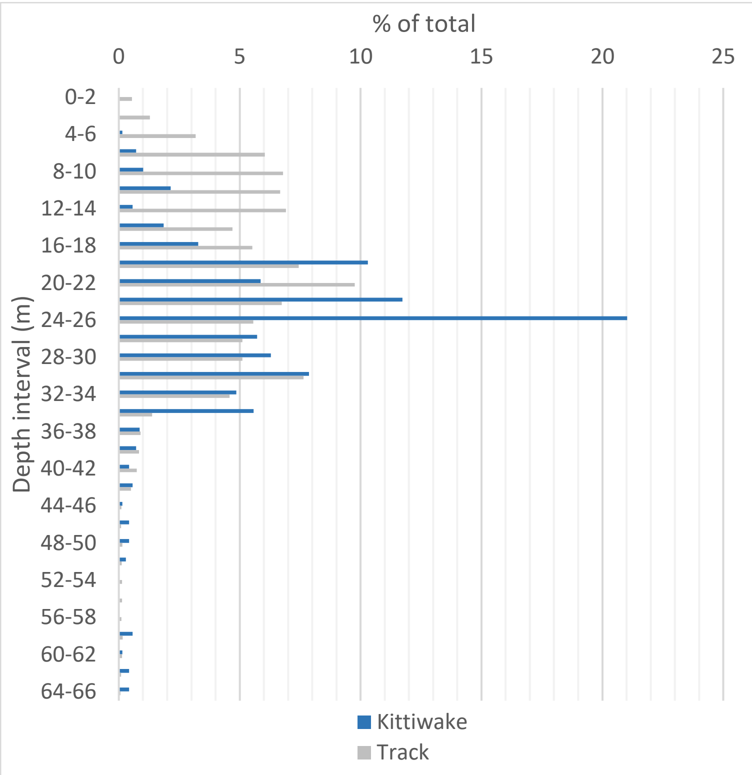

Figure 54. The depth frequency distribution of Kittiwake in the Kattegat Study Area in 2 m depth intervals and expressed as % of total numbers observed. The depth frequency distribution of the covered survey track lines is given for comparison.

Distance Analysis

The average probability of sighting Kittiwakes was estimated to be 0.42 (CV=0.052). This probability was estimated using a hazard rate detection function that varied with observer (Figure 55). As there were very few sightings in band D, these detections were excluded and the strip half width set to be 956m.

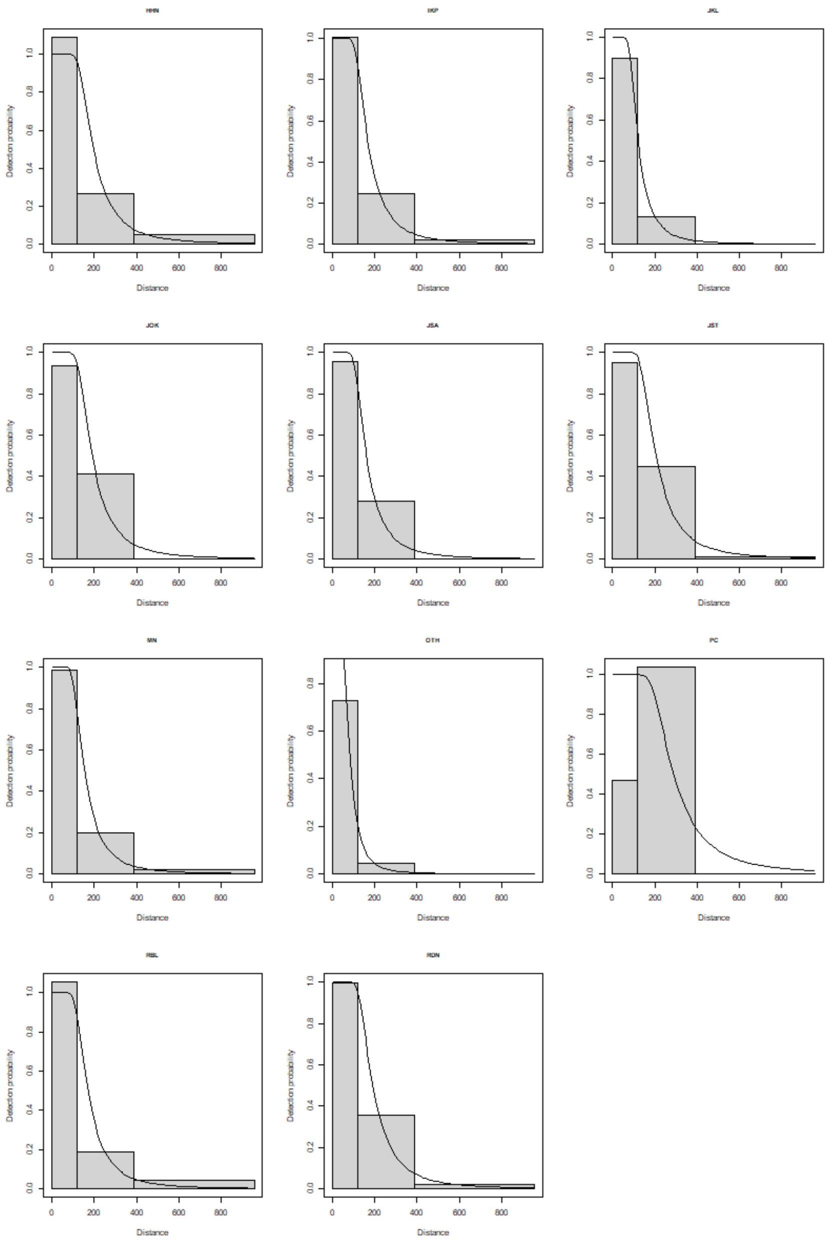

Figure 55: Figure showing the estimated detection function for each of the observers. The histograms are the distances of the observed sightings.

The dataset for the spatial analysis comprised 26,656 segments, 1.3 % of which were segments containing Kittiwake sightings. Table shows the breakdown of survey effort within each of the 11 surveys and Figure shows the distribution of the distance corrected counts. As there were no Kittiwake sightings in surveys MG05 and MG06, these were not included in the spatial analysis.

Table 14: Table showing a summary of the survey effort for the Kittiwake species in each of the 11 surveys.

Survey	Number of Segments	
	With Sightings	Total
W08	154	4930
W13	19	4805
W16	29	4920
MG01	10	1481
MG02	18	1469
MG03	18	1368
MG04	2	1484
MG05	0	1477
MG06	0	1160
MG07	18	1313
W20	66	4886

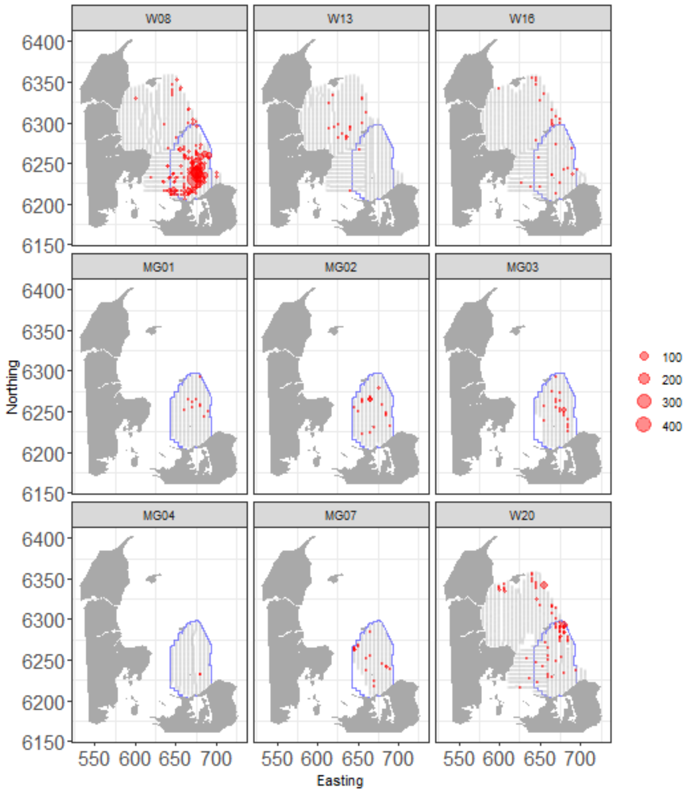

Figure 56: Distance-corrected counts for Kittiwake across nine surveys. The red circles indicate the distance-corrected counts along the transect lines while the grey polygons represent land. The blue line denotes the MG study area.

Model Selection results

There was compelling evidence for spatial patterns in Kittiwake density across eight of the nine surveys (of variable complexity) while a water depth relationship was not selected in any of the models. While in eight surveys, localised spatial patterns were justified (using objective fit criteria), an intercept only model was selected in one case (Table). These model returns just one predicted value across the survey area.

Due to the very low numbers of non-zero counts in these surveys, the spatial surfaces selected were very low dimensional (with between two and nine degrees of freedom) and all models estimated a dispersion parameter larger than one, indicating an over-dispersed approach was justified in these models (Table).

Table 15: Model selection results for the 9 surveys. "N/S" indicates the term was not selected as part of the 10-fold cross validation procedure and df=degrees of freedom for that relationship.

Survey	Depth	s(xpos, y.pos)	Dispersion parameter estimate
W08	N/S	$p < 0.0001$ (df=4)	45.4
W13	N/S	$p < 0.0001$ (df=9)	5.7
W16	N/S	$p < 0.0001$ (df=8)	3.8
MG01	N/S	$p = 0.0002$ (df=3)	5.0
MG02	N/S	$p = 0.1264$ (df=4)	13.0
MG03	N/S	$p = 0.0172$ (df=6)	12.0
MG04	N/S	N/S	6.6
MG07	N/S	$p = 0.0044$ (df=2)	7.5
W20	N/S	$p < 0.0001$ (df=5)	10.1

The estimated abundances in each survey are given in Table . Survey MG04 reported the lowest estimated abundance but the uncertainty associated with all of the estimates for the MG surveys meant no conclusions could be drawn about any genuine differences between them. Of the W surveys, W08 had the largest estimated abundance (significantly higher than all other W surveys for this species), but the remaining W surveys each had sufficient uncertainty to render them indistinct from each other.

Table 16: Table of estimated counts for each survey. The 95 % CI are percentile-based confidence intervals from the 250 bootstraps generated which incorporate the uncertainty from both the detection function estimation and the subsequent spatial analyses.

Survey	Estimated Count	95 % CI
W08	7071.5	(3102.7, 17944.1)
W13	11.9	(1.2, 1302.4)
W16	165.5	(66.1, 405.6)
MG01	121.4	(63.1, 329.6)
MG02	371.8	(124.4, 1035.6)
MG03	270	(104.1, 1739.6)
MG04	32.9	(8.1, 128.9)
MG07	343.6	(118.7, 1305.4)
W20	743.5	(368.8, 1599.2)

For further details on model selection, please see refer to MacKenzie & Scott-Hayward (2021).

Spatial Results

When a common scale was chosen to display the model predictions across all nine surveys, the surfaces were largely dominated by surveys W08 and W20 (Figure). In particular, significantly more Kittiwakes were seen in WG08. When all surveys were treated separately, clearer patterns were evident and there were similar concentrations in the south eastern area in surveys W08, MG01 and MG03 (Figure , Figure and

Figure) with a more central indication in W16 (Figure). Surveys W16 and W20 show increased numbers at the edge of the survey area (Figure and Figure).

These spatial surfaces showed clusters of Kittiwakes inside the existing windfarm footprint in one of the larger surveys (W13), while there was an indication of Kittiwake density in the proposed wind farm footprint in surveys W08, MG01, MG02 and MG03. There was some minimal overlap in MG07 also in the southern tip of the proposed area.

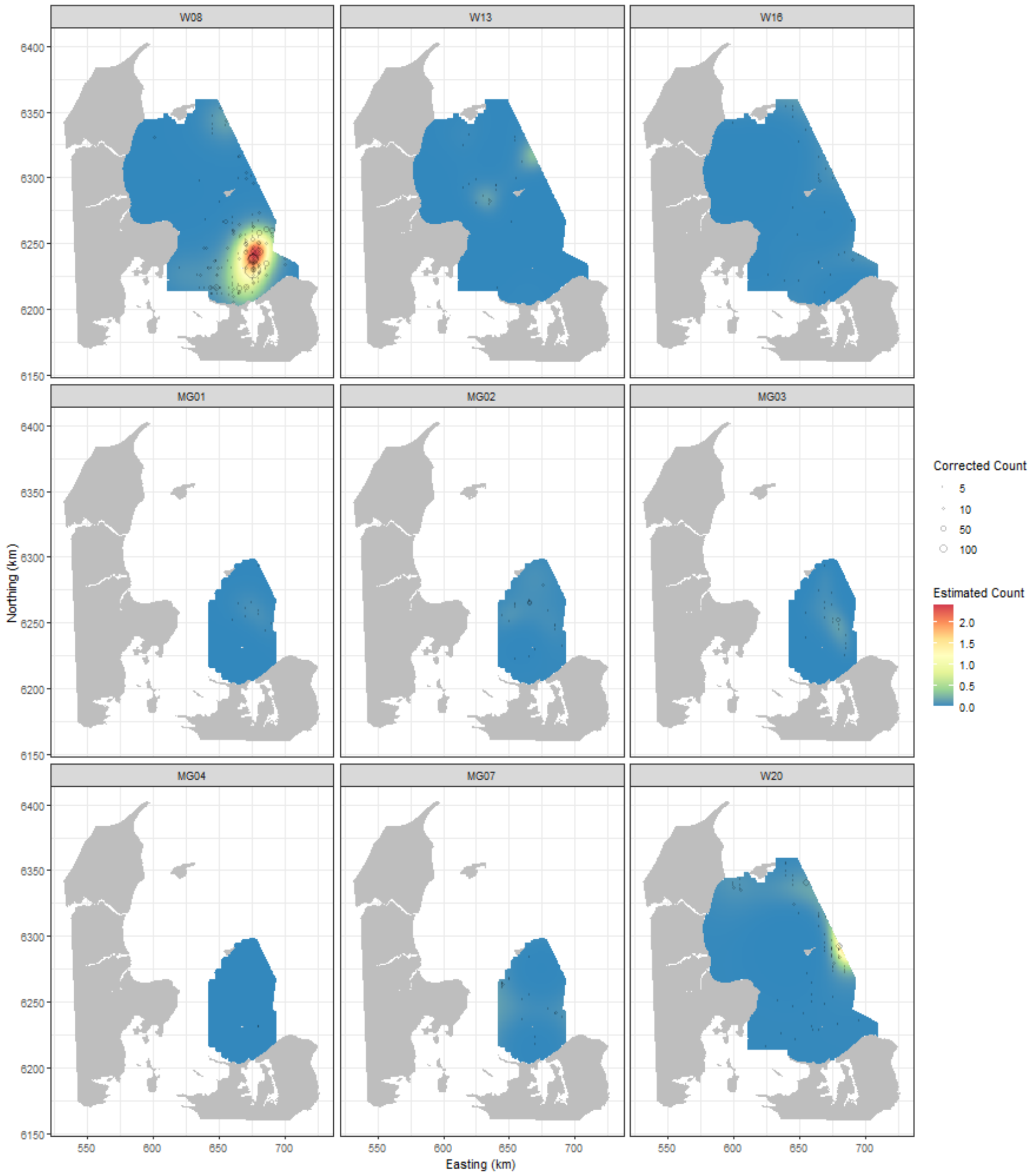

Figure 57: Figure showing the average Kittiwake count across the study site for each of the nine surveys. The counts are per 500x500m grid cell. The open circles show the observed, distance corrected count while the coloured graphics represent the predicted values in each location.

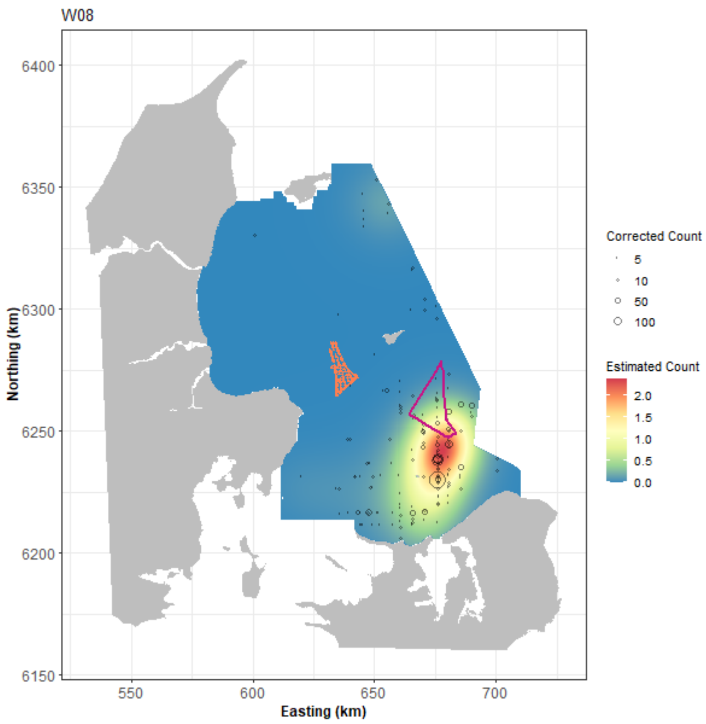

Figure 58: Figure showing the average Kittiwake count across the study site for the W08 survey. The counts are per 500x500m grid cell. The open circles show the observed, distance corrected count while the coloured graphics represent the predicted values in each location.

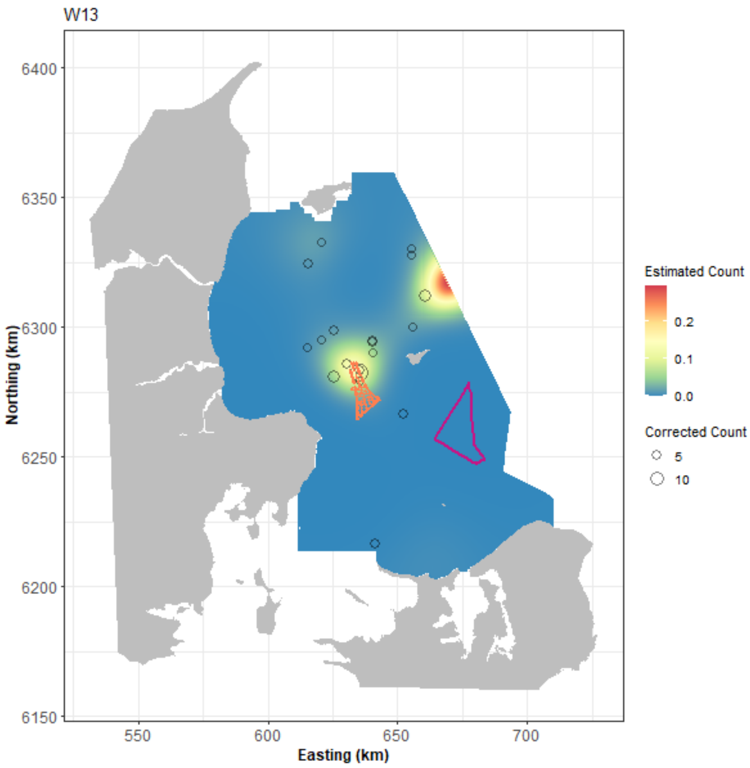

Figure 59: Figure showing the average Kittiwake count across the study site for the W13 survey. The counts are per 500x500m grid cell. The open circles show the observed, distance corrected count while the coloured graphics represent the predicted values in each location.

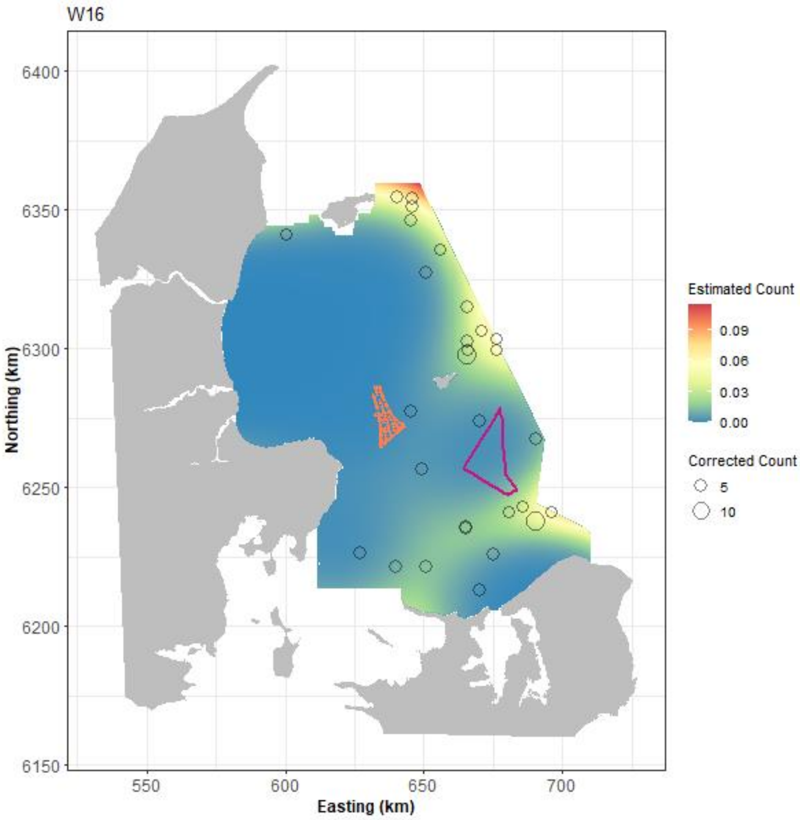

Figure 60: Figure showing the average Kittiwake count across the study site for the W16 survey. The counts are per 500x500m grid cell. The open circles show the observed, distance corrected count while the coloured graphics represent the predicted values in each location.

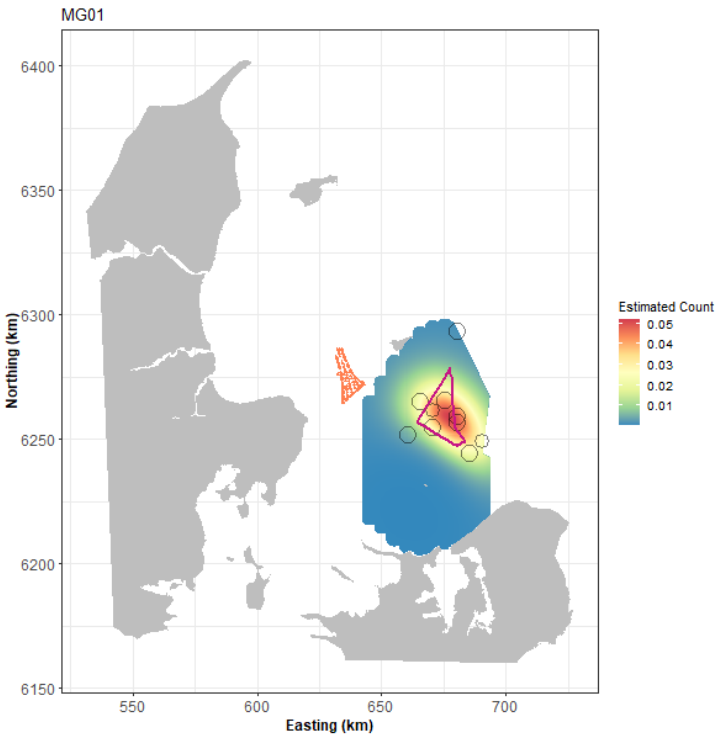

Figure 61: Figure showing the average Kittiwake count across the study site for the MG01 survey. The counts are per 500x500m grid cell. The open circles show the observed, distance corrected count while the coloured graphics represent the predicted values in each location.

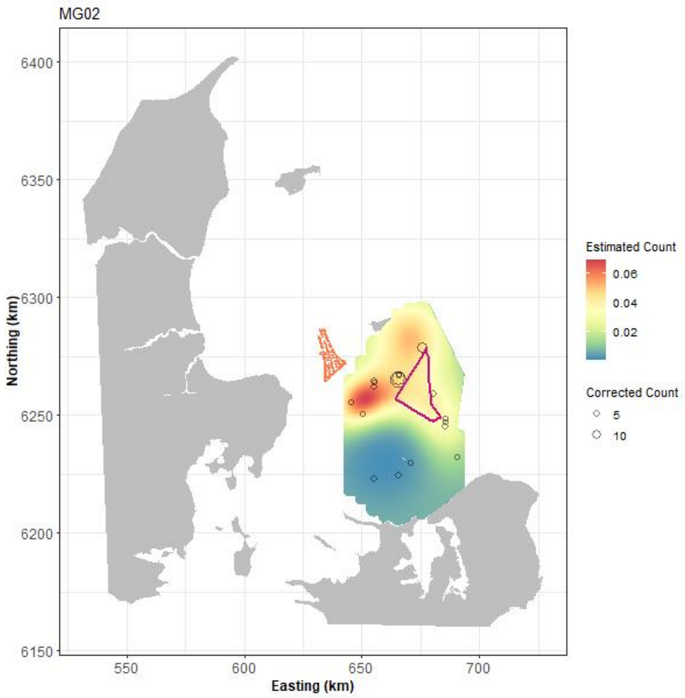

Figure 62: Figure showing the average Kittiwake count across the study site for the MG02 survey. The counts are per 500x500m grid cell. The open circles show the observed, distance corrected count while the coloured graphics represent the predicted values in each location.

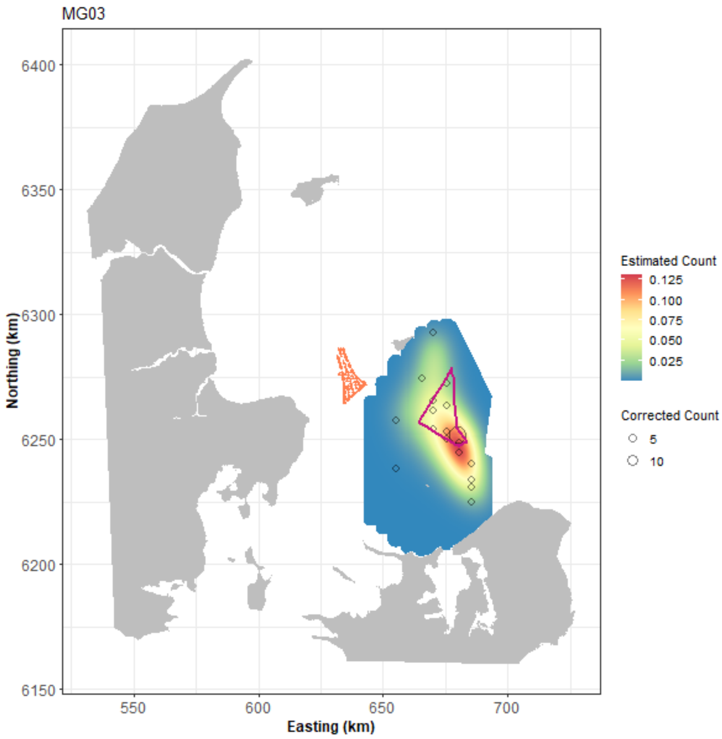

Figure 63: Figure showing the average Kittiwake count across the study site for the MG03 survey. The counts are per 500x500m grid cell. The open circles show the observed, distance corrected count while the coloured graphics represent the predicted values in each location.

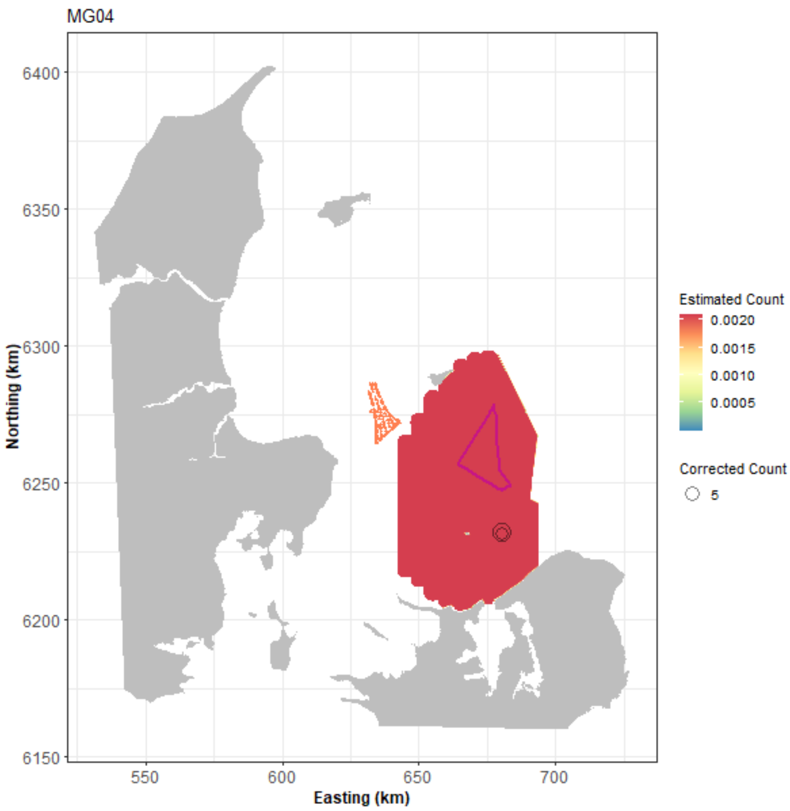

Figure 64: Figure showing the average Kittiwake count across the study site for the MG04 survey. The counts are per 500x500m grid cell. The open circles show the observed, distance corrected count while the coloured graphics represent the predicted values in each location.

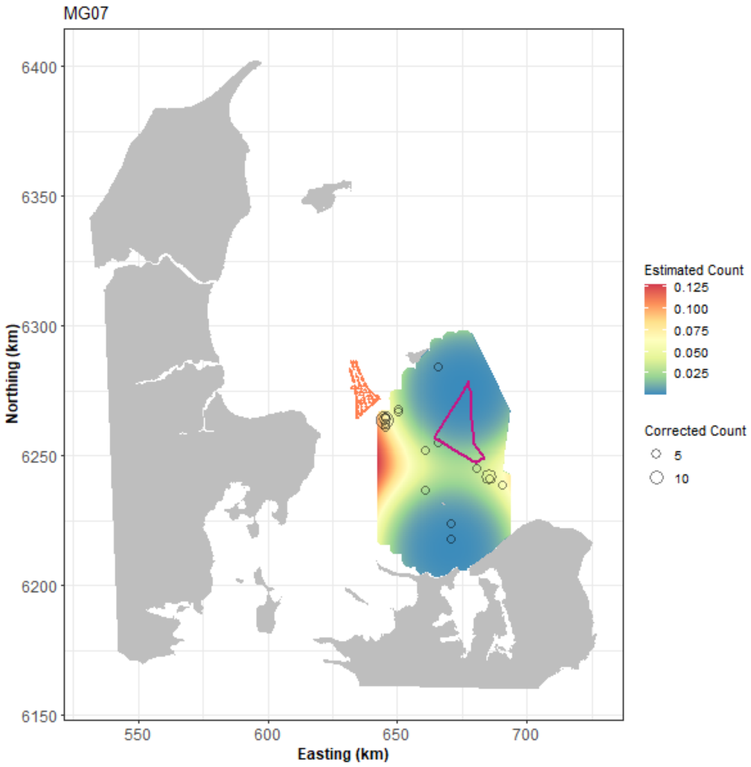

Figure 65: Figure showing the average Kittiwake count across the study site for the MG07 survey. The counts are per 500x500m grid cell. The open circles show the observed, distance corrected count while the coloured graphics represent the predicted values in each location.

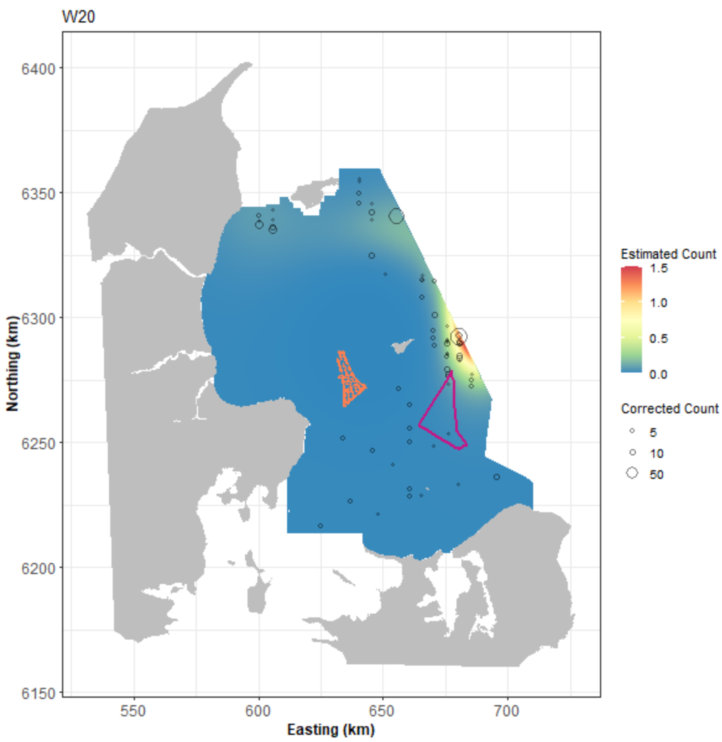

Figure 66: Figure showing the average Kittiwake count across the study site for the W20 survey. The counts are per 500x500m grid cell. The open circles show the observed, distance corrected count while the coloured graphics represent the predicted values in each location.

Uncertainty in the spatial predictions

The highest CV scores were associated with the very smallest predictions, however it is well-known that the CV metric is highly sensitive to any uncertainty for very small predictions and therefore results in no concerns in this case (Figure and Figure). The intercept only models are evident here by their single colour representing the uncertainty about the mean in each case.

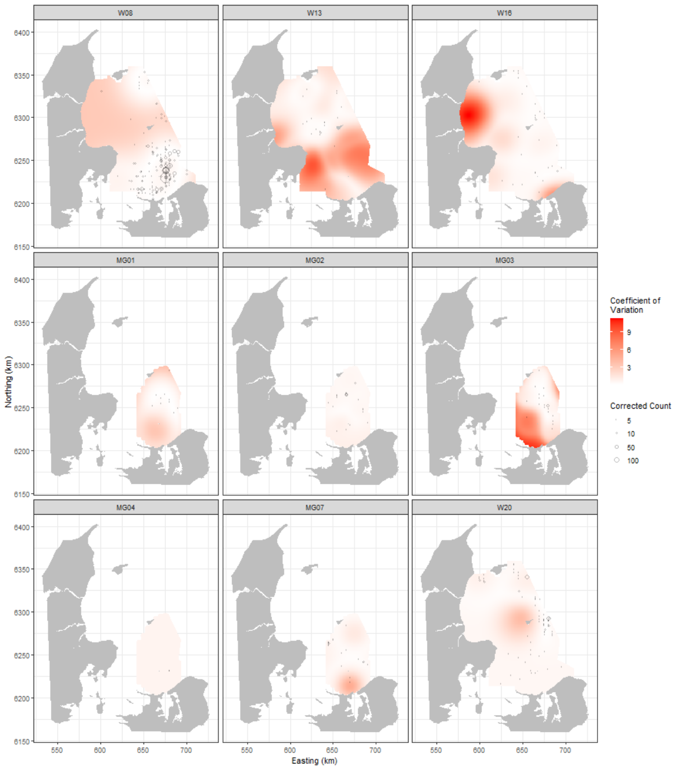

Figure 67: Figure showing the coefficient of variation (untruncated) across the study region for each of the surveys. The open circles show the observed, distance corrected counts.

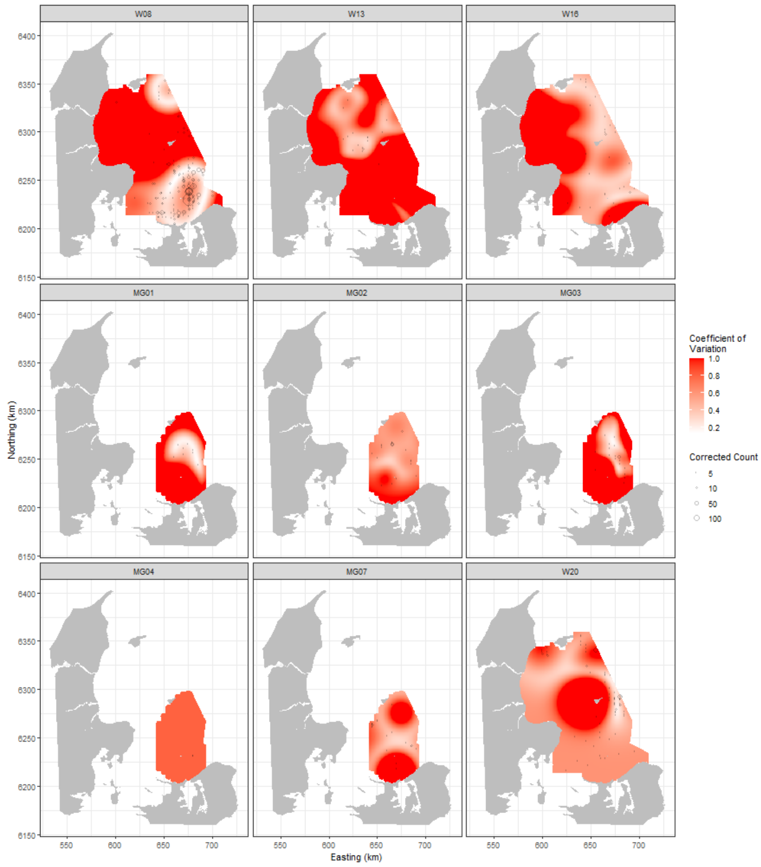

Figure 68: Figure showing the coefficient of variation across the study region for each of the surveys, capped at one. The open circles show the observed, distance corrected counts.

For further information on uncertainty in the spatial predictions, please refer to MacKenzie & Scott-Hayward (2021).

Areas of Persistence

There is evidence of relatively high persistence at the centre and north-eastern edge of the (reduced survey) area, and very low persistence towards the north-western edge of the survey area (Figure). This aligns well with the survey results which show these patterns in these areas (Figure -Figure). The proposed footprint area encloses mostly low-to-moderate (~0.3) levels of persistence.

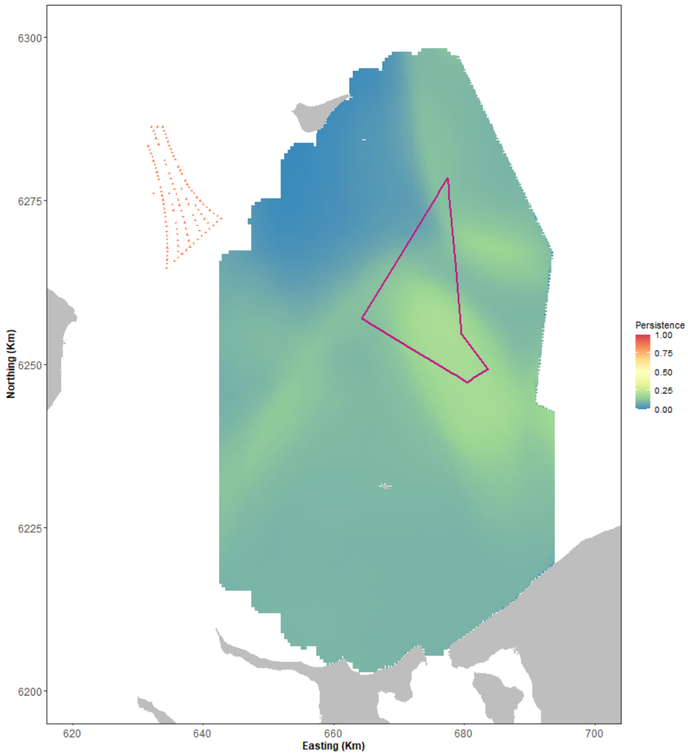

Figure 69: Kittiwake persistence scores across the MG survey area (reduced survey area with consistent overlap).

Razorbill/Guillemot *Alca torda/Uria aalge*

In this report Razorbill and Guillemot are treated as a group because identification to species is challenging and often impossible during the aerial surveys.

More than 13,000 Razorbills/Guillemots was recorded during the 11 surveys, with highly fluctuating numbers between surveys within the same period of time (Table 5). They were concentrated in the eastern and southeastern part of the study area (Figure 70). Of all the Razorbills/Guillemots 11,708 individuals were recorded within the Middelgrund Study Area, and 2,868 birds were recorded within a distance of 2 km from the proposed wind farm area.

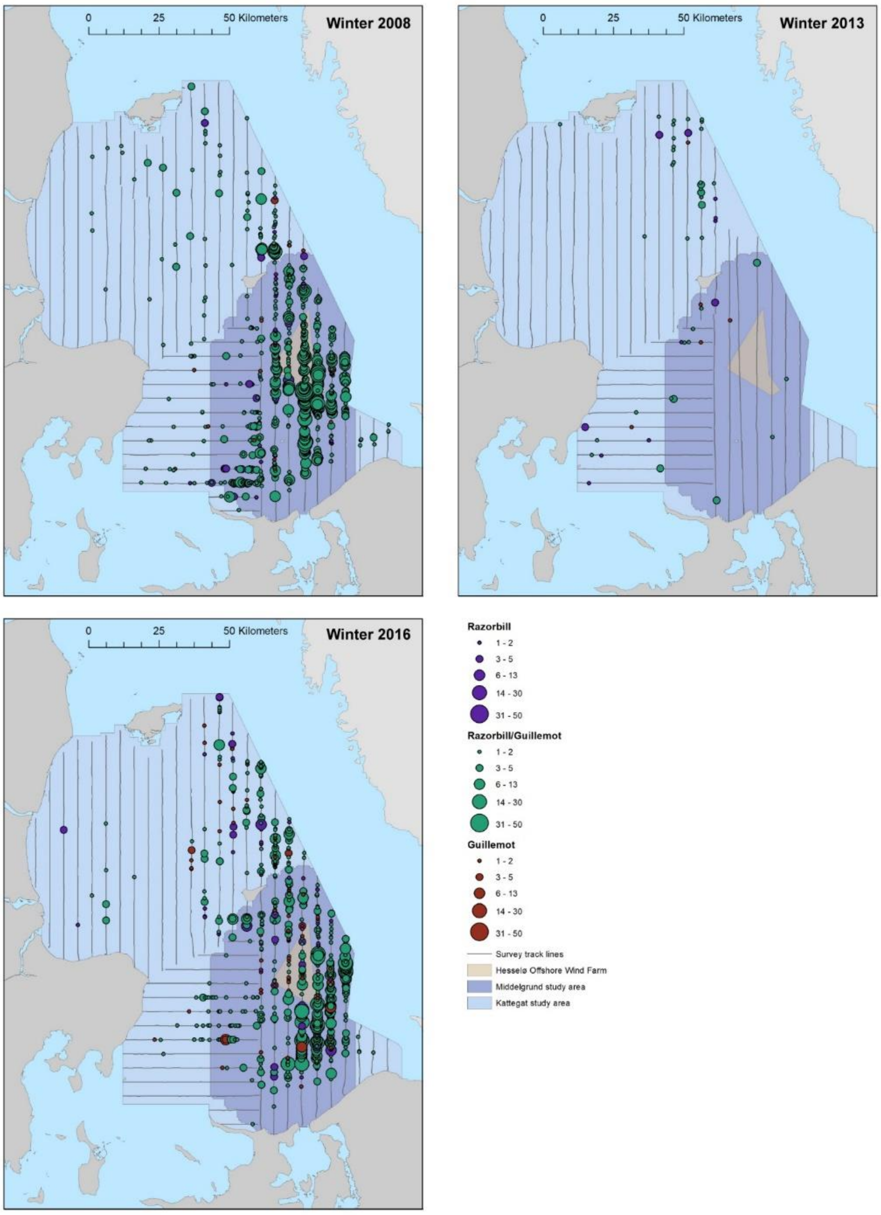

Figure 70. The spatial distribution of observed Razorbill/Guillemot from 11 surveys of birds in the study area between winter 2008 and winter 2020. Survey timing for the individual surveys are given in upper right corner of each map. The survey track lines covered for each survey is also given.

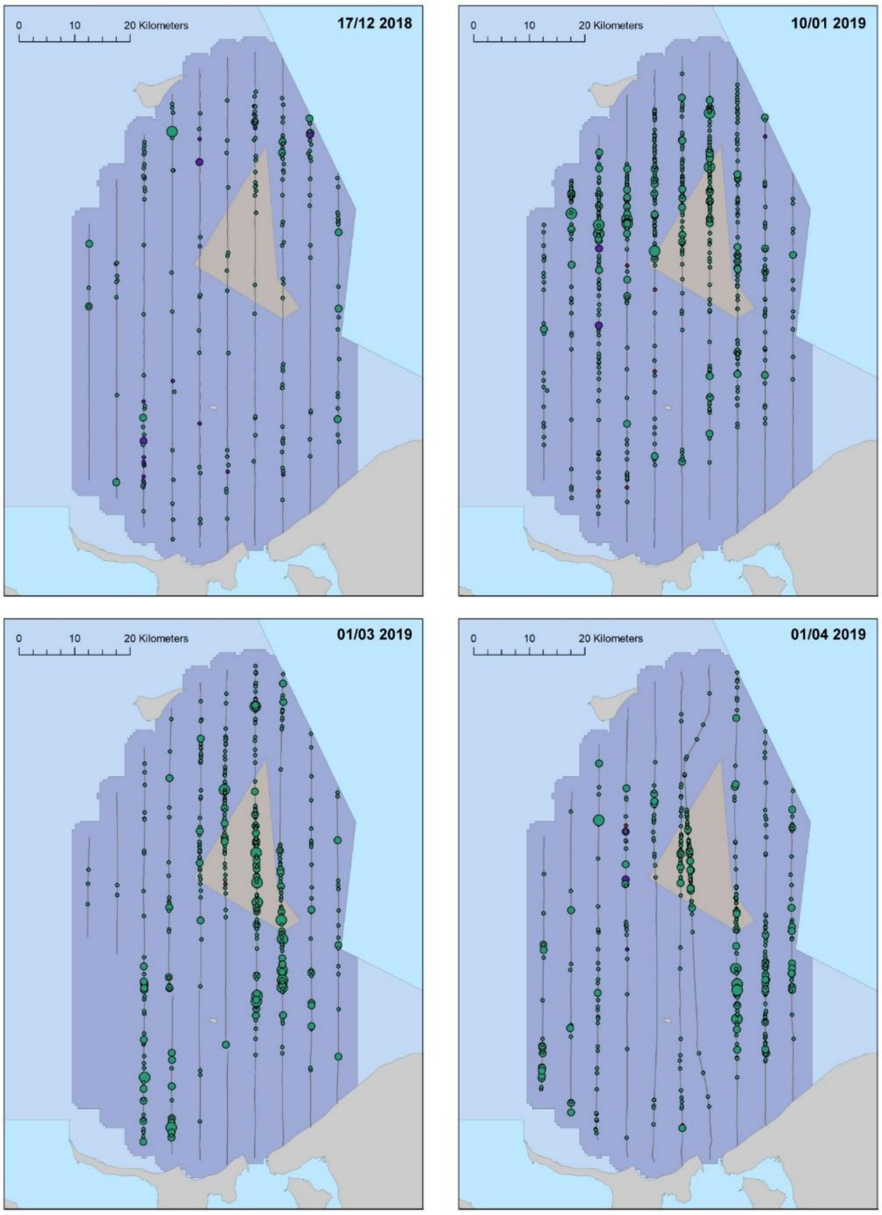

Figure 70. Razorbill/Guillemot, continued.

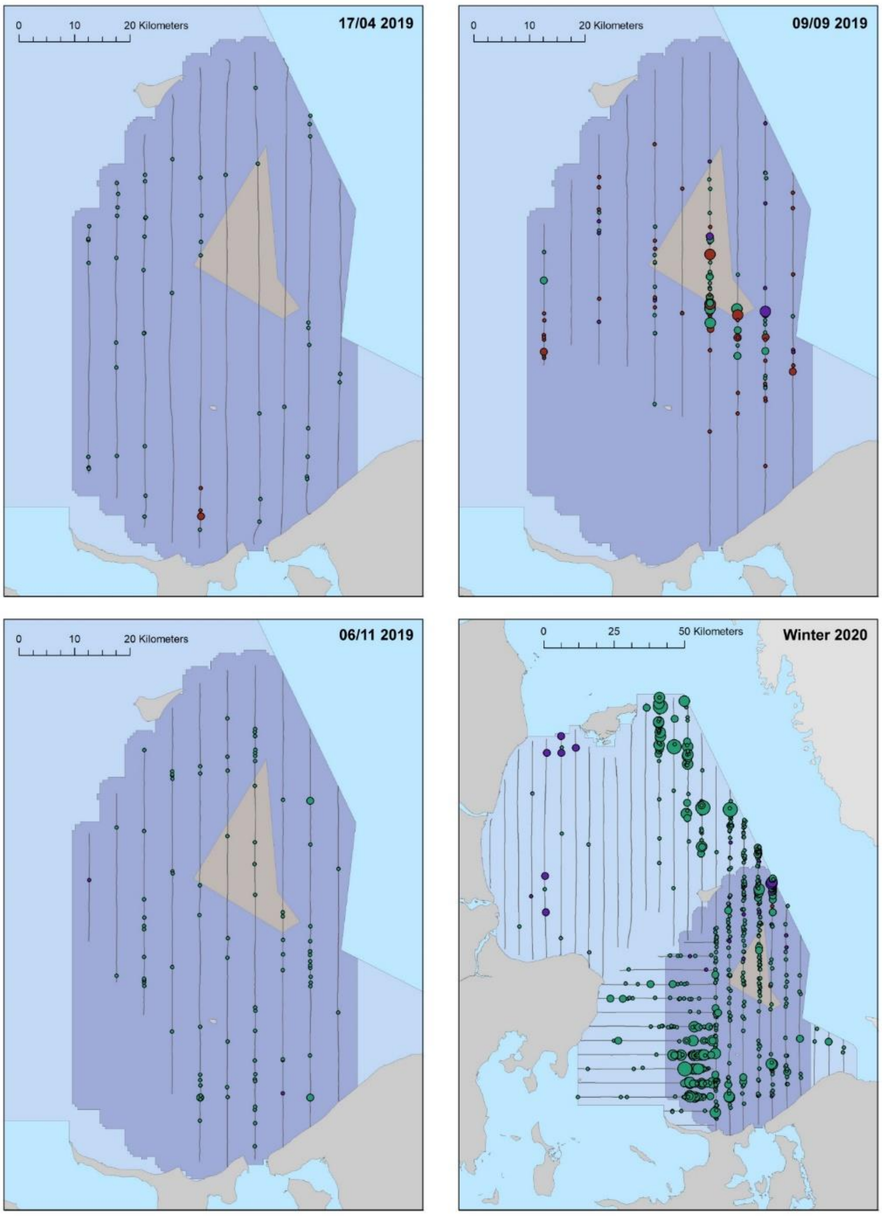

Figure 70. Razorbill/Guillemot, continued.

Razorbills/Guillemots were most abundant in the study area in late winter and early spring, and with generally lower presence in autumn and early winter (Figure 71).

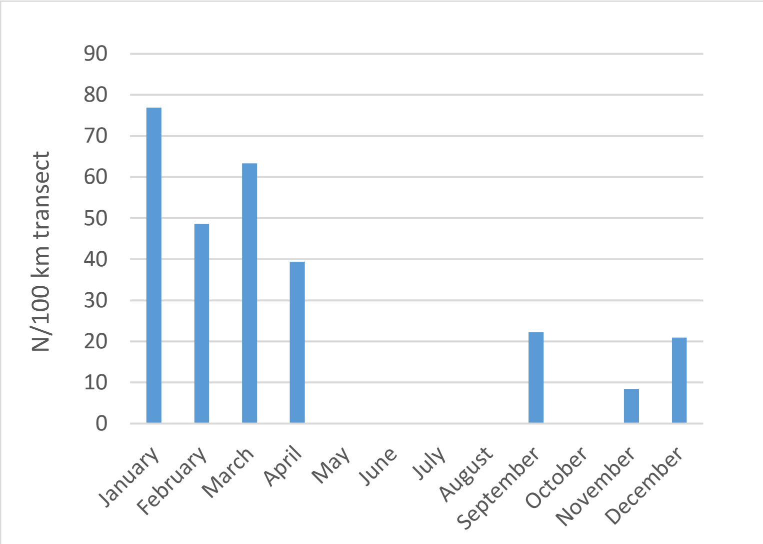

Figure 71. The annual variation in the relative density of Razorbill/Common Guillemot in the Kattegat survey area from 11 surveys included in this report.

Razorbills/Guillemots are pursuit feeders, foraging on small fish in the water column. They are therefore found on deeper waters than for instance diving ducks. The majority of birds were recorded within the water depth interval 20-34 meters, within which 80 % of the birds were observed (Figure 72).

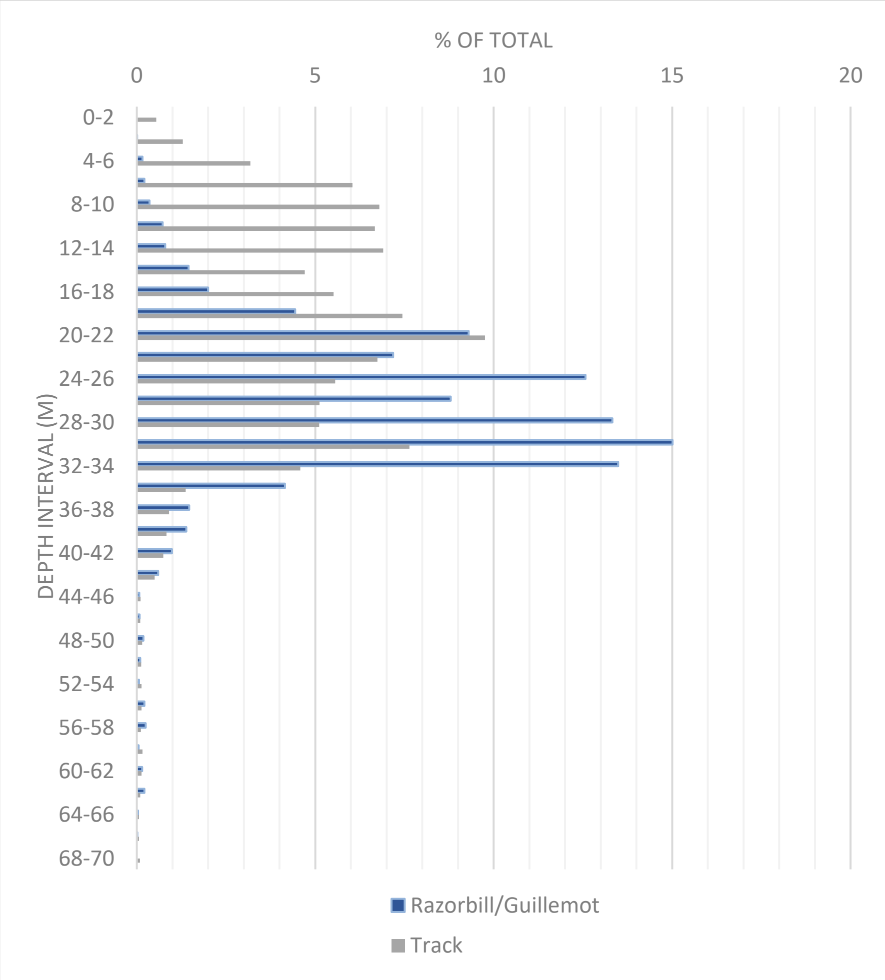

Figure 72. The depth frequency distribution of Razorbill/Guillemot in the Kattegat Study Area in 2 m depth intervals and expressed as % of total numbers observed. The depth frequency distribution of the covered survey track lines is given for comparison.

Distance Analysis

The average probability of sighting Razorbills/Guillemots was estimated to be 0.4 (CV=0.014). This probability was estimated using a hazard rate detection function that varied with observer (Figure). No other covariates were selected. As there were very few sightings in band D, these detections were excluded and the strip half width set to be 956m.

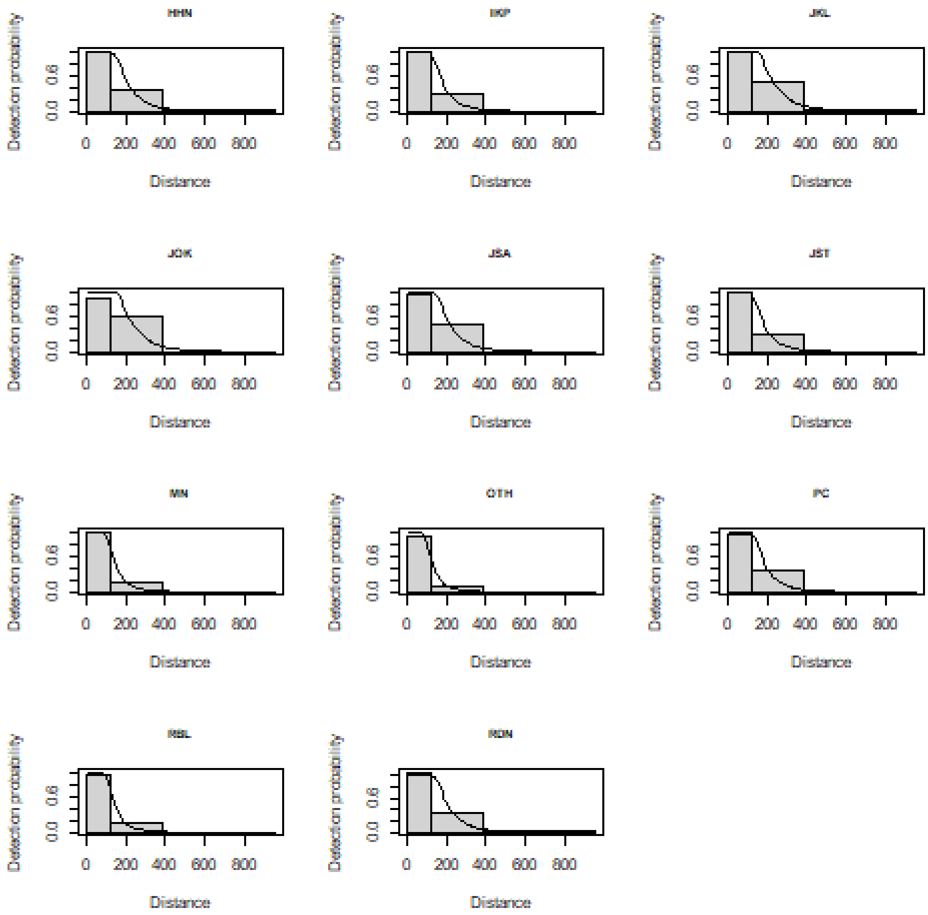

Figure 73: Figure showing the estimated detection function for each of the observers. The histograms are the distances of the observed sightings.

The dataset for the spatial analysis comprised 29,293 segments, 11 % of which were segments containing Razorbills/Guillemots sightings. Table shows the breakdown of survey effort within each of the 11 surveys and Figure shows the distribution of the distance corrected counts.

Table 17: Table showing a summary of the survey effort for the Razorbills/Guillemots species in each of the 11 surveys.

Survey	Number of Segments	
	With Sightings	Total
W08	611	4930
W13	54	4805
W16	605	4920
MG01	187	1481
MG02	439	1469
MG03	333	1368
MG04	311	1484
MG05	52	1477
MG06	102	1160
MG07	86	1313

W20	545	4886

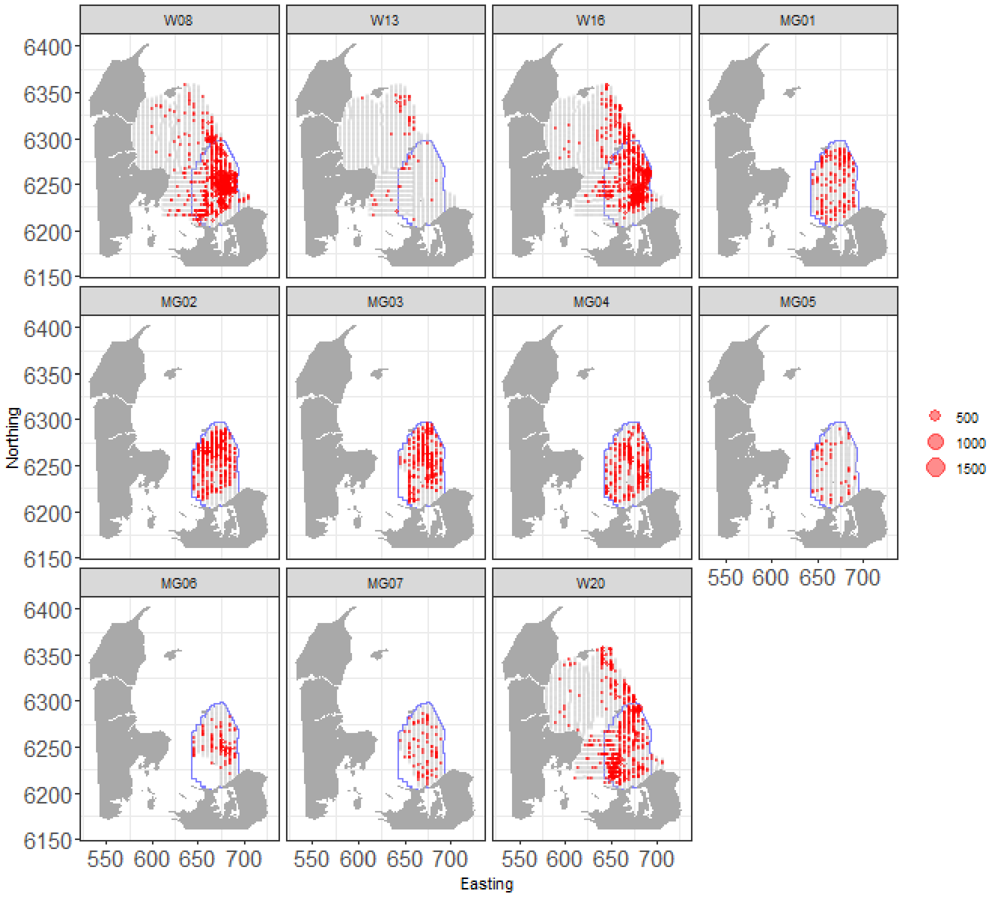

Figure 74: Distance-corrected counts of Razorbills/Guillemots for the 11 surveys. The red circles indicate the distance-corrected counts along the transect lines while the grey polygons represent land. The blue line denotes the MG study area.

Model Selection results

There was compelling evidence for spatial patterns in Razorbills/Guillemots density across 10 of the 11 surveys (of variable complexity) and no evidence for a water depth relationship for any survey. In one survey (MG07), no model terms were selected (using objective fit criteria) returning a single (mean) value for the entire survey area in this case (Table).

Notably, the spatial surfaces selected were relatively low dimensional (with between three and nine degrees of freedom) and all models estimated a dispersion parameter significantly larger than one, indicating an over-dispersed approach was justified (Table).

Table 18: Model selection results for the 11 surveys. "N/S" indicates the term was not selected as part of the 10-fold cross validation procedure and df=degrees of freedom for that relationship

Survey	Depth	s(xpos, y.pos)	Dispersion parameter estimate

W08	N/S	$p < 0.0001$ (df=9)	38.9
W13	N/S	$p < 0.0001$ (df=7)	9.73
W16	N/S	$p < 0.0001$ (df=4)	52.5
MG01	N/S	$p < 0.0001$ (df=3)	67.0
MG02	N/S	$p < 0.0001$ (df=8)	10.3
MG03	N/S	$p < 0.0001$ (df=5)	23.3
MG04	N/S	$p < 0.0001$ (df=6)	15.5
MG05	N/S	$p < 0.0001$ (df=6)	6.5
MG06	N/S	$p < 0.0001$ (df=7)	14.5
MG07	N/S	N/S	6.5
W20	N/S	$p < 0.0001$(df=3)	28.8

The estimated abundances within the Middelgrund Study Area and for each survey are given in Table . Survey W08 had the largest estimated abundance but also the largest uncertainty associated with this estimate (in line with the estimated mean-variance relationship). The uncertainty about this number (and those for W16) also indicated that numbers seen in W08 were statistically indistinct from numbers estimated in W16. W20 exhibited significantly lower numbers than the W08/W16 'group' and significantly lower numbers again were estimated in W13. Of the M-labelled surveys, there were three distinct groups which can be characterized as relatively low (MG05 and MG07), medium (MG01 and MG06) and relatively large abundance (MG02, MG03, MG04) groups.

Table 19: Table of estimated counts for the Middelgrund Study Area and for each survey. The 95 % CI are percentile-based confidence intervals from the 250 bootstraps generated which incorporate the uncertainty from both the detection function estimation and the subsequent spatial analyses.

Survey	Estimated Count	95 % CI
W08	52047	(32610, 84128)
W13	219	(92, 573)
W16	36688	(21514, 65449)
MG01	4027	(2936, 6098)
MG02	14295	(10765, 19989)
MG03	12636	(7932, 21464)
MG04	10742	(7512, 16137)
MG05	1016	(646, 1779)
MG06	4148	(2041, 8700)
MG07	1524	(1261, 1924)
W20	14203	(9879, 21479)

For further details on model selection, please see refer to MacKenzie & Scott-Hayward (2021).

Spatial Results

Figure shows the estimated average counts of Razorbills/Guillemots in each 500m^2 grid cell across each of the 11 surveys. These point estimates show clusters of individuals in the south east of the larger survey area in survey W08 and W16 with a more distributed picture in the W20 survey. Less distinctive (and more variable) patterns were evident in the reduced survey area (MG01-MG07) where numbers generally appeared higher in MG02—MG04 (also Figure).

The concentration of Razorbill/Guillemot numbers in the South East in surveys W08 and W16 are clearer when the scales are free to change across surveys (Figure and Figure). For the surveys restricted to the small study area (MG01-MG07), very low numbers of Razorbills/Guillemots were estimated to be present in the northwestern parts of the Middelgrund Study Area, close to the footprint of the Anholt OWF but the spatial patterns with reference to the proposed footprint suggest that the W08 and W16 surveys had elevated numbers of Razorbills/Guillemots in the southern tip. The W20 survey saw these patterns shift to the north and west of the proposed footprint area (Figure 86).

The reduced survey area applicable in surveys MG01 and MG02 exhibited similar patterns with increased numbers in the north and northwest (Figure and Figure). The spatial patterns shifted toward the centre and south of this area in MG03 (Figure) but became more widely distributed in surveys MG04 and MG05 before a return to this centre in MG06 (Figure). A single mean value was estimated for Razorbill/Guillemot across the survey area in MG07 due to the lack of model terms selected using the objective fit criteria (Figure). Notably, the proposed wind farm area overlaps with moderate-to-high numbers of Razorbill/Guillemot in all MG surveys to some extent, excepting MG05.

Figure 75: Figure showing the average Razorbill/Guillemot count across the study site for each of the 11 surveys. The counts are per 500x500m grid cell. The open circles show the observed, distance corrected count while the coloured graphics represent the predicted values in each location.

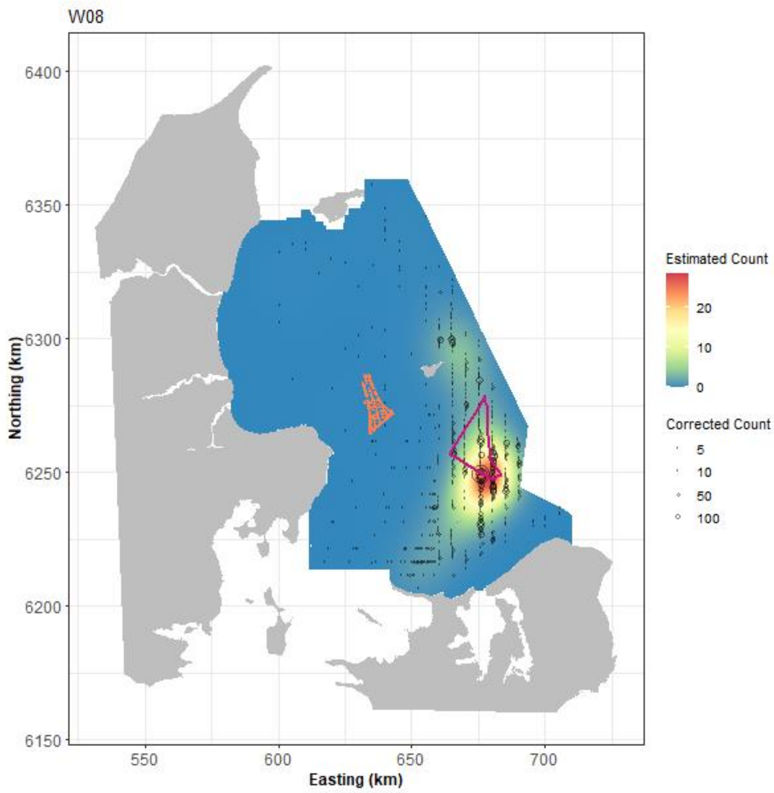

Figure 76: Figure showing the average Razorbill/Guillemot count across the study site for the W08 survey. The counts are per 500x500m grid cell. The open circles show the observed, distance corrected count while the coloured graphics represent the predicted values in each location.

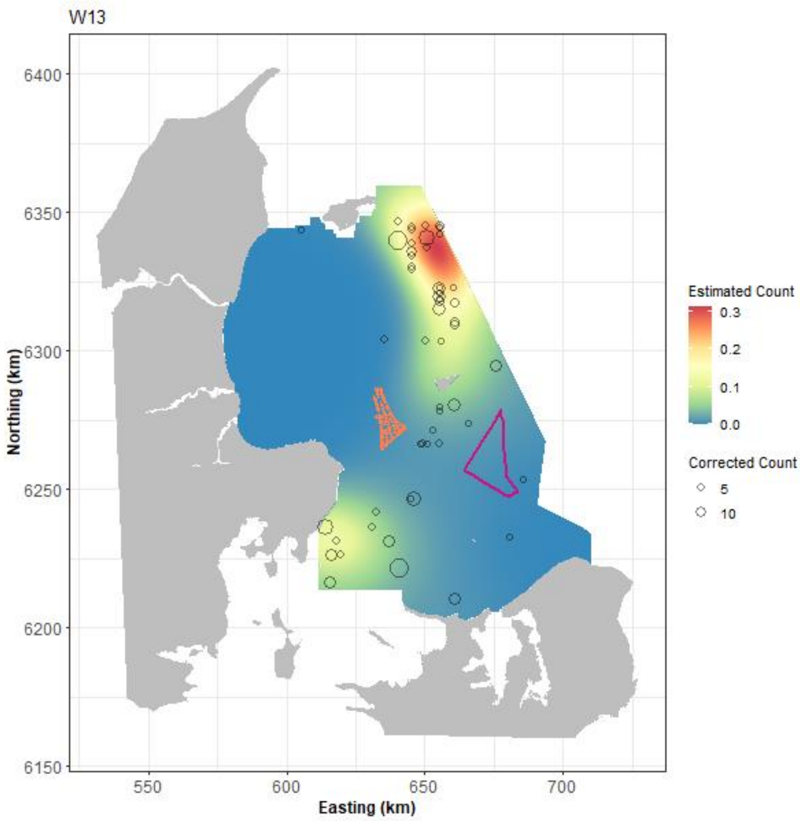

Figure 77: Figure showing the average Razorbill/Guillemot count across the study site for the W13 survey. The counts are per 500x500m grid cell. The open circles show the observed, distance corrected count while the coloured graphics represent the predicted values in each location.

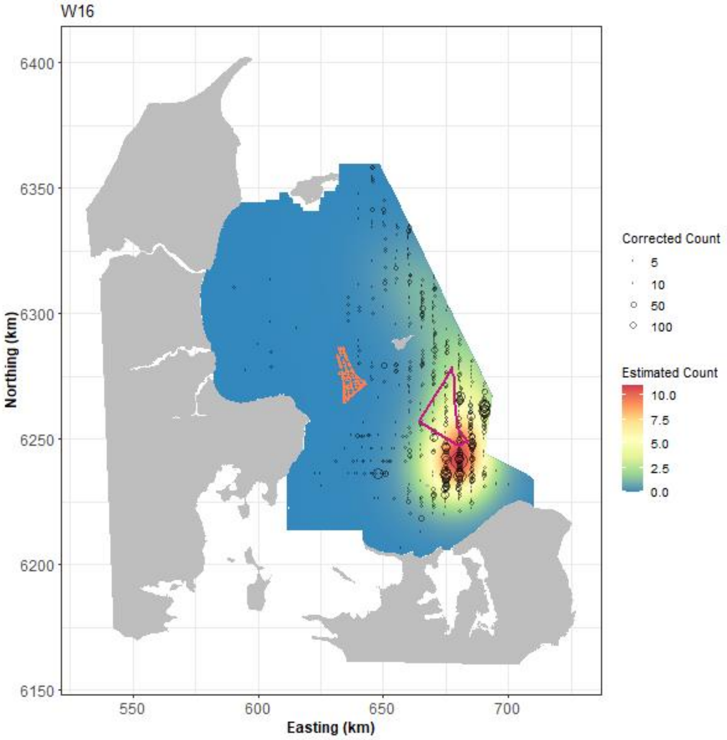

Figure 78: Figure showing the average Razorbill/Guillemot count across the study site for the W16 survey. The counts are per 500x500m grid cell. The open circles show the observed, distance corrected count while the coloured graphics represent the predicted values in each location.

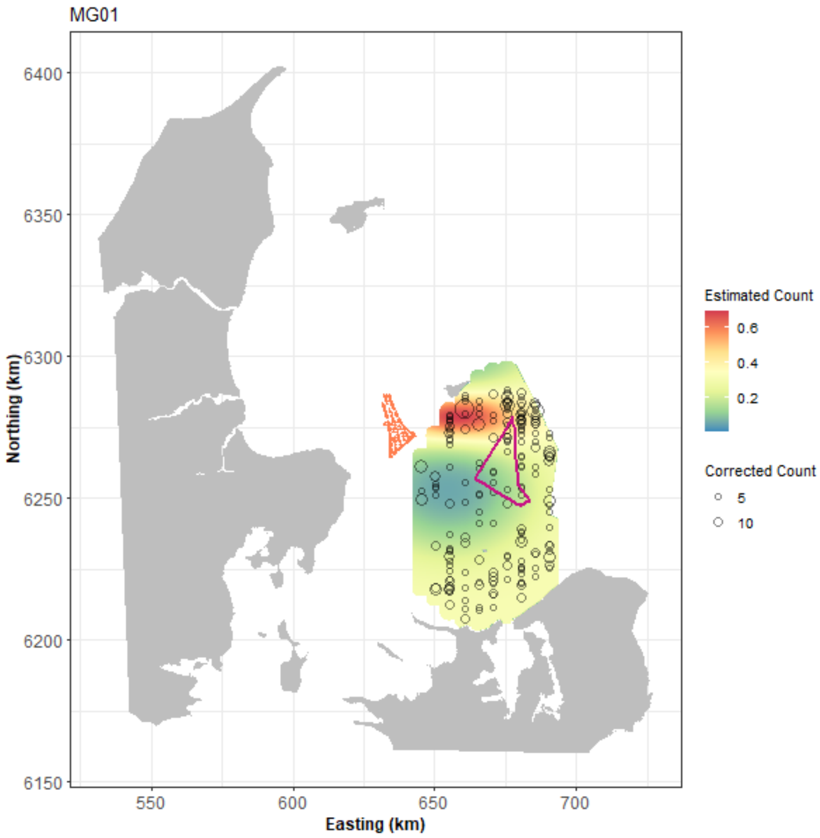

Figure 79: Figure showing the average Razorbill/Guillemot count across the study site for the MG01 survey. The counts are per 500x500m grid cell. The open circles show the observed, distance corrected count while the coloured graphics represent the predicted values in each location.

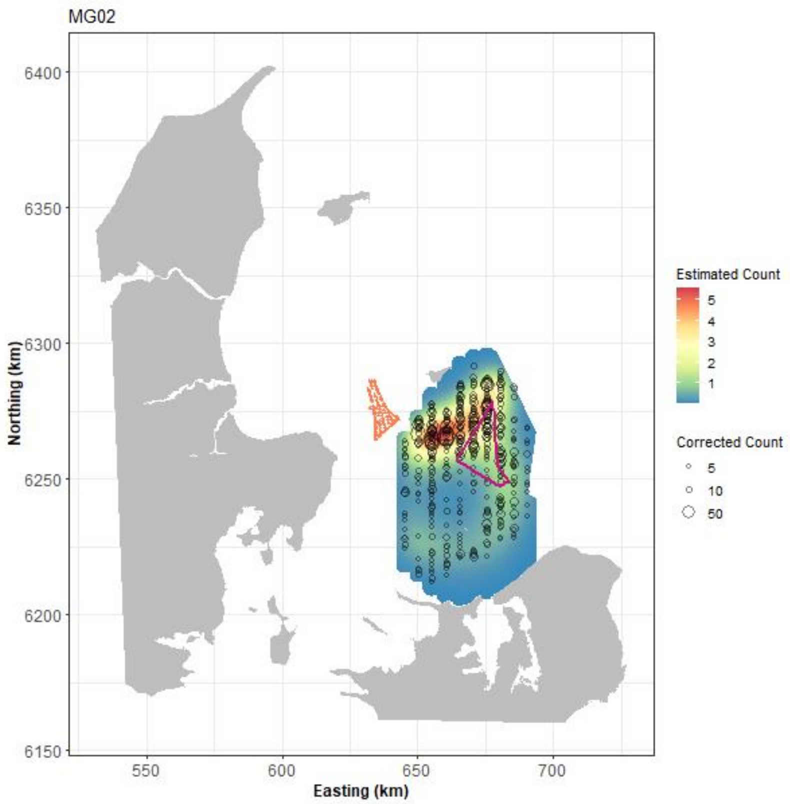

Figure 80: Figure showing the average Razorbill/Guillemot count across the study site for the MG02 survey. The counts are per 500x500m grid cell. The open circles show the observed, distance corrected count while the coloured graphics represent the predicted values in each location.

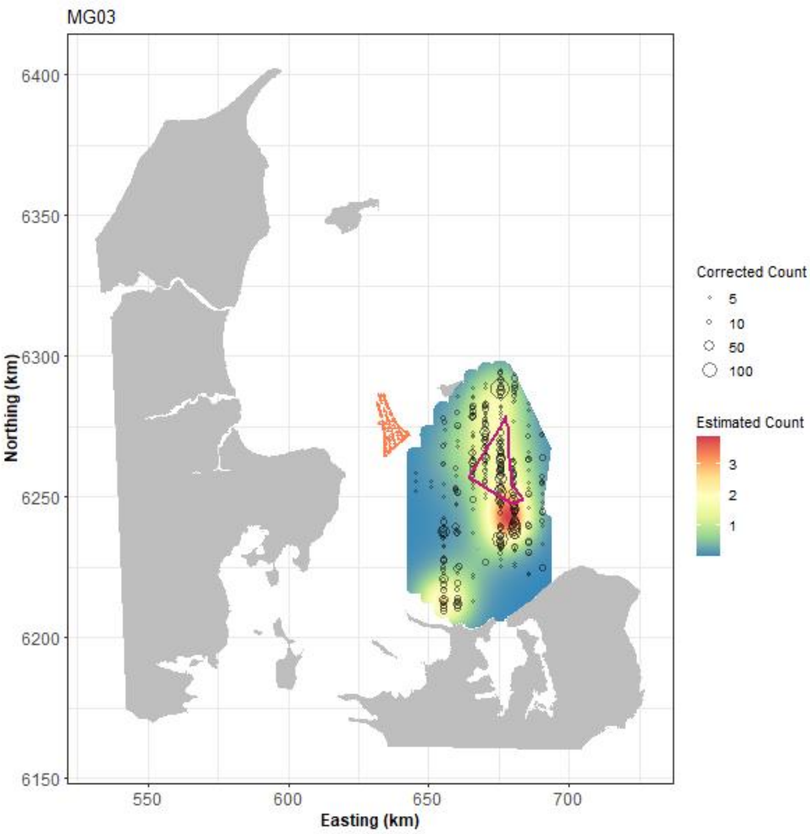

Figure 81: Figure showing the average Razorbill/Guillemot count across the study site for the MG03 survey. The counts are per 500x500m grid cell. The open circles show the observed, distance corrected count while the coloured graphics represent the predicted values in each location.

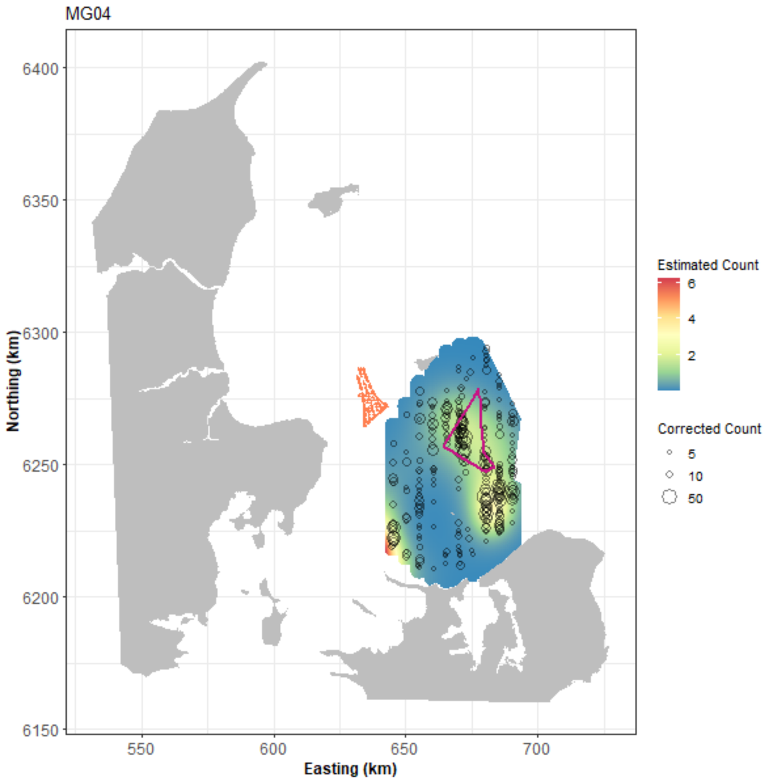

Figure 82: Figure showing the average Razorbill/Guillemot count across the study site for the MG04 survey. The counts are per 500x500m grid cell. The open circles show the observed, distance corrected count while the coloured graphics represent the predicted values in each location.

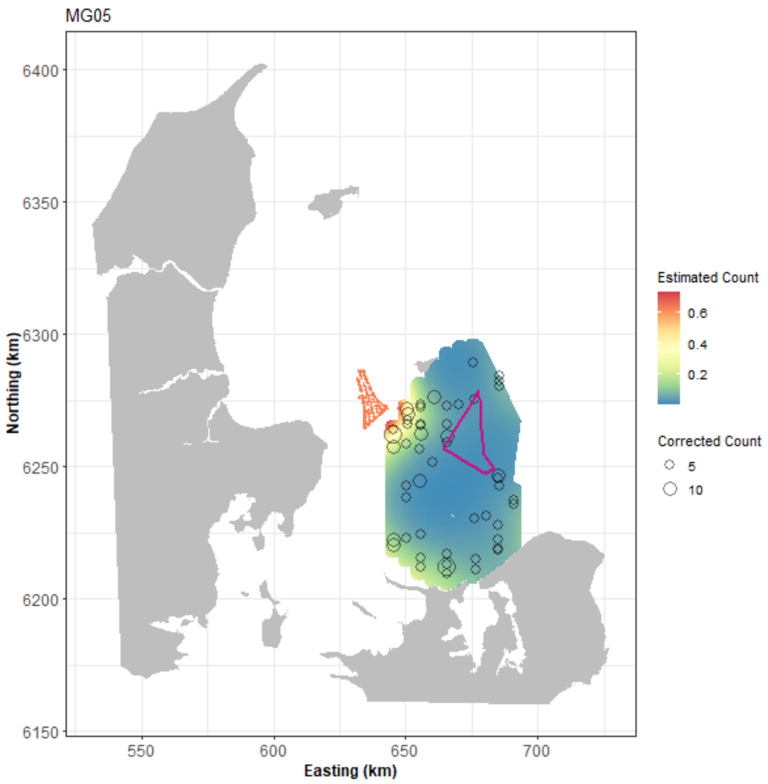

Figure 83: Figure showing the average Razorbill/Guillemot count across the study site for the MG05 survey. The counts are per 500x500m grid cell. The open circles show the observed, distance corrected count while the coloured graphics represent the predicted values in each location.

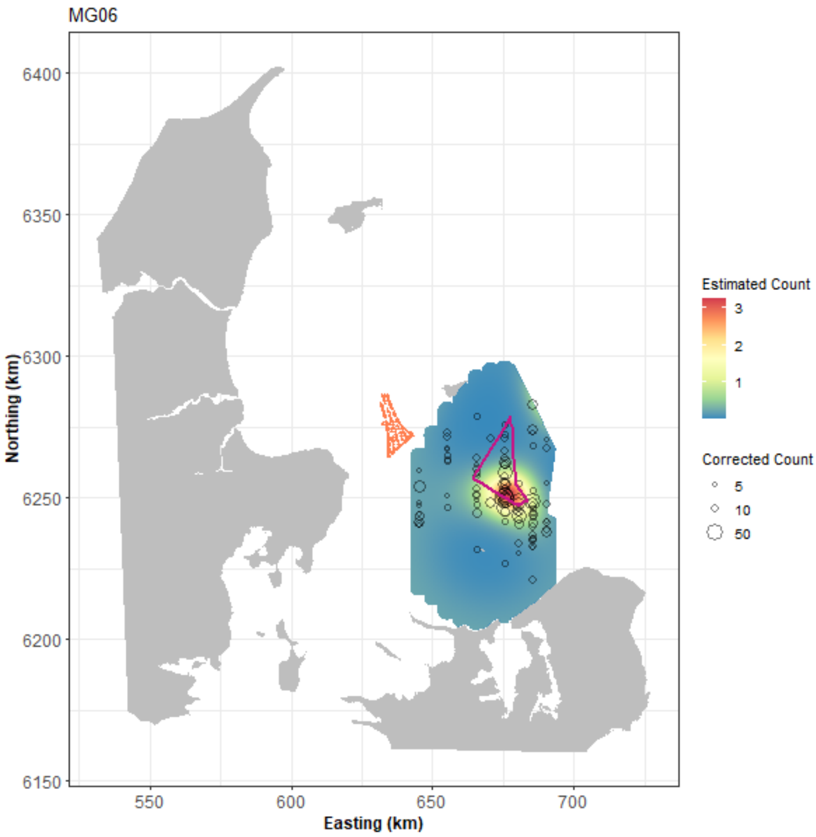

Figure 84: Figure showing the average Razorbill/Guillemot count across the study site for the MG06 survey. The counts are per 500x500m grid cell. The open circles show the observed, distance corrected count while the coloured graphics represent the predicted values in each location.

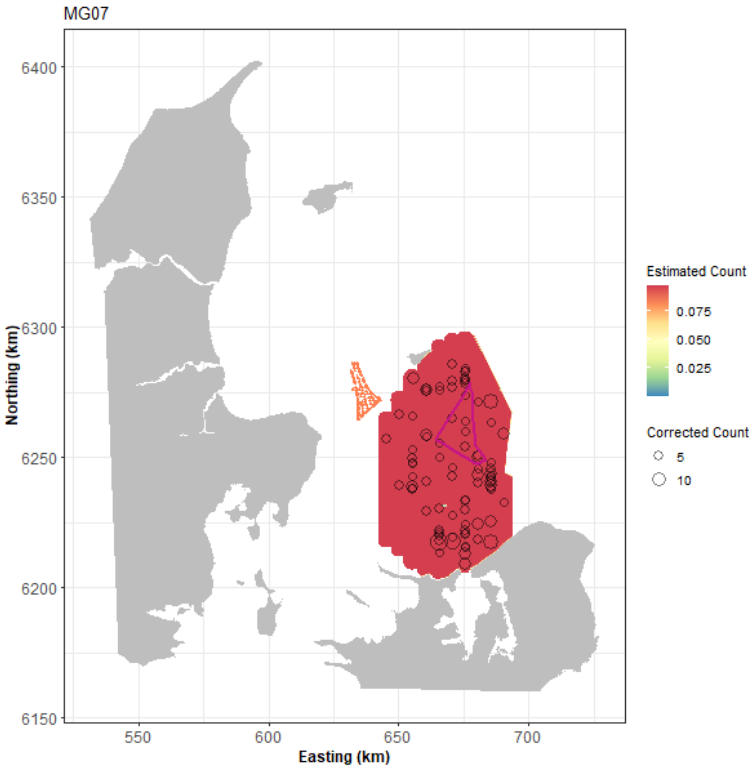

Figure 85: Figure showing the average Razorbill/Guillemot count across the study site for the MG07 survey. The counts are per 500x500m grid cell. The open circles show the observed, distance corrected count while the coloured graphics represent the predicted values in each location.

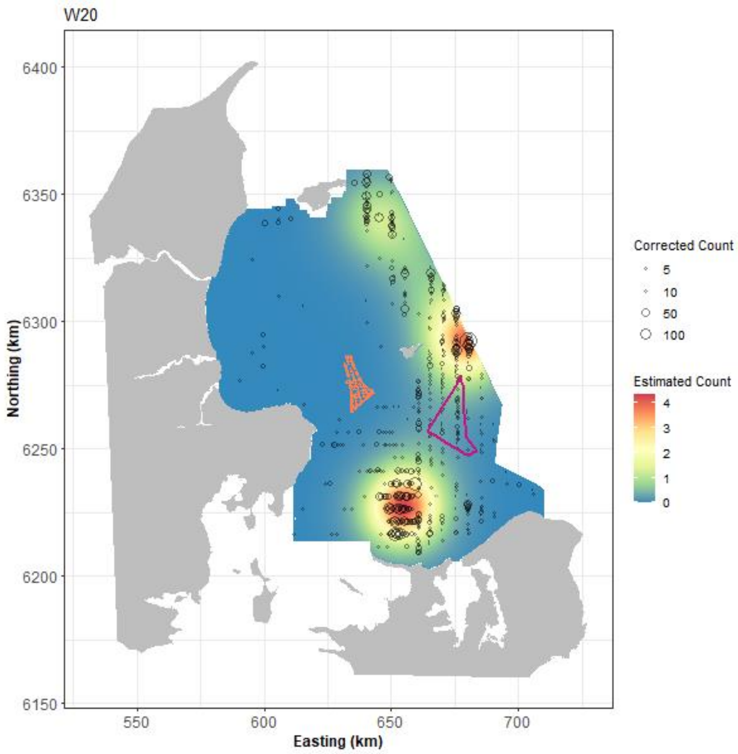

Figure 86: Figure showing the average Razorbill/Guillemot count across the study site for the W20 survey. The counts are per 500x500m grid cell. The open circles show the observed, distance corrected count while the coloured graphics represent the predicted values in each location.

Uncertainty in the spatial predictions

The highest CV scores were associated with the very smallest predictions, however it is well-known that the CV metric is highly sensitive to any uncertainty for very small predictions and therefore results in no concerns in this case (Figure). There was no material overlap between the CV metric and the transect lines/locations with non-zero counts.

Upon closer inspection, when the CV is capped at one (Figure), no concerns are revealed and further demonstrates the relationship between large CV values when there are predictions very close to zero.

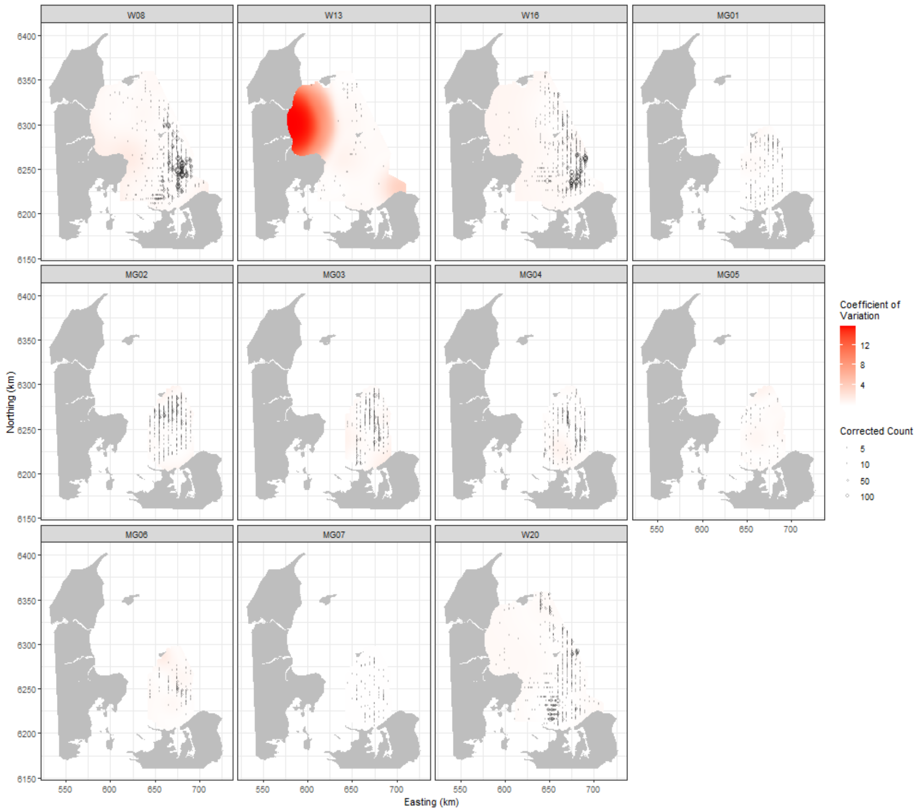

Figure 87: Figure showing the coefficient of variation across the study region for each of the surveys. The open circles show the observed, distance corrected counts.

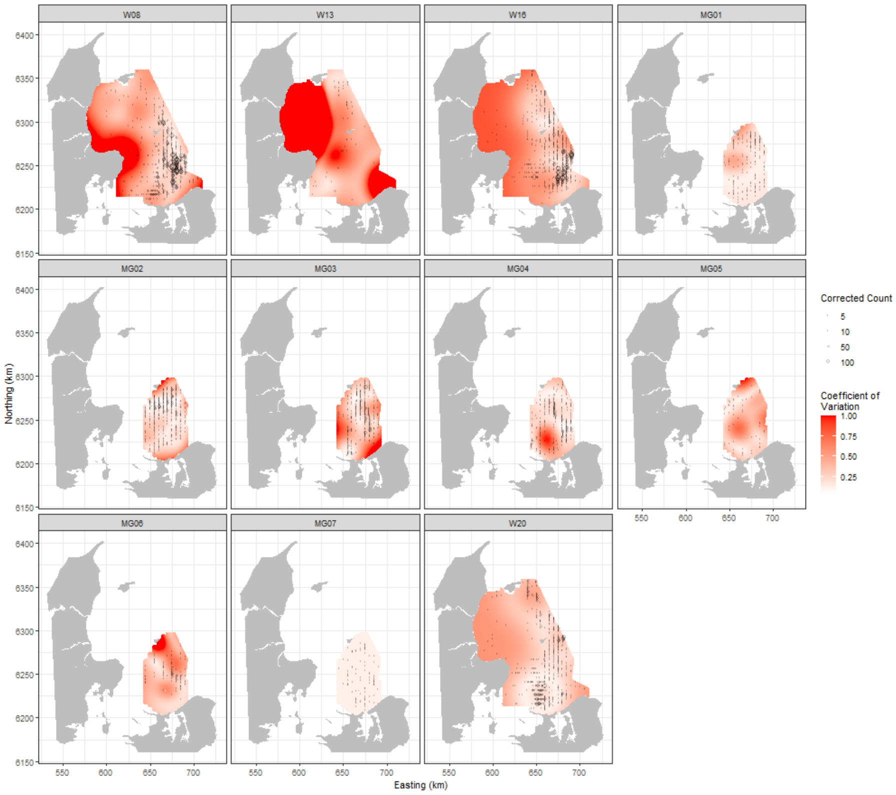

Figure 88: Figure showing the coefficient of variation across the study region for each of the surveys, capped at one. The open circles show the observed, distance corrected counts.

For further information on uncertainty in the spatial predictions, please refer to MacKenzie & Scott-Hayward (2021).

Areas of Persistence

There is evidence of approximately 50 % persistence in the central (and northern) part of the reduced survey area, and very low persistence towards the west and southern edge of the survey area (Figure 89). This moderate persistence also predominantly characterises the proposed wind farm footprint, with a slight elevation of persistence (~0.6) in the southern tip of the proposed footprint.

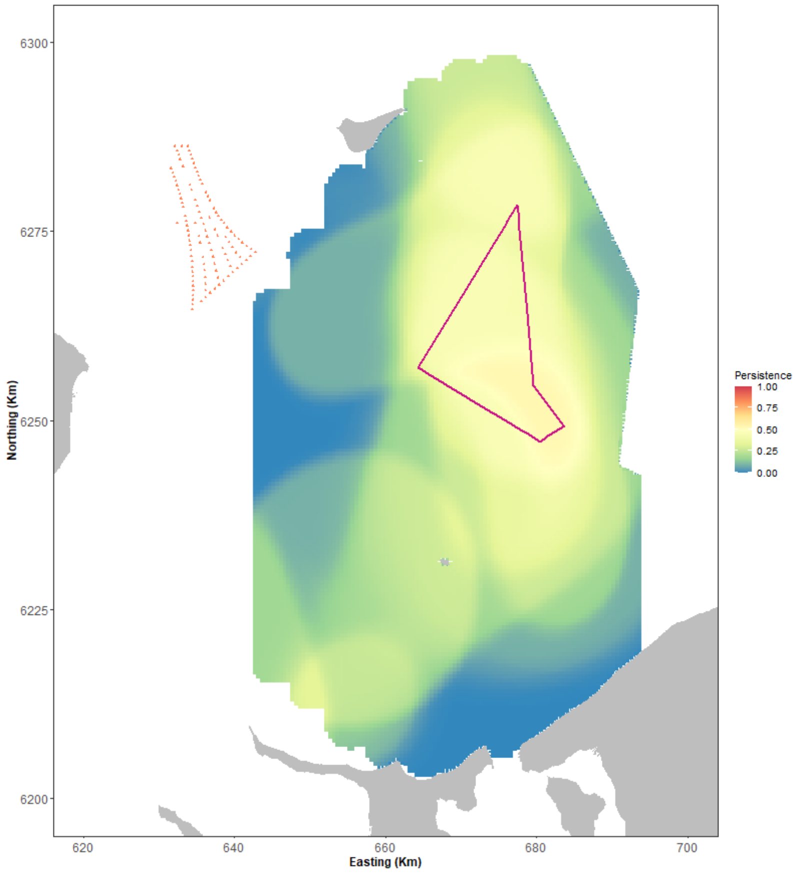

Figure 89: Persistence scores for Razorbill/Guillemot across the MG survey area (reduced survey area with consistent overlap).

Population status of selected species

In this section a population status for selected species/species groups is presented, based on a literature study.

Red-throated Diver/Black-throated Diver *Gavia stellata/Gavia arctica*

The northwest European population of Red-throated Diver is estimated at 210,000 to 340,000 individuals and a 1% criteria at 3,000 birds (2018), while the arctic, northwest European and western Siberian population of Black-throated Diver is estimated at 390,000 to 590,000 individuals and a 1% criteria at 3,500 birds (2012) (Wetlands International 2021).

Gannet *Morus bassanus*

The species is observed in increasing numbers in the Inner Danish Waters and is now fairly common in the appropriate season within Kattegat and is also quite commonly seen from land. Observations of >5,000 birds have been recorded from Skagen, but >1,000 birds also reported from northern Zealand and Djursland (www.dofbasen.dk). The North Atlantic population is estimated at 1,6 million individuals (Table 20).

Table 20. Total population estimate and population 1 % criteria of Northern Gannet from AEWA Conservation Status Report 8 (Wetlands International 2021).

	Population estimate	**Population 1 % (year)**
North Atlantic	1,600,000	25,000 (2018)

Kittiwake *Rissa tridactyla*

One flyway population (Table 21) that is declining in numbers (Wetlands International 2021).

From shore, the species can be seen in high numbers at the right time of year and in the right weather conditions, especially from Skagen, Læsø, Anholt and northern Zealand but also occasionally from northeast Djursland though in lower numbers than from the other sites. The highest counts are from late autumn and in winter (www.dofbasen.dk).

Table 21. Total Kittiwake population estimate and population 1 % criteria from AEWA Conservation Status Report 8 (Wetlands International 2021).

	Population estimate	**Population 1 % (year)**
Ssp. *tridactyla*	6,100,000	66,000 (2012)

Razorbill *Alca torda*

Within Kattegat two subspecies of Razorbill occur, ssp. *islandica* and ssp. *torda* (East Atlantic population).

Breeding areas

- Ssp. *islandica* breeding in Iceland, Faroe Islands, Britain, Ireland, Helgoland and NW France
- Ssp. *torda* (East Atlantic) breeding in the Baltic, West Sweden, Norway and east to the White Sea.

Both of the populations are believed to be increasing in numbers (Wetlands International 2021).

The proportion of birds in Kattegat from the different breeding areas/flyways/subspecies is not known in detail. Based on ring recoveries and corrected for population sizes and ringing effort, Lyngs & Kampp (1996) calculated a composition of 33 % birds from Britain, 59 % from Norway, and 8 % from the Baltic Sea for Razorbills wintering in Denmark. However, this hardly reflects the true composition. The bulk of the world population of Razorbill breeds in Iceland, where only few birds have been ringed in Iceland, and none of these have been recovered in Denmark. Just a single recovery of an Icelandic bird would mean a significant change of the above proportions. Furthermore, it is unlikely, that birds from Norway make up 59 % of the wintering birds in Denmark. The Norwegian population was last estimated to be less than 55,000 pairs (Anker-Nilssen et al. 2015), and the winter population may exceed 200,000 birds in Kattegat alone (Skov et al. 1995).

Baltic breeders (ssp. *torda*) predominantly stay within the Baltic outside the breeding season, though some have been recorded in Kattegat (Lyngs & Kampp 1996). Birds from Norway, the Kola peninsula, and the White Sea (ssp. *torda*) winter along the Norwegian coast into Skagerrak and Kattegat (Lavers et al. 2020).

Birds from the large population of ssp. *islandica* breeding in Iceland probably also winter in Kattegat and Danish waters, though there are no ring recoveries from Denmark (Lyngs & Kampp 1996). Data from birds ringed or equipped with geo-locators in Icelandic breeding colonies have shown that most birds stay around Iceland and the Faroe Islands, but some winter in the North Sea (Linnebjerg et al. 2018). Razorbills ssp. *islandica* breeding in northern England and Scotland also winter in Skagerrak and Kattegat (Lyngs & Kampp 1996, Lavers et al. 2020).

From land in the Kattegat area, the species is primarily recorded from late autumn into early spring. Most birds are recorded from Skagen and northeast Djursland where daily maximum numbers almost annually exceed 10.000 birds, but there are also a few records of >50.000 birds. In late October/November large flocks can be seen daily from northeast Djursland. From December and onwards much fewer birds are recorded here (www.dofbasen.dk).

It is generally not possible to identify the species to subspecies level in the field. The distribution of the different subspecies outside their breeding season is based on knowledge from ring recoveries and telemetry studies.

Table 22. Total population estimate and population 1 % criteria from AEWA Conservation Status Report 8 (Wetlands International 2021). ssp. torda was proposed split into two flyway populations in 2019 with ssp. islandica distributed between these (Nagy 2019a). This split that has been endorsed by the Technical and Standing Committees of AEWA and put forward for final adoption at the 8th Session of the Meeting of Parties to AEWA (Nagy 2019a, AEWA 2021).*

Flyway population	**Population estimate**	**Population 1 % (year)**
Ssp. *islandica*	830,000-2,000,000	13,800 (2018)
Ssp. *torda*, West Atlantic*	130,000	1,300 (2021)
Ssp. torda, East Atlantic*	290,000-350,000	3,200 (2021)

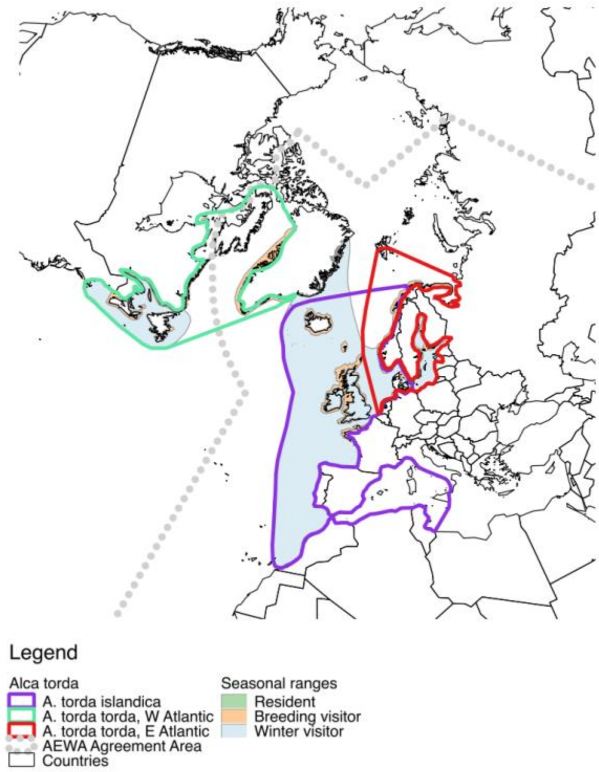

Figure 90. Proposed delineation of the biogeographic populations of A. torda. Map and text from Nagy 2019a

Common Guillemot *Uria aalge*

Three flyway populations are believed to occur regularly within Kattegat, ssp. *albionis*, ssp. *aalge* (Baltic) and ssp. *aalge* (East Atlantic) (Lyngs & Kampp 1996). There are also a few ring recoveries of ssp. *hyperborea* from Denmark, incl. Kattegat (Lyngs & Kampp 1996), but birds from this population predominantly winters further north (Cramp 1985).

Breeding areas

- ssp. *albionis* breeding in Ireland, South Britain, France, Iberia and on Helgoland
- ssp. *aalge* East Atlantic, breeding in Iceland, Faroe Islands, South Norway and Scotland
- ssp. *aalge* Baltic, breeding Sweden, Denmark and Finland.
- ssp. *hyperborea* northern Norway, Svalbard and east to Novaya Zemlya

Both of the populations of ssp. *aalge* and the population of ssp. *albionis* are believed to be increasing in numbers (Wetlands International 2021). On species level, Common Guillemot is considered not threatened (least concern, LC) and with an increasing population trend on the latest European red list from 2021, while it was considered near theatened (NT) on the previous red list from 2015 (BirdLife International 2021). However, a population decline is seen in some areas. The Norwegian population is considered critically endangered (CR) based on a population decline of 85-90 % since the 1960's (Stokke et al. 2021).

The exact proportion of birds in Kattegat from the different breeding areas/flyways/subspecies is not known. Based on ring recoveries and corrected for population sizes and ringing effort, Lyngs & Kampp

(1996) estimated that birds from Britain accounted for 85 % of the autumn/winter population of Common Guillemots in Denmark, with another 5 % coming from the Faeroes. The vast majority of these birds belong to the East Atlantic population of ssp. *aalge*. Of the remaining 10 %, birds from Helgoland (ssp. *albionis*) made out 3 % and Baltic birds (ssp. *aalge*, Baltic) 7 %. The Baltic birds (ssp. aalge) predominantly stay within the Baltic outside the breeding season, and only few immature birds have been recorded further west into the North Sea (Britain and southern Norway, Lyngs & Kampp 1996). On that basis it seems fair to assume, that more than 90 % of the Common Guillemots in Kattegat belong to the East Atlantic population of ssp. aalge.

It is generally not possible to identify the species to subspecies level in the field. The distribution of the different subspecies outside their breeding season is based on knowledge from ring recoveries and telemetry studies.

*Table 23. Total population estimate and population 1 % criteria from AEWA Conservation Status Report 8 (Wetlands International 2021). * ssp. aalge was proposed split into two flyway populations (an East Atlantic and a Baltic) in 2019 (Nagy 2019b). This split that has been endorsed by the Technical and Standing Committees of AEWA and put forward for final adoption at the 8th Session of the Meeting of Parties to AEWA (Nagy 2019b, AEWA 2021).*

Flyway population	**Population estimate**	**Population 1 % (year)**
Ssp. *albionis*	500,000	8,000 (2018)
Ssp. *hyperborea*	600,000-640,000	4,700 (2018)
Ssp. *aalge*, East Atlantic*	4,600,000-5,700,000	51,200 (2021)
Ssp. *aalge*, Baltic*	77,000-100,000	880 (2021)

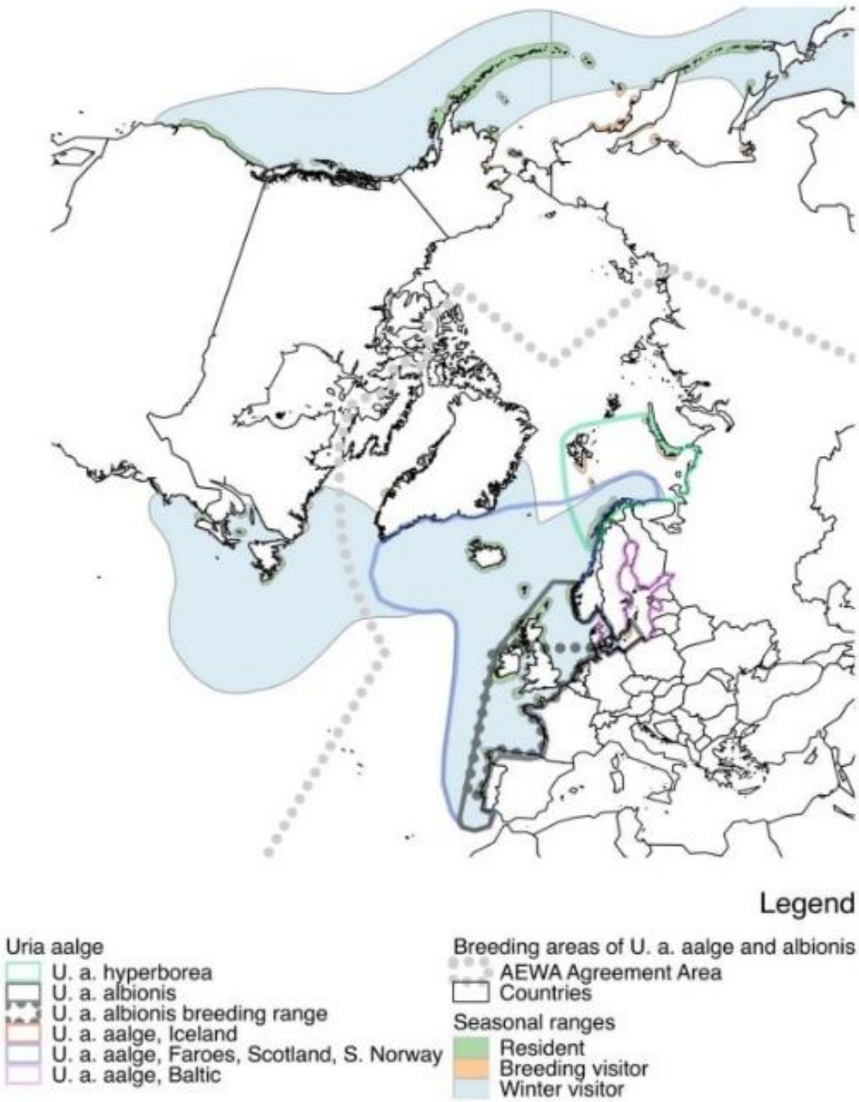

Figure 91. Delineation of the proposed biogeographic populations of U. a. aalge and the delineation of the ranges of the other populations of U. aalge recognised in Table 1 of the AEWA Action Plan. (Note: the range map produced by BirdLife International is only to provide a backdrop for the flyway delineation. It will require update at a later stage to incorporate the correction proposed by experts during the consultation process. Map and text from Nagy 2019b.

Persistency/Sensitivity analyses and cumulative effects

A full evaluation of the cumulative impact of anthropogenic effects on specific bird species will require access to information about anthropogenic effects along the geographical range of the flyway of the species. In the present report we evaluate the potential displacement effect from an offshore wind farm development in the study area, and thus how the displacement part under the proposed Hesselø OWF project may contribute to a cumulative effect on selected bird species. It is important to bear in mind that the number of displaced individuals does not represent a true population decline (because a bird displaced elsewhere is not a dead bird necessarily), but a potential population effect related to increased inter- and/or intra-specific competition that in turn may have impact on mortality rates and/or reproduction rates. The relationship between number of displaced individuals and the numerical impact on a population level is poorly known for all the species considered here.

For the four most relevant species or species groups in this study the total numbers estimated to be present within the identified potential distribution effect zone was calculated, and the total numbers of individuals displaces was estimated, based on the above mentioned effect zones and the percentage reduction within the wind farm effect zone (Table 5, Table 24). These were estimated on the basis of the abundance values from the distribution maps, based on the percentage reduction given in Table 5 and a linear decrease in effect out to the distance to where a distribution effect was assumed to happen.

Table 24. For each of the 11 surveys treated in this report and for each of the four selected bird species/species groups, the numbers of individuals present within the potential effect zone (N within zone) and the estimated number of displaced individuals (reduction within zone) are given.

	Red-throated Diver/ Black-throated Diver		Gannet		Kittiwake		Razorbill/Guillemot	
Survey	N within Zone	reduction within zone	N within Zone	reduction within zone	N within Zone	reduction within zone	N within Zone	reduction within zone
Winter 2008	250	109	4	0	983	154	16064	6458
Winter 2013	349	145	2	0	0	0	17	7
Winter 2016	256	71	0	0	9	1	7664	3032
17. DEC 2018	185	87	39	9	54	9	363	139
10. JAN 2019	139	65	24	2	67	11	3164	1240
01. MAR 2019	284	88	6	1	101	17	2993	1200
01. APR 2019	130	56	809	160	4	1	2327	956
17. APR 2019	27	7	528	89	NA	NA	38	15
09. SEP 2019	NA	NA	58	10	NA	NA	1530	629
06. NOV 2019	NA	NA	40	6	15	2	163	64
Winter 2020	187	68	28	5	55	8	615	229

For the divers, the distribution persistency analysis showed high persistency in the southwestern parts of the Middelgrund Study Area, and low persistency in the northeastern and eastern areas (see Figure 22). Under the displacement scenario used in this report, between 27 and 349 divers were estimated to be present within that zone, and a wind farm in the proposed wind farm area would displace between seven and 145 divers (Table 24). The vast majority of these divers are likely to be Red-throated Divers, with a flyway population of 210,000 to 340,000 individuals. Thus, the displaced individuals will represent between 0.003 and 0.04 % of the flyway population. This is estimated on the background of the Middelgrund Study Area. The fact that part of the 16 km impact zone reaches into the Swedish EEZ zone was not accounted for because the spatial model area does not cover Swedish waters. The estimated number of displaced birds will therefore be slightly lower that would have been the case if Swedish waters had been included in the model. Due to low numbers of divers present in the Middelgrund Study Area in September and November 2019 spatial models could not be performed for those surveys.

The number of Gannets within the Middelgrund Study Area and the impact zone fluctuated markedly between surveys. The persistency analyses showed highest persistency in the northern and northeastern parts of the Middelgrund Study Area, with lower persistency in the southern central parts around the island of Hesselø (see Figure 42). Under the displacement scenario used in this report, a total of 0 to 890 Gannets was estimated to be present within that zone, and the proposed Hesselø OWF would under that scenario displace between 0 and 160 individuals (Table 24). With an estimated population of 1.6 million individuals wind farm construction in the planned area would displace less than 0.01 % of the population.

Like for the Gannets, the number of Kittiwakes within the Middelgrund Study Area and the impact zone fluctuated markedly between surveys. The persistency analyses showed general low persistency, with highest persistency in the central, southern and northeastern parts of the Middelgrund Study Area, with lower persistency in the northwestern parts around the island of Hesselø (see Figure 69). Under the displacement scenario used in this report, a total of 0 to 983 Kittiwakes was estimated to be present within that zone, and the proposed Hesselø OWF would displace between 0 and 154 individuals (Table 24). With an estimated population of 6.1 million individuals wind farm construction in the planned area would displace less than 0.003 % of the population.

The number of Razorbills/Guillemots within the Middelgrund Study Area and the impact zone fluctuated markedly between surveys. The persistency analyses showed highest persistency in the central, eastern and northeastern parts of the Middelgrund Study Area and lower persistency in the northwestern and the southeastern parts (see Figure 89). Under the displacement scenario used in this report, between 38 and 16,064 Razorbills/Guillemots were estimated to be present within that zone, and a wind farm in the proposed area would displace between seven and 6,458 individuals (Table 24). The fact that this species group represent two species of highly differing population sizes and that each of the species have subpopulations of highly varying population sizes, the estimation of the percentage impact from a potential wind farm in the Hesselø area is complicated. It is not possible to determine the ratio between Razorbills and Guillemots in this data. At the same time, it is unclear which proportion of a subpopulation the birds may derive from. Razorbills from both *A.t. torda* and *A.t. islandica* forms are potentially present in the study area and both subspecies of Guillemot potentially occur (*U.a. albionis* and the eastern Atlantic part of the *U.a. aalge*). The Baltic subpopulation of *U.a. aalge* is believed to have little exchange with the rest of the subpopulation, and is therefore not considered in this context. In order to assess the magnitude of displaced birds in relation to population sizes we have assumed that all Razorbills/Guillemots within the area belonged to one species and to one subpopulation of the species, being well aware that this is not the case. On that basis, the percentage of the total subpopulation could be estimated. Using the subpopulation estimates given above and the highest and lowest displacement estimate from the 11 modelled surveys the percentage of the displaced birds from the different subpopulations was calculated (Table 25). The smaller populations are represented by higher percentages, with the guillemot subspecies *U.a. albionis* showing the highest value.

Table 25. A theoretical estimate of the percentage of a subpopulation of Razorbills/Guillemots that would be displaced (for upper-lower population estimate) for each subpopulation and for maximum numbers of displaced birds from the 11 surveys. The presence of Razorbills/Guillemots is a mixture of species and populations, and the indicated percentages are calculated under the assumption that all Razorbills/guillemots in the calculation was of the same population.

Species	Population	Max. abundance displaced (%)
Razorbill	*A.t. torda*	1.8-2.2
	A.t. islandica	0.32-0.78
Common Guillemot	*U.a. aalge (east Atlantic)*	0.11-0.14
	U.a. albionis	1.3

The relative proportion of Razorbills versus Common Guillemots in Kattegat is likely to vary through the year and between different parts of the area. Generally, Common Guillemots arrive earlier in the autumn to Kattegat than Razorbills. Many Common Guillemots arrive during August and September, and it has been estimated that an average of around 30,000 birds were present in Kattegat during September-October in 1980-1994 (Skov et al. 1995). Razorbills mainly arrive to the area from late October/early November (Skov et al. 1995).

During winter (generally December-February), Skov et al. (1995) estimated for 1980-1994, that a total of approximately 65,000 Common Guillemots and 228,000 Razorbills were present in Kattegat (total number for the Danish and Swedish part). According to this, Razorbills should make out 78 % of the Auks in Kattegat during winter. Durinck et al. (1994) estimated for the period 1988-1993, that around 66,000 Common Guillemots and 132,000 Razorbills wintered in Kattegat, corresponding to 66.5 % Razorbills.

A more realistic estimate of the affected proportion of the involved populations can be achieved by assuming the following:

1) the Common Guillemot:Razorbill ratio is 30:70 in Kattegat during winter (and that this is also applies to the potential wind farm area),
2) the Razorbills are 33 % ssp. *torda* and 67 % *islandica*, and
3) the Common Guillemots are 90 % ssp. *aalge* (East Atlantic) and 10 % ssp. *albionis*.

If we then use the mean of the lower and upper population estimates and the highest number of displaced individuals (Table 24), the theoretical estimate of the proportions of the different populations that would potentially be displaced, would be approximately 0.5 % for Razorbill ssp. *torda*, 0.2 % for Razorbill ssp. *islandica*, 0.03 % for Common Guillemot ssp. *aalge* (East Atlantic), and 0.04 % for Common Guillemot ssp. *albionis*. It must be stressed, that accurate data on the ratio between the two species in the area is missing and likewise for the ratio between birds of the different populations, especially for Razorbill.

Redistribution of displaced birds

The displacement of birds will lead to redistributions. The exact mechanisms for a redistribution can be modelled, assuming a spread by the same mechanisms as used for the spatial modelling of bird densities, apart from the effect of displacement from the wind farm. Such an approach has been used here for each of the selected bird species. In this way, the potential effect on bird abundance within SPAs within the model area can be estimated. The analysis was made for the four surveys with a wider Kattegat model result, which is winter 2008, 2013 and 2016, compared to the most recent survey from the winter of 2020. The numbers under this model vary slightly from the numbers given in Table 24 because they derive from different models, but they fall within the 95 % confidence intervals.

By using distributions of birds from the 2020 survey data as compared to the winter data from 2008, 2013 and 2016, changes between 2020 and the other wintering data could be detected.

The calculation of redistribution of birds can lead to reductions or increases of the number of birds estimated within SPAs within the study area. The birds will seek to optimize their conditions by choice of location. A displacement is therefore potentially a conditional disadvantage, given that conditions on the alternative position are, even marginally, reduced.

It is important to notice that the mechanisms for redistribution can be different from the ones used here, and that a redistribution is calculated within the model area. Thus, the lack of redistributions into the neighbouring Swedish areas remain a shortcoming for the analysis.

Divers:

Distributional in the winter of 2020 as compared to other mid-winter surveys.

The general trend between winter 2020 distribution and the mid-winter surveys of 2008, 2013 and 2016 was a significant increase in an area to the south of Anholt offshore wind farm and decreases to the north and north east (Figure and Figure). Apart from a small region in the north of the proposed windfarm area between W08 and W20 (between 2008 and 2020) there were no significant differences in the region of the proposed Hesselø OWF (Figure and Figure).

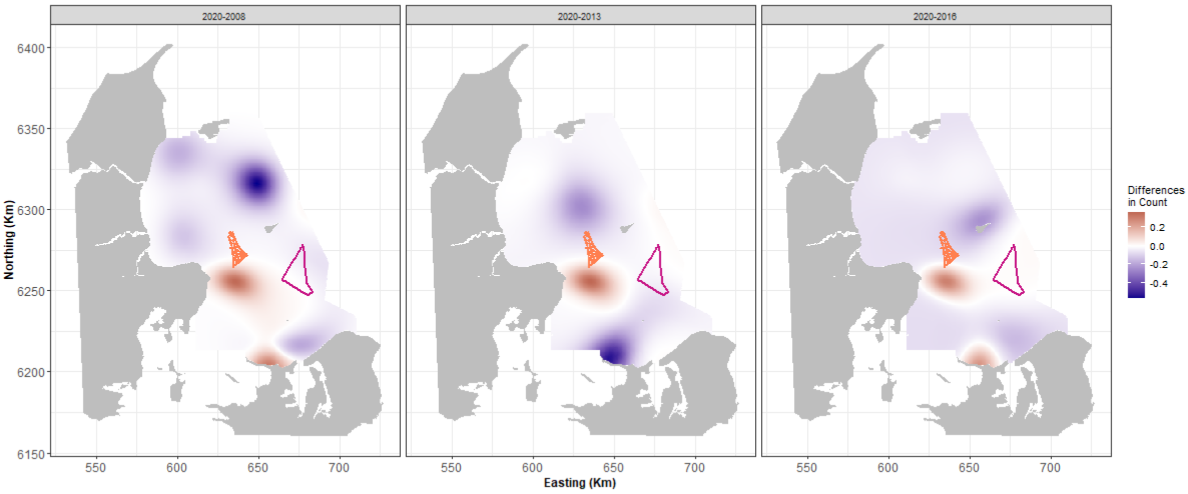

Figure 92: Maps showing differences in diver counts between 2020 and 2008, 2013 and 2016. Red areas indicate an increase in numbers in 2020 and blue areas show a decrease. The significance of these differences is shown in Figure . The Anholt windfarm is in orange and the proposed Hesselø site is purple.

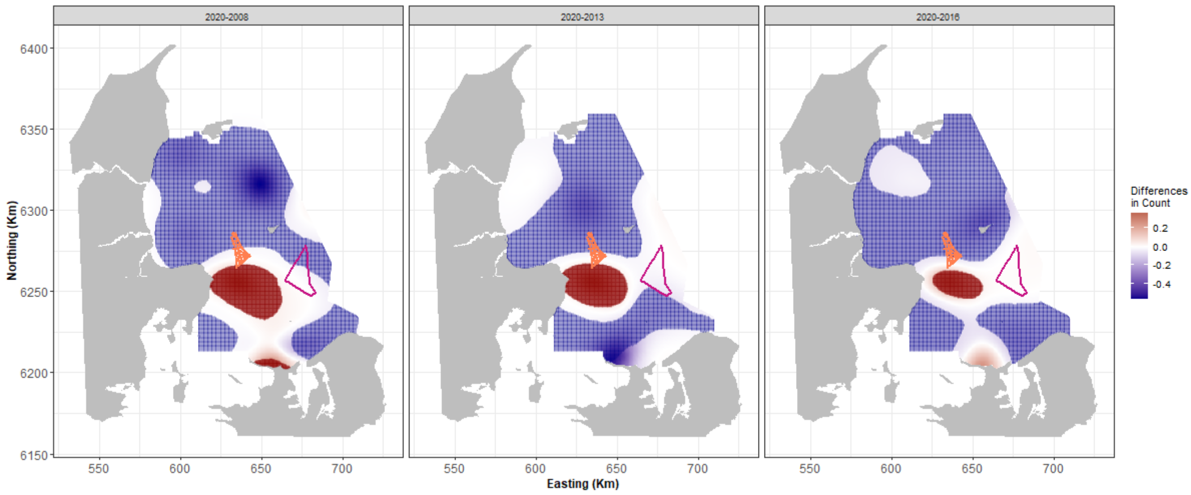

Figure 93: Maps showing significant differences in diver counts between 2020 and 2008, 2013 and 2016. Red areas indicate an increase in numbers in 2020 and blue areas show a decrease. Areas highlighted by dark red or dark blue show a significant difference in bird numbers between the two years. The Anholt windfarm is in orange and the proposed Hesselø site is purple.

Scenario Planning

The scenario for divers was an 80 % decline in the footprint of the proposed Hesselø OWF with a linear return to no change in a 16 km buffer. This led to a decline of approximately 13 birds in the footprint and 71 birds in the footprint plus buffer area (Table). These birds were re-distributed to the remainder of the study area in line with their estimated distribution in W20. The main hotspot areas for divers in W20 (estimated as part of the analysis described in this report) was not found to be close to the proposed site and so the numbers of birds impacted was relatively small. Figure shows an example scenario based on one of the bootstrap replicates.

Table 26: Table showing the effect of scenario implementation on diver numbers in the proposed Hesselø OWF footprint and buffer regions. "Estimated numbers for W20" is the estimated bird count for the W20 survey while "Estimated numbers under the scenario" represents the estimated bird count under the scenario described. The "95 % CI" figures represent the 95 percentile based confidence intervals for each estimate.

Region	Estimated numbers for W20	95 % CI (W20)	Estimated numbers under the scenario	95 % CI Scenario
Inside Footprint	15.9	(8.7, 26.5)	3.2	(1.7, 5.3)
Outside Footprint	1543.5	(1141.7, 2031.6)	1556.2	(1153.1, 2045.5)
Footprint including 16km buffer area	193.9	(120.3, 291.9)	123.2	(78.6, 183.8)
Outside Footprint including 16km buffer area	1365.6	(982.5, 1859.4)	1436.2	(1046.3, 1931.5)

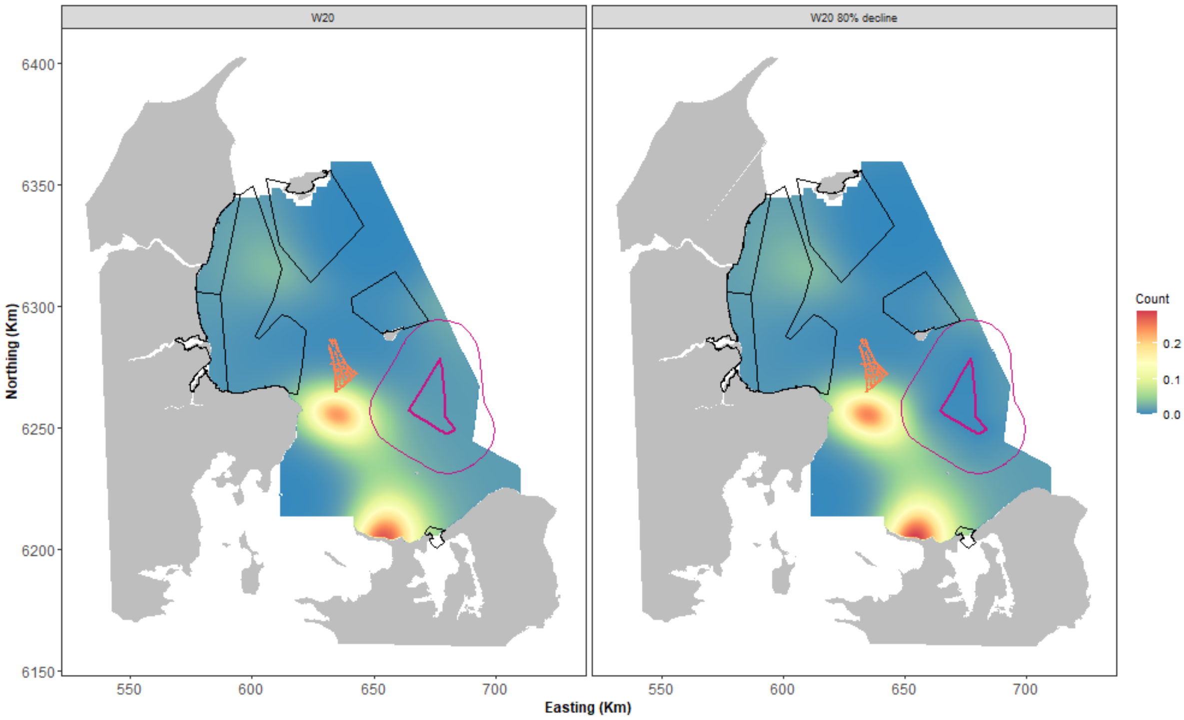

Figure 94: Example of scenario for diver sp. On the left is one of the estimated bootstrap predictions from the W20 model. On the right is the same set of predictions but with the scenario imposed. The footprint is shown by the thick purple line and the buffer the thinner purple line. The black lines denote the SPA areas.

The impact of this scenario on diver numbers in the SPA regions was estimated to be minimal (Table) and in all cases, the confidence intervals for the number of birds in each site overlapped substantially. This suggests that the underlying abundances in each case may not be statistically distinct, which is unsurprising given the small number of birds that were re-distributed over a very large area in this case. Although very small and non-significant changes, the impacted SPAs were 112 and 10.

Table 27: Table of SPA areas showing the effect of scenario implementation on bird numbers. N is the estimated bird count for either the W20 survey or for the scenario and 95 % CI is the 95 percentile based confidence interval for N. N/A in the SPA column represents the rest of the study area that is not contained within an SPA.

SPA	Area (Kmsq)	N (W20)	95 % CI (W20)	N Scenario	95 % CI Scenario
SPA10	904.7	35.7	(18.9, 68.7)	37.6	(19.8, 72.6)
SPA102	20.3	6.4	(3.5, 10.2)	6.8	(3.7, 11)
SPA112	1758.9	100.4	(61.8, 154)	105.7	(65, 164.1)
SPA15	297.2	13.2	(7.4, 24.6)	14	(7.6, 26.1)
SPA2	296.1	22.5	(13.4, 37.3)	23.8	(13.8, 40.2)
SPA32	463	17.9	(4.8, 46.2)	18.9	(5.0, 47.5)
N/A	8567.9	1363.2	(981.2, 1854.1)	1352.6	(969.7, 1847)

Gannet:

Distributional in the winter of 2020 as compared to other mid-winter surveys.

The general trend between results from the mid-winter 2020 data and and the mid-winter surveys of the 2008, 2013 and 2016 data was a significant increase to the south and east of Anholt offshore wind farm (in 2020 compared with 2008 and 2013) and including in Anholt itself in 2020 compared with 2016 (Figure and Figure).   A much smaller area of significant decrease was evident to the east of the farm in 2008 compared with 2020 (Figure) but otherwise a decrease is not seen until the 2016-2020 comparison and then only in the far north east of the study area. There were small but significant increases in parts of the Hesselø OWF footprint for all comparisons.

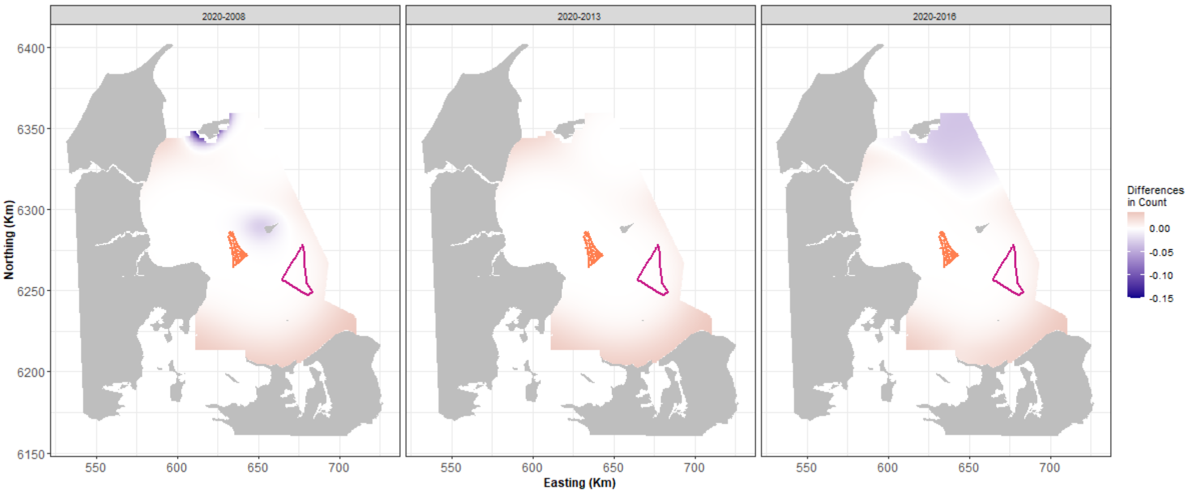

Figure 95: Maps showing differences in gannet counts between 2020 and 2008, 2013 and 2016. Red areas indicate an increase in numbers in 2020 and blue areas show a decrease. The significance of these differences is shown in Figure . The Anholt windfarm is in orange and the proposed Hesseloe site is purple.

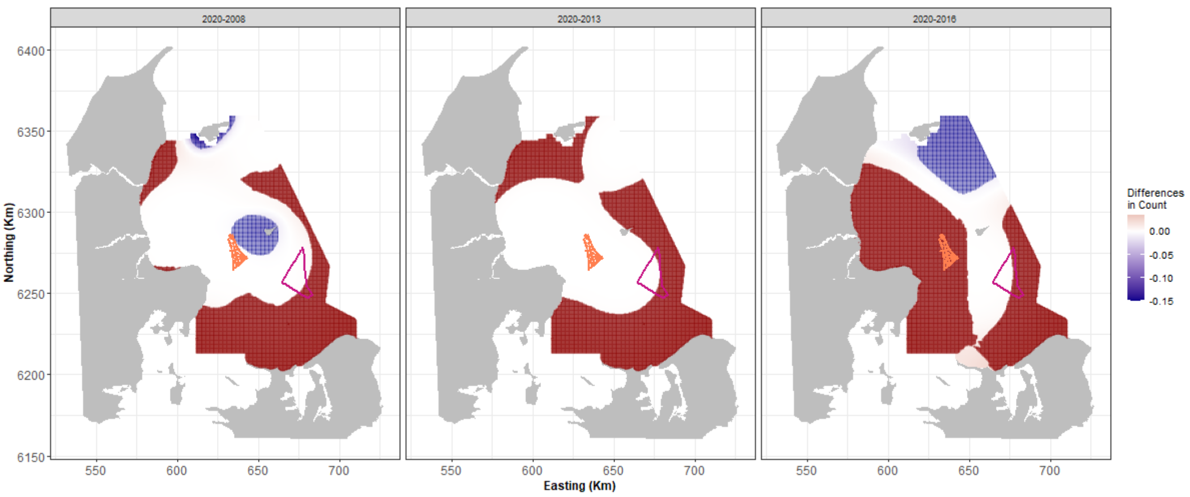

Figure 96: Maps showing significant differences in gannet counts between 2020 and 2008, 2013 and 2016. Red areas indicate an increase in numbers in 2020 and blue areas show a decrease. Areas highlighted by dark red or dark blue show a significant difference in bird numbers between the two years. The Anholt windfarm is in orange and the proposed Hesseloe site is purple.

Scenario Planning

The scenario for Gannets was a 37 % decline in the footprint of the proposed wind farm with a linear return to no change in a 15 km buffer. This led to a decline of approximately 1 bird in the footprint and 5 birds in the footprint plus buffer area (Table). These birds were re-distributed to the remainder of the study area in line with their estimated distribution in W20. The main hotspot areas for gannets in W20 (estimated as part of the analysis described in this report) was not found to be close to the proposed site and so the numbers of birds impacted was relatively small. Figure shows an example scenario based on one of the bootstrap replicates.

Table 28: Table showing the effect of scenario implementation on Gannet numbers in the proposed wind farm footprint and buffer regions. "Estimated numbers for W20" is the estimated bird count for the W20 survey while "Estimated numbers under the scenario" represents the estimated bird count under the scenario described. The "95 % CI" figures represent the 95 percentile based confidence intervals for each estimate.

Region	Estimated numbers for W20	95 % CI (W20)	Estimated numbers under the scenario	95 % CI Scenario
Inside Footprint	1.9	(0.4, 5.4)	1.2	(0.3, 3.4)
Outside Footprint	313.5	(165, 532.1)	314.2	(165.6, 533.2)
Footprint including 15km buffer area	32.6	(14.2, 73)	27.2	(11.9, 59.6)
Outside Footprint including 15km buffer area	282.8	(144.3, 485.4)	288.2	(147.3, 490.7)

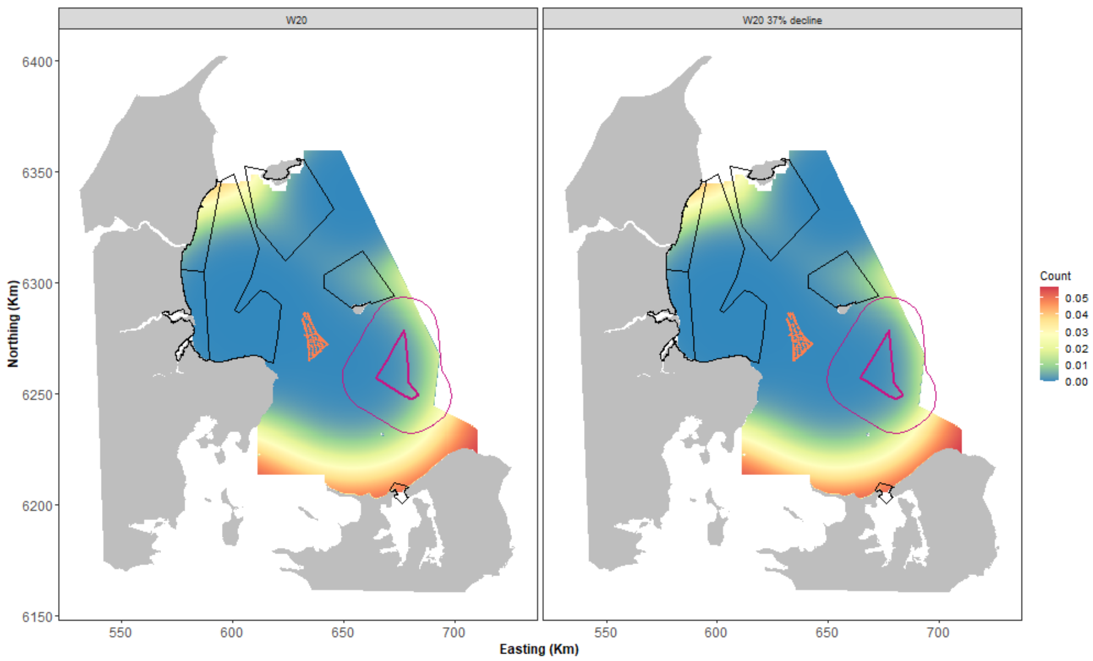

Figure 97: Example of scenario for Gannet. On the left is one of the estimated bootstrap predictions from the W20 model. On the right is the same set of predictions but with the scenario imposed. The footprint is shown by the thick purple line and the buffer the thinner purple line. The black lines denote the SPA areas.

The impact of this scenario on Gannet numbers in the SPA regions was estimated to be trivial (Table) and in all cases, the confidence intervals for the number of birds in each site overlapped almost entirely. This suggests that the underlying abundances in each case may not be statistically distinct, which is unsurprising given the small number of birds that were re-distributed over a very large area in this case.

Table 29: Table of SPA areas showing the effect of scenario implementation on Gannet numbers. N is the estimated bird count for either the W20 survey or for the scenario and 95 % CI is the 95 percentile based confidence interval for N. N/A in the SPA column represents the rest of the study area that is not contained within an SPA.

SPA	Area (Kmsq)	N (W20)	95 % CI (W20)	N Scenario	95 % CI Scenario
SPA10	904.7	18.6	(8, 36.5)	18.9	(8.3, 37)
SPA102	20.3	2.7	(1.1, 5.6)	2.8	(1.1, 5.6)
SPA112	1758.9	19.3	(8, 43.6)	19.6	(8.2, 44.1)
SPA15	297.2	1.2	(0.1, 6.9)	1.2	(0.1, 7)
SPA2	296.1	11.6	(5.2, 24)	11.9	(5.3, 24.2)
SPA32	463	6.9	(3.9, 11)	7	(4, 11.3)
N/A	8567.9	255.1	(129, 458.3)	254	(127.8, 455.3)

Kittiwake:

Distributional in the winter of 2020 as compared to other mid-winter surveys.

The general trend between mid-winter survey data and the corresponding mid-winter surveys of 2008, 2013 and 2016 was a significant increase in an area to the north east of the proposed Hessleoe site (Figure and Figure). There were mixed results when comparing kittiwake numbers between 2008, 2013, 2016 & 2020, but largely the comparisons saw increased numbers in this proposed footprint area since 2013. There was no change seen in the area of the Anholt OWF site between 2008/2016 and 2020 however, there was a very small but significant decrease in Kittiwake numbers between 2013 and 2020.

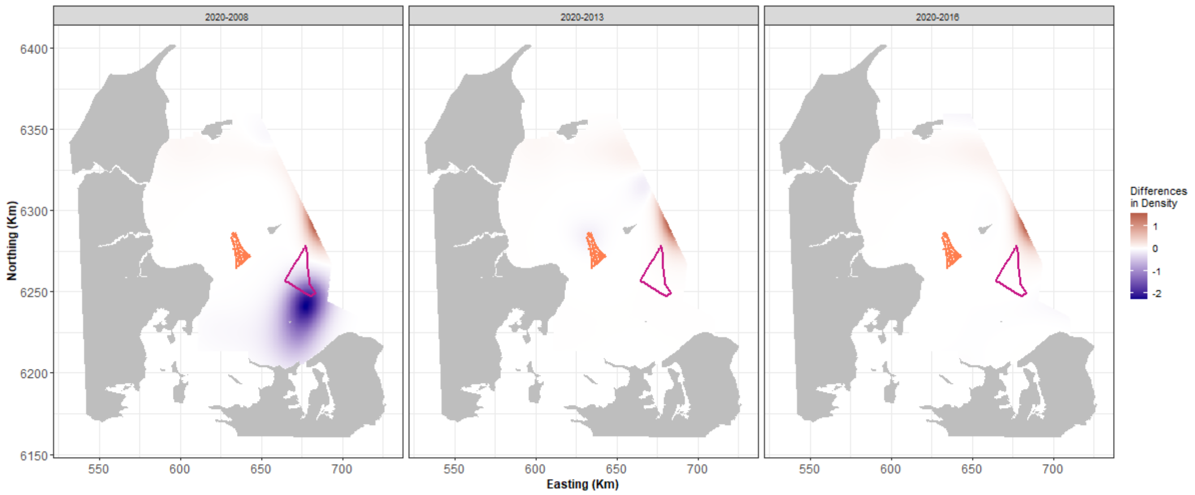

Figure 98: Maps showing differences in Kittiwake counts between 2020 and 2008, 2013 and 2016. Red areas indicate an increase in numbers in 2020 and blue areas show a decrease. The significance of these differences is shown in Figure . The Anholt windfarm is in orange and the proposed Hesselø site is purple.

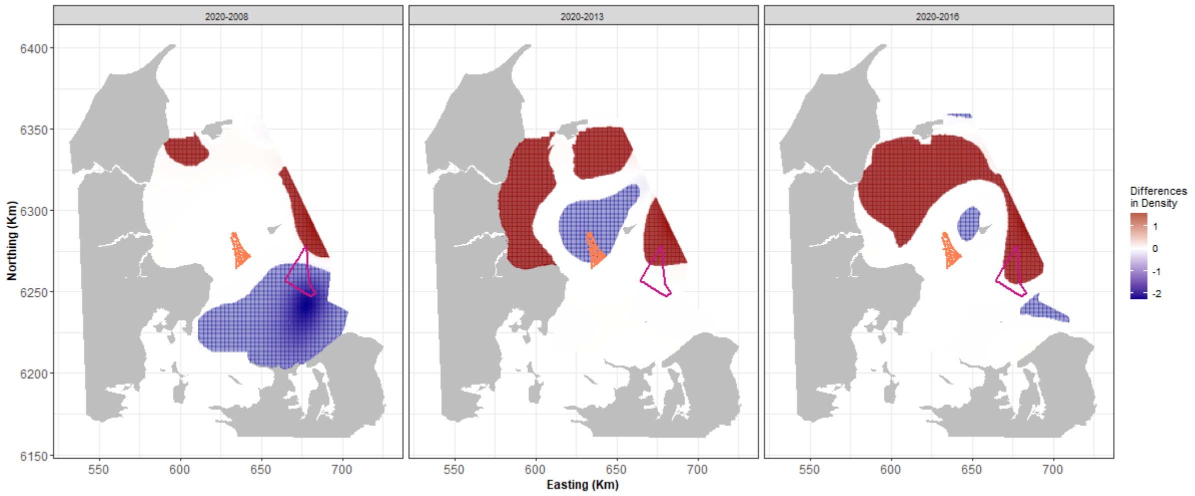

Figure 99: Maps showing significant differences in Kittiwake counts between 2020 and 2008, 2013 and 2016. Red areas indicate an increase in numbers in 2020 and blue areas show a decrease. Areas highlighted by dark red or dark blue show a significant difference in bird numbers between the two years. The Anholt windfarm is in orange and the proposed Hesselø site is purple.

Scenario Planning

Two scenarios were undertaken for kittiwakes. The first was a 20 % decline in the footprint of the proposed wind farm with a linear return to no change in a 2 km buffer. The second was a 20 % increase in the footprint with a linear return to no change in a 2 km buffer.

The first scenario led to a decline of approximately 5 birds in the footprint and 8 birds in the footprint plus buffer area (

Table). These birds were re-distributed to the remainder of the study area in line with their estimated distribution in W20. The main hotspot area for Kittiwakes in W20 (estimated as part of the analysis described in this report) was to the north east of the proposed site and so the numbers of birds impacted was relatively small. Figure shows an example scenario based on one of the bootstrap replicates.

Table 30: Table showing the effect of scenario implementation on Kittiwake numbers in the proposed wind farm footprint and buffer regions. "Estimated numbers for W20" is the estimated bird count for the W20 survey while "Estimated numbers under the scenario" represents the estimated bird count under the scenario described. The "95 % CI" figures represent the 95 percentile based confidence intervals for each estimate.

Region	Estimated numbers for W20	95 % CI (W20)	Estimated numbers under the scenario	95 % CI Scenario
Inside Footprint	26.3	(13.9, 49.6)	21	(11.2, 39.7)
Outside Footprint	1678.2	(1183.5, 2739.8)	1683.4	(1187.9, 2745)
Footprint including 2 km buffer area	57.1	(34.1, 98)	49	(29.4, 83.6)
Outside Footprint including 2 km buffer area	1647.3	(1158.1, 2707.2)	1655.4	(1164.7, 2715.3)

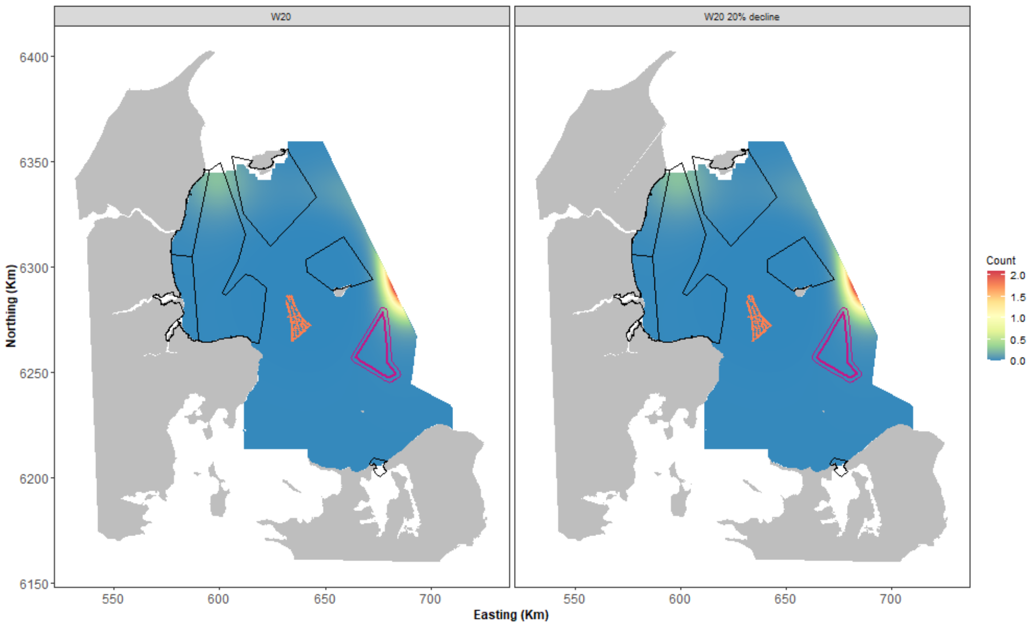

Figure 100: Example of scenario for Kittiwake. On the left is one of the estimated bootstrap predictions from the W20 model. On the right is the same set of predictions but with the scenario imposed. The footprint is shown by the thick purple line and the buffer the thinner purple line. The black lines denote the SPA areas.

The impact of this scenario on kittiwake numbers in the SPA regions was estimated to be minimal (Table) and in all cases, the confidence intervals for the number of birds in each site overlapped substantially. This suggests that the underlying abundances in each case may not be statistically distinct, which is unsurprising given the small number of birds that were re-distributed over a very large area in this case. Although very small and non-significant changes, the impacted SPAs were 10 and 112.

Table 31: Table of SPA areas showing the effect of scenario implementation on Kittiwake numbers. N is the estimated bird count for either the W20 survey or for the scenario and 95 % CI is the 95 percentile based confidence interval for N. N/A in the SPA column represents the rest of the study area that is not contained within an SPA.

SPA	Area (Kmsq)	N (W20)	95 % CI (W20)	N Scenario	95 % CI Scenario
SPA10	904.7	189.5	(87.1, 372.3)	190.4	(87.5, 373.3)
SPA102	20.3	0.6	(0.2, 1.5)	0.6	(0.2, 1.5)
SPA112	1758.9	134.0	(47.9, 350.3)	134.7	(48.1, 351)
SPA15	297.2	9.2	(3.2, 22.3)	9.2	(3.2, 22.4)
SPA2	296.1	38.9	(11.8, 98)	39.1	(11.8, 98.4)
SPA32	463	14.1	(2.1, 47.3)	14.2	(2.1, 47.8)
N/A	8567.9	1318.2	(892, 2158.5)	1316.3	(890.1, 2157.1)

The second scenario led to an increase of approximately 5 birds in the footprint and 8 birds in the footprint plus buffer area (Table). These birds were removed from the remainder of the study area in line with their estimated distribution in W20. The main hotspot area for kittiwakes in W20 (estimated as part of the analysis described in this report) was to the north east of the proposed site and so like the first scenario, the numbers of birds impacted by this scenario was relatively small. Figure shows an example scenario based on one of the bootstrap replicates.

Table 32: Table showing the effect of scenario implementation on Kittiwake numbers in the proposed wind farm footprint and buffer regions. "Estimated numbers for W20" is the estimated bird count for the W20 survey while "Estimated numbers under the scenario" represents the estimated bird count under the scenario described. The "95 % CI" figures represent the 95 percentile based confidence intervals for each estimate.

Region	Estimated numbers for W20	95 % CI (W20)	Estimated numbers under the scenario	95 % CI Scenario
Inside Footprint	26.3	(13.9, 49.6)	31.5	(16.7, 59.5)
Outside Footprint	1678.2	(1183.5, 2739.8)	1672.9	(1179, 2734.6)
Footprint including 2 km buffer area	57.1	(34.1, 98)	65.3	(38.8, 112.4)
Outside Footprint including 2 km buffer area	1647.3	(1158.1, 2707.2)	1639.2	(1151, 2699)

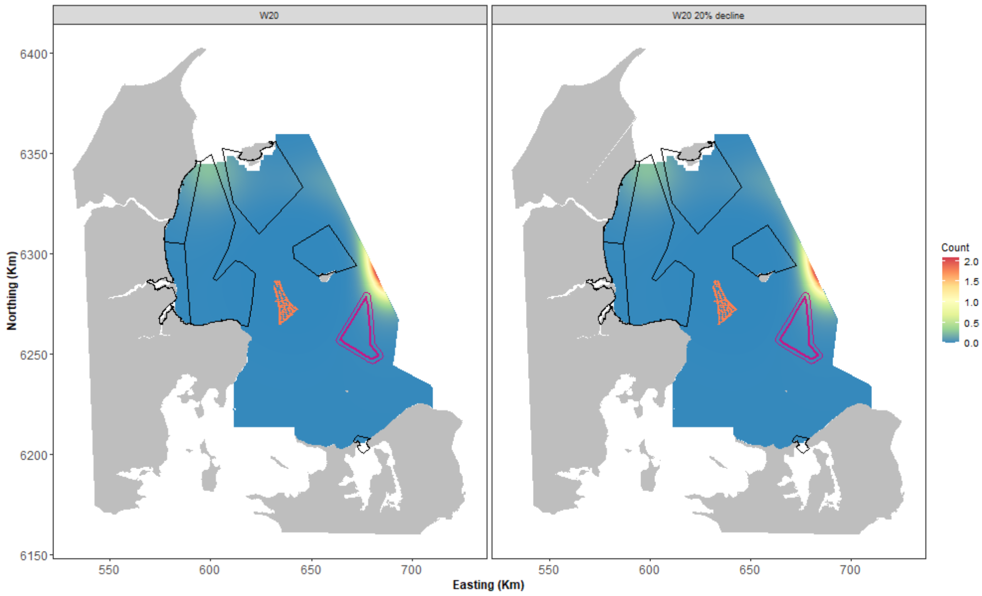

Figure 101: Example of scenario or Kittiwake. On the left is one of the estimated bootstrap predictions from the W20 model. On the right is the same set of predictions but with the scenario imposed. The footprint is shown by the thick purple line and the buffer the thinner purple line. The black lines denote the SPA areas.

The impact of this scenario on kittiwake numbers in the SPA regions was estimated to be minimal (Table) and in all cases, the confidence intervals for the number of birds in each site overlapped substantially. This suggests that the underlying abundances in each case may not be statistically distinct, which is unsurprising given the small number of birds that were re-distributed over a very large area in this case. Although very small and non-significant changes, the impacted SPAs were 10 and 112.

Table 33: Table of SPA areas showing the effect of scenario implementation on Kittiwake numbers. N is the estimated bird count for either the W20 survey or for the scenario and 95 % CI is the 95 percentile based confidence interval for N. N/A in the SPA column represents the rest of the study area that is not contained within an SPA.

SPA	Area (Kmsq)	N (W20)	95 % CI (W20)	N Scenario	95 % CI Scenario
SPA10	904.7	189.5	(87.1, 372.3)	188.6	(86.7, 371.2)
SPA102	20.3	0.6	(0.2, 1.5)	0.6	(0.2, 1.5)
SPA112	1758.9	134	(47.9, 350.3)	133.4	(47.7, 349.6)
SPA15	297.2	9.2	(3.2, 22.3)	9.1	(3.2, 22.1)
SPA2	296.1	38.9	(11.8, 98)	38.7	(11.7, 97.5)
SPA32	463	14.1	(2.1, 47.3)	14	(2.1, 46.8)
N/A	8567.9	1318.2	(892, 2158.5)	1320.1	(893.9, 2159.8)

Razorbill/Guillemot:

Distributional in the winter of 2020 as compared to other mid-winter surveys.

The general trend between the mid-winter survey data and the corresponding data from the mid-winter surveys of 2008, 2013 and 2016 was a significant increase in an area to the far south of the Anholt OWF site and an increase to the far north of the Kattegat Study Area (Figure and Figure). Notably, there were significant (and substantial) decreases in Razorbill/Guillemot numbers in the proposed Hesselø site between 2008 and 2016 (compared with 2020) while in 2013 significant fewer Razorbills/Guillemots were observed in the proposed wind farm footprint, than in 2020 (Figure and Figure).

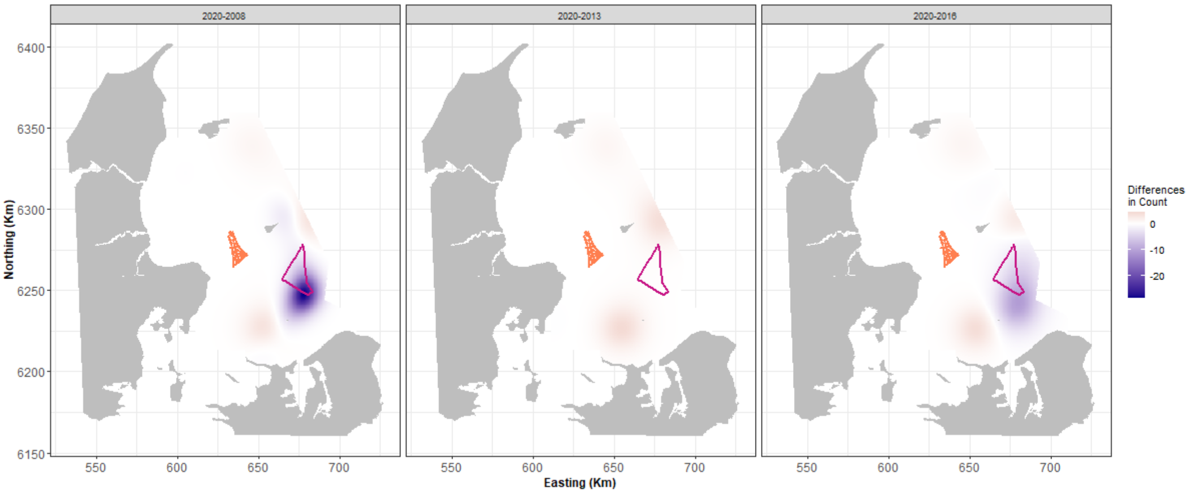

Figure 102: Maps showing differences in Razorbill/Guillemot counts between 2020 and 2008, 2013 and 2016. Red areas indicate an increase in numbers in 2020 and blue areas show a decrease. The statistical significance of these differences is shown in Figure . The Anholt OWF is in orange and the proposed Hesselø site is purple.

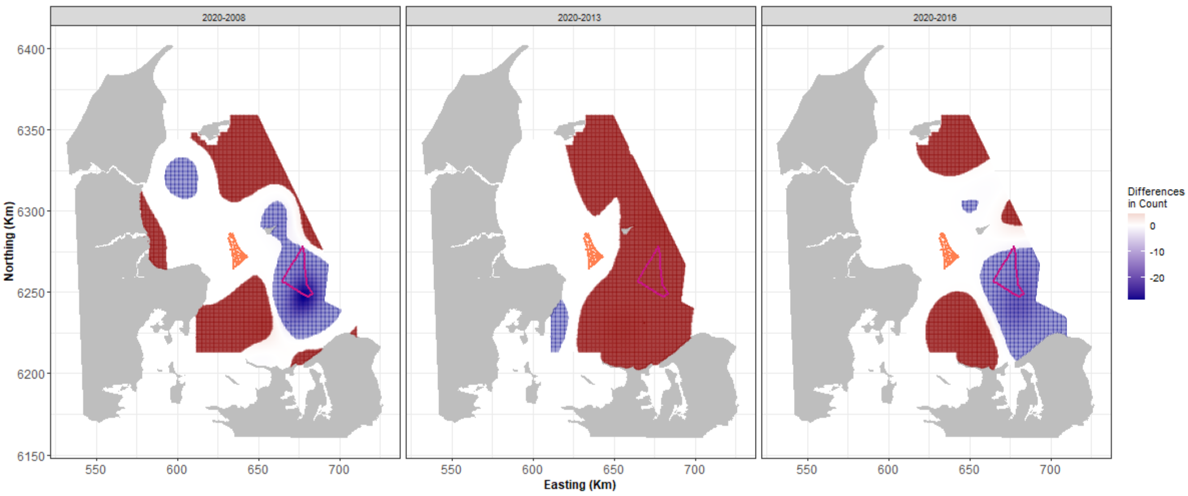

Figure 103: Maps showing significant differences in Razorbill/Guillemot counts between 2020 and 2008, 2013 and 2016. Red areas indicate an increase in numbers in 2020 and blue areas show a decrease. Areas highlighted by dark red or dark blue show a

significant difference in bird numbers between the two years. The Anholt windfarm is in orange and the proposed Hesselø site is purple.

Scenario Planning

The scenario for Razorbill/Guillemot was a 50 % decline in the footprint of the proposed wind farm with a linear return to no change in a 2 km buffer. This led to a decline of approximately 163 birds in the footprint and 237 birds in the footprint plus buffer area (Table). These birds were re-distributed to the remainder of the study area in line with their estimated distribution in W20. The main hotspot areas for Auks in W20 (estimated as part of the analysis described in this report) was not found to be close to the proposed site and so the numbers of birds impacted was relatively small. Figure shows an example scenario based on one of the bootstrap replicates.

Table 34: Table showing the effect of scenario implementation on Razorbill/Guillemot numbers in the proposed wind farm footprint and buffer regions. "Estimated numbers for W20" is the estimated bird count for the W20 survey while "Estimated numbers under the scenario" represents the estimated bird count under the scenario described. The "95 % CI" figures represent the 95 percentile based confidence intervals for each estimate.

Region	Estimated numbers for W20	95 % CI (W20)	Estimated numbers under the scenario	95 % CI Scenario
Inside Footprint	326.4	(231.8, 461.1)	163.2	(115.9, 230.5)
Outside Footprint	21939	(17332, 27916)	22102	(17472, 28114)
Footprint including 2km buffer area	634.7	(453.5, 899.5)	398.0	(283.7, 559.8)
Outside Footprint including 2km buffer area	21631	(17074, 27542)	21867	(17275, 27821)

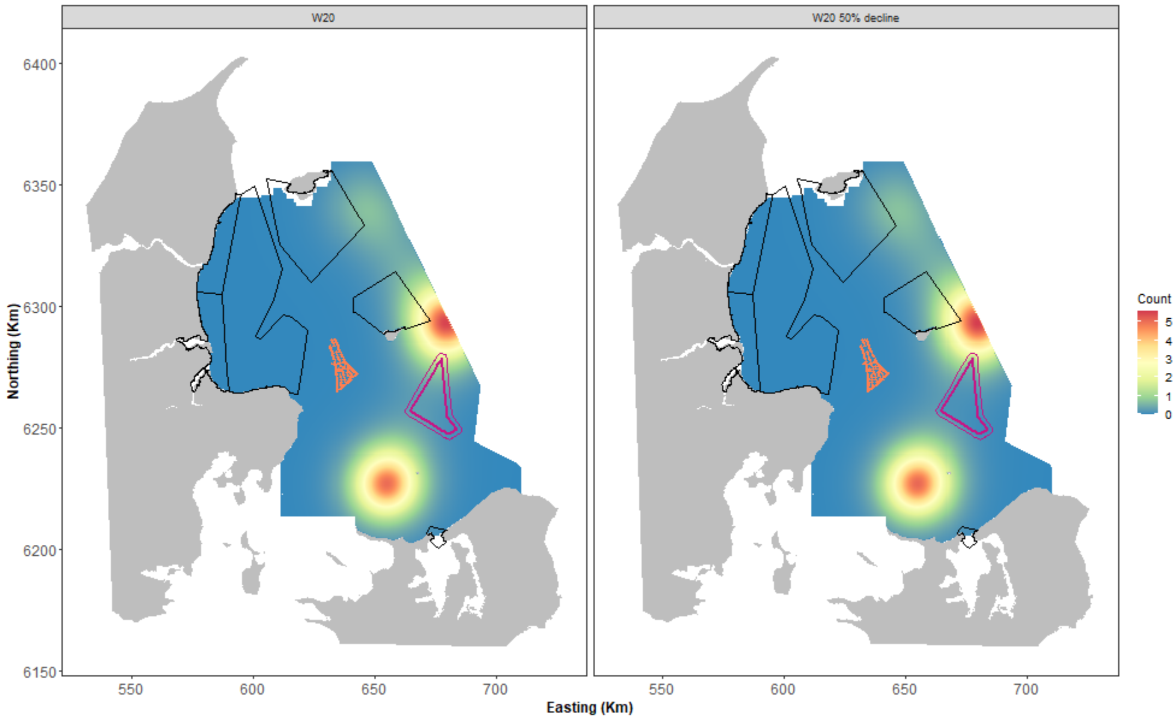

Figure 104: Example of scenario for Razorbill/Guillemot. On the left is one of the estimated bootstrap predictions from the W20 model. On the right is the same set of predictions but with the scenario imposed. The footprint is shown by the thick purple line and the buffer the thinner purple line. The black lines denote the SPA areas.

The impact of this scenario on Razorbill/Guillemot numbers in the SPA regions was estimated to be minimal (Table) and in all cases, the confidence intervals for the number of birds in each site overlapped substantially. This suggests that the underlying abundances in each case may not be statistically distinct, which is unsurprising given the small number of birds that were re-distributed over a large area. The majority of the re-distributed birds were not placed in an SPA region however, those that were ended up in SPA 32 and 10.

Table 35: Table of SPA areas showing the effect of scenario implementation on Razorbill/Guillemot numbers. N is the estimated bird count for either the W20 survey or for the scenario and 95 % CI is the 95 percentile based confidence interval for N. N/A in the SPA column represents the rest of the study area that is not contained within an SPA.

SPA	Area (Kmsq)	N (W20)	95 % CI (W20)	N Scenario	95 % CI Scenario
SPA10	905.0	1011	(462, 1840)	1021	(467, 1854)
SPA102	20.3	11.7	(7.7, 17.2)	11.9	(7.8, 17.4)
SPA112	1759.0	64.9	(21.4, 154.7)	65.6	(21.6, 156.6)
SPA15	297.2	8.3	(2.5, 20.8)	8.4	(2.5, 21.1)
SPA2	296.1	9.4	(2.9, 22.9)	9.5	(2.9, 23.2)
SPA32	463.0	1134	(753, 1626)	1147	(761, 1648)
N/A	8568.0	20026	(15895, 25282)	20002	(15872, 25257)

Discussion and conclusion

The results of a series of surveys conducted across many years, and those undertaken more intensively in 2018/2019, confirm that the Middelgrund and Kattegat Study Areas consistently hold large numbers of waterbirds throughout the year. Some species are characteristically restricted to shallow, coastal areas, whereas others occur only in deeper waters, generally reflecting their feeding ecology. Likewise, some species are found in the study area all year, while others are more seasonally restricted to a specific period of the year.

Of the 50 species of birds and four species groups recorded in the study area, 30 were not encountered in total numbers that exceeded 100 across all eleven survey flights, most of which were never encountered near the area for the proposed site for Hesselø OWF. These species or species groups can thereforebe ignored in any further analysis. Several diving duck species (Common Eider, Common Scoter, Velvet Scoter, Red-breasted Merganser *Mergus serrator*, Common Goldeneye *Bucephala clangula* and Greater Scaup *Aythya marila*) some of which occur in internationally important numbers in the Kattegat Study Area and are designation criteria for several of the SPAs in this area, were never encountered in substantial numbers in the vicinity of the area of the proposed Hesselø OWF. This is because they rest and forage in shallow waters closer to the coast and as such can also be eliminated from further assessment of the potential effects on their future distribution patterns. Likewise Cormorant, dabbling ducks and waders that were detected in aerial surveys but were completely confined to near coastal areas are also not relevant to any assessment of impacts from the proposed Hesselø OWF. This effectively only the leaves the divers, Gannet, gulls (especially Kittiwakes) and Razorbill/Guillemot (all of which tend to forage further offshore) as species needing a thorough assessment in relation to the proposed development of Hesselø OWF.

Given the geographical overlap of the distribution of the bird species with the planning area for the Hesselø OWF and the conservation status of the bird species, for the purposes of this report, the focus was concentrated on a more detailed analysis of the potential displacement effects on four bird species or species groups, namely Red-throated Diver/Black-throated Diver, Gannet, Kittiwake and Razorbill/Guillemot. For these species total numbers was estimated and their spatial distribution was modelled at a high geographical resolution (500 x 500 meter grid cells), excluding surveys with too few observations to permit spatial modelling. This process generated high resolution species distribution surfaces in and around the area of the proposed Hesselø OWF, which suggested that all four species/species groups occurred at relatively low densities, with the possible exception of Razorbills/Guillemots.

Clearly any effects on birds of a given species arising from the construction of an offshore wind farm will depend not only on their local abundance, but also how those birds respond to the development. Some bird species (such as divers) have been shown to be reticent to swim within a kilometer or more of an unfamiliar moving object in the marine environment such as for instance ship traffic (Fliessbach et al. 2019), despite the persistence of a viable food supply in waters between the turbines. Such a behavioural response effectively precludes birds from foraging anywhere within and in an area up to one kilometer out from peripheral turbines, causing displacement and effective habitat loss to that species. Other species (such as some large gulls and Cormorant) are actually attracted to turbines and hence potentially can show increases in local density within an offshore wind farm than was the case prior to construction. Yet other species may show no detectable change in density inside and outside the wind farm and are effectively unaffected by its construction. To effectively contribute to a strategic environmental assessment of the effects of a wind farm construction on any one species therefore requires some assessment of the proportional changes in numbers within and outside the development area to understand the potential impact on the population as a whole.

In this report, it was chosen to model the potential increase or decrease in numbers of each of the four focal species or species groups based on the observed changes in numbers of these species reported in the literature from other studies of offshore wind farms comparing pre and post construction densities. Following a literature study for the selected bird species/species groups, we extracted two parameters from the results of previous studies, firstly the degree of change within the footprint of the wind farm site was assessed, and secondly the distance around the wind farm out to which a significant effect was detected. One potential drawback with this approach was that for some of these species the results varied considerably between sites and studies, while for all species, the number of studies providing robust results for these species were generally highly restricted. Nevertheless, the chosen scenarios are expected to generate the best available potential scenarios for displacement/attraction given the existing literature from previous studies.

With input from the modelled density surfaces, persistency maps for each species/species group could be modelled. These persistency values indicate which areas, within the study area, are of higher importance than others, calculated across all available density model results, and can also be named sensitivity maps. The results show that the persistency for Red-throated Diver/Black-throated Diver in the area of the proposed Hesselø OWF area was low as compared to the general area. The corresponding persistency scores for Gannet and Kittiwake was intermediate, while it was high for Razorbills/Guillemots. Of the selected species, the Razorbills/Guillemots was at the same time present in highest numbers in the area of the proposed Hesselø OWF area.

Based on percentage displacement/attraction rates reported in the literature, the potential numbers of displaced individuals from the area of the proposed Hesselø OWF area could be estimated for each of the species/species group and for each survey data set. For the Red-throated/Black-throated Diver this amounted to between seven to 145 individuals (the minimum and maximum for the 11 surveys). Since the majority of the small unidentified divers in this category is considered to be Red-throated Divers, this would amount to 0.003 % to 0.04 % of the flyway Red-throated Diver population (Wetlands International 2021).

For Gannet, the corresponding calculation estimated the displacement of 0 to 160 individuals under the displacement scenario used <0.01 % of the flyway population of the species.

In the case of the Kittiwake, it should be noticed that Kittiwakes have been reported to be both displaced and attracted to offshore wind farms. So for this species we estimated both displacement and attraction of 0 to 154 individuals or 0.003 % of the population. Since the scenarios for displacement and attraction were the same under this calculation, an offshore wind farm could potentially attract additional Kittiwakes at a numerical scale equal to the displacement scenario.

Finally for Razorbill/Guillemot, displacement estimates varied greatly between surveys, ranging from seven to 6,458 individuals. Attempting to establish the magnitude of these changes on the population level are impossible given the mixing of populations and sub-populations present and foraging in these non-breeding areas. This is because it is not possible to differentiate Razorbills from Guillemots with confidence from aircraft and because the survey area supports birds that originate from a mixture of different subpopulations of both species. At present good data on the subpopulation composition of the two species in the Kattegat area is missing. Being well aware of the caveats, we calculated the percentages assuming that all birds present belonged to one subpopulation. While for the larger subpopulations the percentage of displaced birds represented low values, for the smaller subpopulations of Razorbills (*Alca torda torda*) and Guillemot (*Uria aalge albionis*) these values represented much higher percentages of birds being displaced which potentially could have serious consequences for those subpopulations were the birds in the impact area to all be derived from among their number. While this is perhaps unlikely as a worst case scenario, our current inability to designate the birds from our surveys to specific subpopulations makes any true assessment almost impossible based on current knowledge, which should take account of potential impacts on the most vulnerable subpopulations.

When birds are either displaced or attracted to offshore wind farms, this will have an impact on the bird distribution, not only in the wind farm and a buffer zone, but also in the surrounding area outside of these areas. In this report, we have modelled the spatial pattern of redistribution scenario for the four selected bird species, using the mid-winter 2020 data set. The spatial model used the same model parameters as used for the estimation of densities and for the 2020 data set, but reducing densities within and around the proposed wind farm site according to the displacement scenarios used. The model re-distributed the displaced birds, so for species with reduced abundances in and around the wind farm site had corresponding increased densities over the rest of the model area. Thus, the number of birds present in the surrounding SPA's was estimated to increase. It is challenging to estimate the population impact from displacement of birds. In theory, birds locate themselves to optimize their conditions, taking access to food availability and risk of predation into consideration. From this starting point, therefore, any displacement has a potential adverse effect on a given individual, either because it is displaced to an area of less suitable foraging (e.g. lower food density or enhanced competition from other occupying the area), greater predation risk or a combination of the two. The present redistribution data was modelled on the background of modelling results from the 2020 data set, which represents another shortcoming, as these birds vary enormously in numbers over space and time, and data from one year may not be fully representative of all other years.

Furthermore, our estimation of abundance of displaced individuals is limited to calculating effects within the modelled area. If displaced birds from the area of the proposed Hesselø OWF moved outside the limit of the modelled area, the number of displaced individuals will be underestimated. In this study, displacement distances of 16 km was used for divers and 15 km for Gannets, but the shortest distance from the proposed wind farm area to the edge of the model area was ca. 8 km, so such a scale effect is a likely feature of our approach. Likewise in our re-distribution modelling, the relocation of birds was restricted to occurring within the modelled area, even though redistribution of birds into areas outside the modelled area is very likely to occur. The results of this part of the modelling should therefore be treated with caution.

The effect of a potential offshore wind farm on birds in the Hesselø area is generally expected to have little effect on bird distributions. For a number of bird species, as for instance coastal birds and species that forage on shallow water, there is a general geographical segregation between their distribution and the wind farm site, and there is thus no distributional effect from a wind farm on those species. For more marine species, such as for instance Gannets, Kittiwakes and Razorbills/Guillemots, the geographical overlap is much higher. Divers are also found in the proposed wind farm site, but in low numbers. The number of displaced Red-throated/Black-throated Divers, Gannet and Kittiwakes represent very low proportions of the flyway populations. They thus contribute marginally to a cumulative effect of these populations. For the Razorbills/Guillemots the situation is more challenging to assess because of the inability to differentiate birds into sub-populations. If the birds present in the area are dominated by birds from the smaller subpopulations, as Razorbills of the eastern Atlantic *A.t. torda* subpopulation or the

Guillemots of the *U.a. albionis* subpopulation, then displacement may reach percentages that contribute markedly to a cumulative impact of those subpopulations.

Finally, we wish to reiterate that this report assesses the potential effect of the proposed Hesselø OWF area only on the distribution of birds and the potential post-construction distributional effects in terms of potential displacement/attraction based on literature descriptions. It cannot account for the fitness effects (such as loss of reproductive potential or reduced survival) on individuals that accrue from such displacements, which could have potential population impacts. Nor can this report address in any way the potential effect of collisions on population changes in any of these (or other) species, because data on bird flight intensity and altitudes were not available to this study.

References

AEWA 2021. Draft resolution 8.2 Adoption of amendments to the AEWA Annexe. Doc. AEWA/MOP8 DR.2. https://www.unep-aewa.org/sites/default/files/document/aewa_mop8_dr2_adoption_of_amendments.pdf)

Buckland, S.T., Anderson, D.R., Burnham, K.P., Laake, J.L., Borchers, D.L., Thomas, L., 2001. Introduction to Distance Sampling: Estimating Abundance of Biological Populations. Oxford University Press, New York.

Buckland, S.T., Rexstad, E.A., Marques, T.A., Oedekoven, C.S., 2015. Distance Sampling: Methods and Applications. Springer International Publishing, Switzerland.

Cramp, S. (ed.) 1985: Handbook of the Birds of Europe the Middle East and North Africa. Oxford University Press.

Dierschke, V. 2002. Durchzug von Sterntauchern Gavia stellata und Prachttauchern G. arctica in der Deutschen Bucht bei Helgoland. – Vogelwelt 123:203-211.

Dierschke, V., Furness, R.W. & Garthe, S. 2016. Seabirds and offshore wind farms in European waters: Avoidance and attraction. – Biological Conservation 202: 59-68.

Fliessbach, K.L., Borkenhagen, K., Guse, N., Markones, N, Schwemmer, P. & Garthe, S. 2019. A Ship Traffic Disturbance Vulnerability Index for Northwest European Seabirds as a Tool for Marine Spatial Planning. – Front.Mar.Sci. 6:192. https://doi.org/10.3389/fmars.2019.00192

Fox, A.D. & Petersen, I.K. 2019. Offshore wind farms and their effects on birds - Dansk Orn. Foren. Tidsskr. 113: 86-101.

Heinänen, S., Zydelis, R., Kleinschmidt, B., Dorsch, M., Burger, C., Morkunas, J., Quillfelt, P. &Nehls, G. 2020. Satellite telemetry and digital aerial surveys show strong displacement of red-throated divers (*Gavia stellata*) from offshore wind farms. – Marine Environmental Research 160, 104989.

Holm, T.E., Nielsen, R.D., Clausen, P., Bregnballe, T., Clausen, K.K., Petersen, I.K., Sterup, J., Balsby, T.J.S., Pedersen, C.L., Mikkelsen, P. & Bladt, J. 2021. Fugle 2018-2019. NOVANA. Aarhus Universitet, DCE – Nationalt Center for Miljø og Energi. Videnskabelig rapport fra DCE - Nationalt Center for Miljø og Energi nr. 420. novana.au.dk.

Lavers, J., J. M. Hipfner, and G. Chapdelaine 2020. Razorbill (*Alca torda*), version 1.0. - In Birds of the World (S. M. Billerman, Editor). Cornell Lab of Ornithology, Ithaca, NY, USA. https://doi.org/10.2173/bow.razorb.01

Linnebjerg, J.F., Frederiksen, M., Kolbeinsson, Y. et al. Non-breeding areas of three sympatric auk species breeding in three Icelandic colonies. - Polar Biol 41, 1951–1961 2018. https://doi.org/10.1007/s00300-018-2334-1

Marques, F. F. C. and Buckland, S. T. 2004. Advanced Distance Sampling, chapter Covariate models for the detection function, pages 31-47. Oxford University Press.

Marques, T. A., Thomas, L., Fancy, S. G., and Buckland, S. T. 2007. Improving estimates of bird densities using multiple covariate distance sampling. The Auk 124, 1229{1243.

Nagy, S. 2019a. Delineation of biogeographic populations of the Razorbill (*Alca torda*). Proposal to change population delineations. Doc AEWA/TC 15.11. Doc AEWA/TC 15.11. https://www.unep-aewa.org/sites/default/files/document/aewa_tc15_11_delineation_biogeographic_populations_razorbill_en.pdf

Nagy, S. 2019b. Delineation of biogeographic populations of the Common Murre (*Uria aalge*). Proposal to change population delineations. Doc AEWA/TC 15.11. Doc AEWA/TC 15.14 Rev. 1. https://www.unep-aewa.org/sites/default/files/document/aewa_tc15_14_delineation_biogeographic_populcations_common_murre_Rev1.pdf

Peschko, V., Mendel, B., Mercker, M., Dierschke, J. & Garthe, S. 2021. Northern gannets (*Morus bassanus*) are strongly affected by operating offshore wind farms during the breeding season. - Journal of Environmental Management 279 111509.

Petersen, I.K. & Fox, A.D. 2009: Faktorer der påvirker fordelingen af sortænder i fældningsperioden i Ålborg Bugt. Rapport rekvireret af Vattenfall Vindkraft. Danmarks Miljøundersøgelser, Aarhus Universitet. 20 pp.

Petersen, I.K., Fox, A.D. & Clausager, I. 2003. Distribution and numbers of birds in Kattegat in relation to the proposed offshore wind farm south of Læsø – Ornithological impact assessment. - Report request. Commisioned by Elsam Engineering A/S. National Environmental Research Institute Ministry of the Environment. 116 pp.

Petersen, I.K., Nielsen, R.D. & Mackenzie, M.L. 2014. Post-construction evaluation of bird abundances and distributions in the Horns Rev 2 offshore wind farm area, 2011 and 2012. Report commissioned by DONG Energy. Aarhus University, DCE – Danish Centre for Environment and Energy. 51 pp.

Petersen, I.K. & Sterup, J. 2019a. Number and distribution of birds in and around two potential offshore wind farm areas in the Danish North Sea and Kattegat. Aarhus University, DCE – Danish Centre for Environment and Energy, 40 pp. Scientific Report. No. 327. http://dce2.au.dk/pub/SR327.pdf

Petersen, I.K. & Sterup, J. 2019b. Bird distributions in parts of the Danish North Sea and in Kattegat, autumn 2019. Aarhus University, DCE – Danish Centre for Environment and Energy, 14 pp. Research Note from DCE.

Scott-Hayward, L. 2013. Novel Methods for species distribution mapping including spatial models in complex regions: Chapter 5 for SALSA2D methods. PhD Thesis, University of St Andrews.

Scott-Hayward L, Mackenzie, M, Donovan, C and G Walker 2014. CReSS – Complex Region Spatial Smoother. Journal of Computational and Graphical Statistics. 23 (2) 340-360

Scott-Hayward LAS, Oedekoven CS, Mackenzie ML, Walker CG 2019a. MRSea package v1.01: Statistical Modelling of bird and cetacean distributions in offshore renewables development areas. University of St. Andrews: Contract with Marine Scotland: SB9 (CR/2012/05)

Scott-Hayward LAS, Oedekoven CS, Mackenzie ML, Walker CG 2019b. Vignette for the MRSea Package v1.01: Statistical Modelling of bird and cetacean distributions in offshore renewables development areas. - University of St. Andrews.

Vallejo, G.C., Grellier, K., Nelson, E.J., Ross M., McGregor, R.M., Canning, S.J., Caryl, F.M. & McLean, N. 2017. Responses of two marine top predators to an offshore wind farm. - Ecology and Evolution 7:8698–8708.

Vanermen, N., Onkelinx, T., Courtens, W., Van dewalle, M., Verstraete, H., et al., 2015. Seabird avoidance and attraction at an offshore wind farm in the Belgian part of the North Sea. Hydrobiologia 756, 51–61.

Verena Peschko, V., Mendel, B., Müller, S., Markones, N., Mercker, M. & Garthe, S. 2020. Effects of offshore windfarms on seabird abundance: Strong effects in spring and in the breeding season. – Marine Environmental Research 162 105157.

Walker, C., M. Mackenzie, C. Donovan and M. O'Sullivan 2010. SALSA - a Spatially Adaptive Local Smoothing Algorithm. Journal of Statistical Computation and Simulation, 81(2):179-191

Welcker, J. & Nehls, G. 2016. Displacement of seabirds by an offshore wind farm in the North Sea. - Mar Ecol Prog Ser. 554: 173–182. doi: 10.3354/meps11812

Wetlands International 2021. Waterbird Population Estimates. - Retrieved from wpe.wetlands.org on Thursday 16 Sep 2021

Zuur, A.F. 2018. Effects of wind farms on the spatial distribution of Guillemots. – Report from Highland Statistics Ltd.